Dissertation

submitted to the
Combined Faculty of Natural Sciences and Mathematics
of the Ruperto Carola University Heidelberg, Germany
for the degree of Doctor of Natural Sciences

Presented by
Robin Wanjiru Njenga, M.Sc.
born in Nairobi, Kenya
Oral examination: 17th April 2020

Characterizing the Interaction of Adeno-Associated Virus (AAV) with Factors of the Ubiquitin-Proteasome System

Referees: Prof. Dr. Martin Müller
Prof. Dr. Oliver Müller

Summary

The Adeno-associated virus (AAV) presents itself as an attractive vector for gene therapy due to its broad tissue tropism, ease of manipulation and lack of pathogenicity. So far, three FDA approved AAV-based gene therapies are available, with more than 100 ongoing clinical trials. However, aspects of the AAV life cycle still limit its transduction capacities such as receptor binding, intracellular trafficking, uncoating, single-strand to double strand conversion and interaction with host cell factors. Although technologies have been developed to tackle most of these challenges, there is still a gap in knowledge on the restriction through the interaction with host cell factors. Bridging this gap in AAV biology shall additionally enable the generation of more efficient gene therapy vectors. In this study, the restriction of AAV through the ubiquitin-proteasome system was evaluated. The speckled-type POZ protein (SPOP) is a member of the E3-ubiquitin ligase complex with Cullin 3. Both Cullin 3 and SPOP were previously identified though a tandem-affinity purification as putative interaction partners of AAV capsid protein VP1. In addition, a yeast 2 hybrid screen also confirmed the interaction with SPOP. In this study, CRISPR-Cas9 technology was employed to knockout SPOP and Cullin 3; and evaluate their effects on AAV. SPOP was found to restrict AAV in both parts of the life cycle. During entry, SPOP had a 2-fold effect on AAV transduction and regulated the turnover of capsids (up to 3 fold more capsids were seen in the absence of SPOP). However, an increase of transduction through proteasome inhibition in the SPOP knockout cells indicated that it was not the sole E3 ubiquitin ligase complex involved in the restriction of AAV transduction. After de novo synthesis of capsid proteins, SPOP was able to regulate the turnover of both assembled capsids and unassembled capsid proteins. The latter could be visualized as distinct VP clusters in the nuclei of SPOP knockout cells. A restoration of SPOP in the knockout cells was able to destabilize the capsid proteins but wash not able to reach the levels seen in the parental condition, although the functionality of restored SPOP could not be confirmed as other endogenous SPOP substrates showed variable patterns. Proteasome inhibition was able to stabilize unassembled capsid proteins to comparable levels as the absence of SPOP but had no additive effect upon combination. Cullin 3 did not have a significant effect in either part of the AAV life cycle. The results of this study provide more concrete information about the involvement of the ubiquitin-proteasome system in the restriction of AAV.

Zusammenfassung

Das Adeno-assoziierte Virus (AAV) stellt aufgrund seines breiten Gewebetropismus, seiner einfachen Handhabung und seiner geringen Pathogenität einen attraktiven Vektor für die Gentherapie dar. Bislang gibt es drei von der FDA zugelassene AAV-basierte Gentherapien, mit mehr als 100 laufenden klinischen Studien. Jedoch schränken manche Aspekte des AAV-Lebenszyklus, wie Rezeptorbindung, intrazellulärer Transport, Entpacken, Einzelstrang-zu-Doppelstrangkonvertierung und die Interaktion mit Wirtszellfaktoren immer noch die Anwendung ein. Obwohl Technologien entwickelt wurden, um die meisten dieser Herausforderungen zu bewältigen, gibt es immer noch eine Wissenslücke bezüglich der Interaktion von AAV mit Wirtszellenfaktoren. Das Schließen dieser Lücke soll die Entwicklung effizienterer Gentherapievektoren ermöglichen. In dieser Studie wurde die Inhibition von AAV durch das Ubiquitin-Proteasom-System untersucht. Das Speckle-type POZ-Protein (SPOP) ist zusammen mit Cullin 3 ein Mitglied eines E3-Ubiquitin-Ligasekomplexes. Sowohl Cullin 3 als auch SPOP wurden in voran gegangenen Studien durch eine *Tandem-Affinitätsaufreinigung* als mutmaßliche Interaktionspartner des AAV-Kapsidproteins VP1 identifiziert. Darüber hinaus bestätigte ein *yeast-two-hybrid screen* ebenfalls die Interaktion von VP1 und SPOP. In dieser Studie wurde die CRISPR-Cas9 Technologie eingesetzt, um einen *knockout* von SPOP und Cullin 3 zu erreichen und deren Auswirkungen auf AAV zu bewerten. Es wurde festgestellt, dass SPOP in frühen und späten Phasen des Lebenszyklus AAV inhibiert. Während der Transduktion zeigt SPOP einen 2-fachen Effekt auf die AAV Transduktion und reguliert den Abbau von Kapsiden (in Abwesenheit von SPOP wurden bis zu 3-fach mehr Kapside nachgewiesen). Ein Anstieg der Transduktion durch eine Proteasom Inhibition in den SPOP-*knockout*-Zellen zeigte jedoch, dass neben SPOP auch andere E3-Ubiquitin-Ligasen an der Hemmung der AAV-Transduktion beteiligt sind. Nach der Translation der Kapsidproteine konnte SPOP sowohl den Umsatz der assemblierten Kapside als auch der nicht-assemblierten Kapsidproteine regulieren. Letztere konnten als deutliche VP-Akkumulationen in den Kernen von SPOP-*knockout*-Zellen visualisiert werden. Eine Rekonstitution von SPOP in den *knockout*-Zellen konnte den Effekt, der im ursprünglichen Zustand zu beobachten war, nicht umkehren, mit der Einschränkung, dass die vollständige Wiederherstellung der Funktionalität von SPOP mittels Analyse von bekannten SPOP Substraten nicht bestätigt werden konnte. Die Proteasom-Hemmung war in der Lage, nicht-assemblierte Kapsidproteine auf vergleichbare Niveaus wie das Fehlen von SPOP zu stabilisieren, aber kein additiver Effekt bei der Kombination. Cullin 3 hatte in keinem der beiden Teilen des AAV-Lebenszyklus einen signifikanten Effekt. Die Ergebnisse dieser Studie liefern konkretere Informationen über die Beteiligung des Ubiquitin-Proteasomsystems an der Hemmung von AAV zu unterschiedlichen Phasen des viralen Lebenszyklus.

Table of Contents

1 Introduction

1.1 Adeno-associated virus history and biology

In 1965, a novel parvovirus was discovered as a contaminant of a simian adenovirus type 15 culture, the scientists proceeded to name an 'adeno-associated virus'. The initial tests showed that the virus was incapable of self-replication, needing the adenovirus to do so. The first experiments also eluded to its non-pathogenic nature both *in vitro* when several tissue types were inoculated and *in vivo* when newborn mice and hamsters were infected via different routes [1]. From that point immense amounts of research have gone into the study, classification and application of the virus.

It was taxonomically classified under the sub-family of *dependoparvovirus* due to its inability to enter the lytic cycle without the presence of a helper virus, later herpesviruses, vaccinia and HPV were also identified as helper viruses [2], [3]. In the absence of a helper virus, AAV was found to enter a latent state by integrating into the host genome [4]. The biphasic life cycle character of the virus along with its inability to cause disease, presented its potential for development as a gene therapy vector.

Thirteen different serotypes and 108 isolates from human/non-human primates, have been discovered to date and AAV2 is the best studied serovar [5]–[7]. The serotypes share varying levels of homology, for example AAV2, 3 and 6 share 85% homology of *rep* ORF and 80% of *cap* ORF sequences; while AAV5- which is considered the most unique serotype, only sharing 54.5% sequence homology of *rep* sequences [8], [9]. These differences are thought to confer the specific tissue tropism seen among the serotypes, which can be exploited when targeting different organs/cell types (Table 1.1).

The serotypes also utilize different cellular receptors and co-receptors. The adeno-associated virus receptor (AAVR) has been recently identified as the main receptor for most serotypes, except AAV4 which is independent and AAV5 which shows only partial dependence on AAVR [10], [11]. Other receptors implicated in the attachment of AAV include- the heparan sulfate proteoglycan (HSPG) for AAV2 and 3, O-linked sialic acid for AAV4, the platelet-derived growth factor receptor (PDGF-R) for AAV5 and a 37/67-kilodalton laminin receptor for AAV8, 2, 3, and 9[12]–[18].

Table 1.1 Tissues transduced by the different AAV serotypes [19]

Tissue	Serotype
Kidney	AAV2
Lung	AAV4, AAV5, AAV6, AAV9
CNS	AAV1, AAV2, AAV4, AAV5, AAV8, AAV9
RPE (Retinal Pigment Epithelium)	AAV1, AAV2, AAV4, AAV5, AAV8
Photoreceptor Cells	AAV2, AAV5, AAV8
Liver	AAV7, AAV8, AAV9
Pancreas	AAV8
Skeletal Muscle	AAV1, AAV6, AAV7, AAV8, AAV9
Heart	AAV1, AAV8, AAV9

1.1.1 The genome structure of the Adeno-associated virus

AAV has a linear, single stranded, 4.7kb DNA genome that encodes for inverted terminal repeats (ITRs) that flank the three genes: *rep*, *cap* and AAP (Figure 1.1) [20]–[23]. The ITRs are 145-bp palindromic, *cis*-acting hairpin structures that act as primers for AAV replication [24]. In the 1980s, when initial efforts to develop AAV as a gene therapy vector began, which included the successful virus production from a plasmid construct, Samulski and colleagues found that the ITRs were the most essential part of the genome, as 96% of the sequences could be replaced by a transgene but the ITRs (which make up 4%) were essential for replication [25]. The other genes act in *trans* and are further described below.

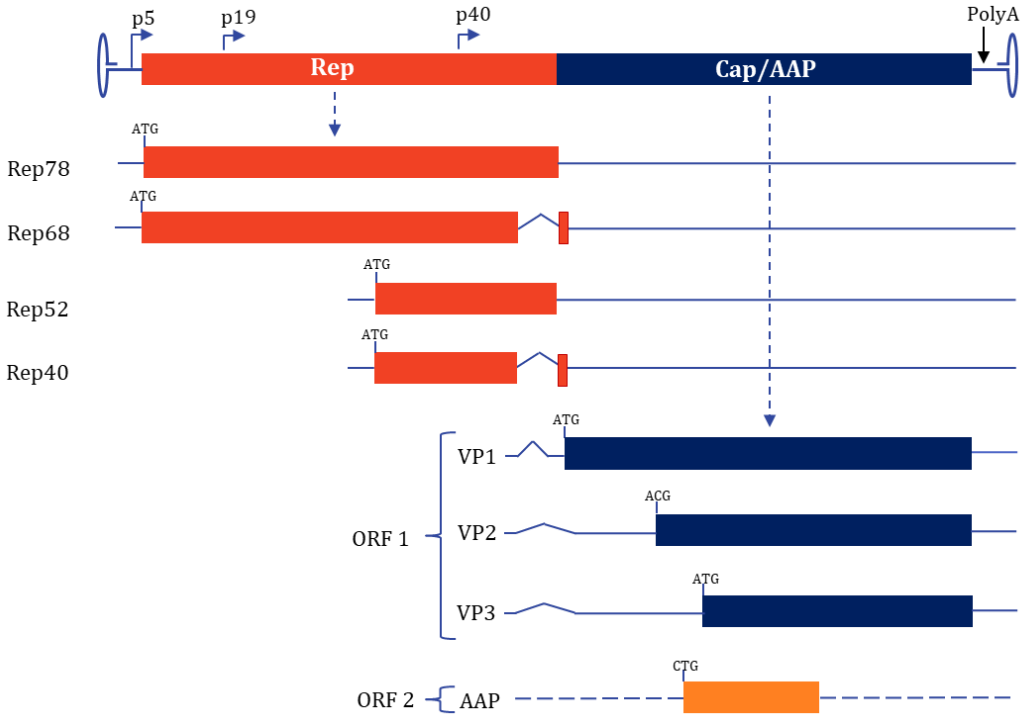

Figure 1.1 Adeno-associated type 2 genome organization. Adeno-associated type 2 genome organization (Adapted from Galibert and Merten, 2011 [26]). The hairpin structures on either side are the ITRs and all transcripts have a poly-adenylation signal present at position 96. The left ORF encodes for the Rep proteins (Rep 78, Rep 68, Rep 52, Rep 40- in red) which are driven by the p5 and p19 promotors with alternative splicing. The right ORF encodes for capsid proteins (VP1, VP2 and VP3-blue) from two transcripts via alternative splicing and the assembly activating protein (AAP-orange) which is located on a separate ORF; and arise from the p40 promotor. Other serotypes show a similar organization. ORF- Open Reading Frame.

1.1.1.1 The Replication Proteins (rep)

The function of the left side of the genome was not known initially, however a replication function was assumed. Four non-structural Rep proteins were identified: Rep78, Rep68, Rep52 and Rep40-the number denotes the molecular weights- all possessing ATPase and helicase activity. Rep 78 and Rep 68 are alternative splice products driven by the P5 promoter and have regulatory roles throughout the AAV life cycle. They are required for DNA replication and regulate the expression of AAV genes in a positive or negative manner depending on the presence or absence of a helper virus, respectively [27]. The smaller Rep proteins-Rep52 and Rep40- are alternative splice products driven by P19 promotor, involved transcriptional regulation and in viral packaging- by accumulating the single stranded AAV DNA which is thereafter packaged into capsids (Figure 1.1) [28], [29].

The q arm of chromosome 19 was found to contain Rep binding elements, dubbed the AAVS1 site. During the latent natural infection, the Rep proteins facilitate the site-specific integration of AAV [30]. Rep52 and Rep78 have also been recently shown to act in the rescue from latency [31].

1.1.1.2 The Capsid Proteins (cap)

The right side of the genome encodes for the viral capsid proteins VP1, VP2 and VP3 and the assembly activating protein (AAP) on a separate ORF (Figure 1.1). The viral capsid proteins are driven by the p40 promoter and share the same C-terminus but have varying N-termini due to alternative splicing. VP1 is a 87kDa unspliced variant that has a N-terminal unique region that contains a PLA-2 domain which is critical for viral infectivity by facilitating endosomal escape and nuclear entry [32], [33]. It has also been recently shown to have protease activity [34]. VP2 and VP3 are both translated from the more abundant major spliced mRNA transcript, but due to the non-canonical ACG start codon on VP2, it is translated less efficiently producing a 72kDa protein [35]. VP2 is considered non-essential, as ΔVP2 capsids were still infectious [36]. VP3 is the most abundant protein, with a molecular weight of 62kDa. When expressed alone it can form capsids in some serotypes but otherwise requires the expression of AAP [37], [38].

1.1.1.3 The Assembly-Activating Protein (AAP)

AAP is encoded on a separate ORF, overlapping with the *cap* ORF (Figure 1.1). It is transcribed through a non-canonical CTG start codon and encodes a 23kDa protein [23]. It shows high homology among the different serotypes and is essential for the capsid assembly of most types [37]. However, it has been found to be non-essential only for AAV4, 5 and 11 [38]. AAP is thought to act as a scaffold for newly synthesized capsids to assemble. It is located in the nucleolus for AAV2 but in other nuclear bodies for the other serotypes [38], [39].

1.1.2 The organization of the AAV Capsid

The AAV capsid proteins are expressed in a molar ratio of 1:1:10, resulting in 60 subunits- 5 VP1, 5 VP 2 and 50 VP3- that assemble to form a ~25nm icosahedral capsid with T=1 symmetry [40]. VP3 is contained in all three proteins, and VP2 is part of VP1, but VP1 has a unique N-terminus (VP1u) with an extra 137 amino acids. The VP1u domain is hidden within the capsid and becomes exposed during virus entry. This has been demonstrated *in vitro* upon heat treatment and thought to act in a similar manner once it enters the endosomes, due to its low pH and the concerted actions of cathepsin B and L [41], [42].

The structure of the monomeric subunit is a conserved β-barrel core. The outer surface of the capsid is composed of long intrastrand loop insertions-named according to where they flank, with β-ribbons and other secondary structural elements. The longest interstrand loop is the GH loop and the extensive interaction between 3 VP proteins at the 3-fold symmetry axis results in a spike. At the 5-fold symmetry axis, a cylindrical structure is formed by an antiparallel β-ribbon from 5 DE-loops each, forming a canyon. A depression (dimple) is found at the 2-fold axis. The peaks and valleys of the 3-fold axis have been linked to the high variability between the G-H β-strands (Figure 1.2). The variable regions are thought to moderate interactions with different cellular receptors and antibodies [43].

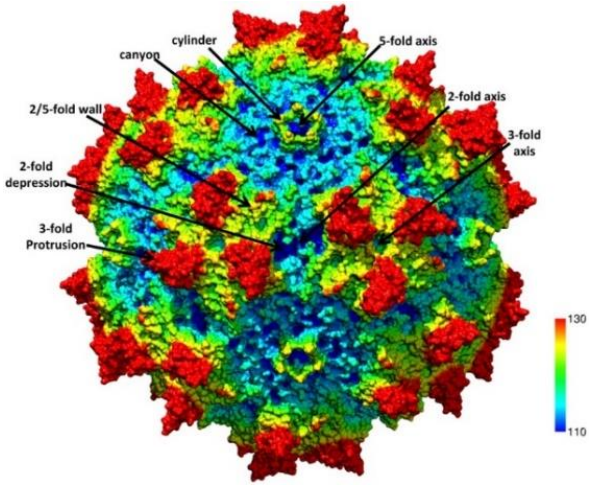

Figure 1.2 The adeno-associated virus 1 capsid (adapted from Tseng and Mckenna, 2014[44]) Heat map of the ~110–130 Å AAV1 capsid-from centre to surface. The capsid is composed of 60 monomers of VP. The features and 2-,3- and 5- fold axes are displayed.

1.1.3 The life cycle of Adeno associated virus

AAV2 is the best studied AAV serotype, with numerous studies about its life cycle as a model for the other serotypes (Figure 2.3). AAVs commonly attach to glycans as the primary receptor, the heparin sulfate proteoglycan (HSPG) was identified as the main receptor of AAV2 and 3[15], [17]. N-linked galactose for AAV9 and O- and N-linked sialic acid moieties for AAV1, 4, 5 and 6 [45]–[48]. No glycan receptors have been identified for AAV7, 8 and 10-12 so far. Apart from the glycans, different proteinaceous receptors have been examined as co-receptors that aid entry. For AAV2 these are aVβ5 integrin, CD9 tetraspanin, fibroblast growth factor receptor-1 (FGFR1) and hepatocyte growth factor receptor (c-MET) [13], [14], [49], [50]. For the other serotypes, several co-receptors have been named, the most wide-spanning are the laminin receptor (LamR) aids entry of AAV2, 3, 8, and 9; and the recently discovered adeno-associated virus receptor (AAVR) is involved in the entry of AAV1, 2, 3B, 5, 6, 8 and 9 [10], [12].

After receptor attachment the AAV particles are internalized into endosomes. There is evidence that this occurs through the action of the GPI-enriched endocytic compartment (CLIC/GEEC), micropinocytosis, caveolar endocytosis, or through clathrin-mediated endocytosis pathways. Although most of particles do not culminate in productive transduction, and different routes have shown differing efficiencies [51]–[53]. In the endosomes, the low pH and the actions of cathepsin B and L play a role in triggering a conformational change that triggers the exposure of the VP1 N-terminus from the capsid [41], [42], [54]. The VP1u region contains the PLA2 domain which is required for the escape from endosomes [55]–[59]. The virus relies on the host cell machinery for trafficking to the nucleus via the network of microtubules and through the trans-golgi network (Figure 2.3) [60], [61].

Two of the three short basic amino acid sequence elements (basic clusters [BCs]) in the VP1/2 common region contain a non-classical nuclear localization signal (NLS) that facilitates the entry of the capsids [59]. Once in the nucleus, AAV2 particles are readily transported into the nucleolus before they reenter the nucleoplasm. The exact reason for this sequestration is unknown especially given that the siRNA knockdown of nucleolar factors increases transduction up to 15-fold and together with hydroxyurea has an additive effect up to 50-fold. Nevertheless, this sequestration is thought to permit uncoating and gene transduction [62]. After egress into the nucleoplasm the capsids undergo uncoating, however it is also believed that full disassembly of the capsids is not required for the release of the genome as proven with other autonomous parvoviruses [63], [64]. The kinetics of the release of the DNA depends on the serotype and the cells being transduced [65], [66].

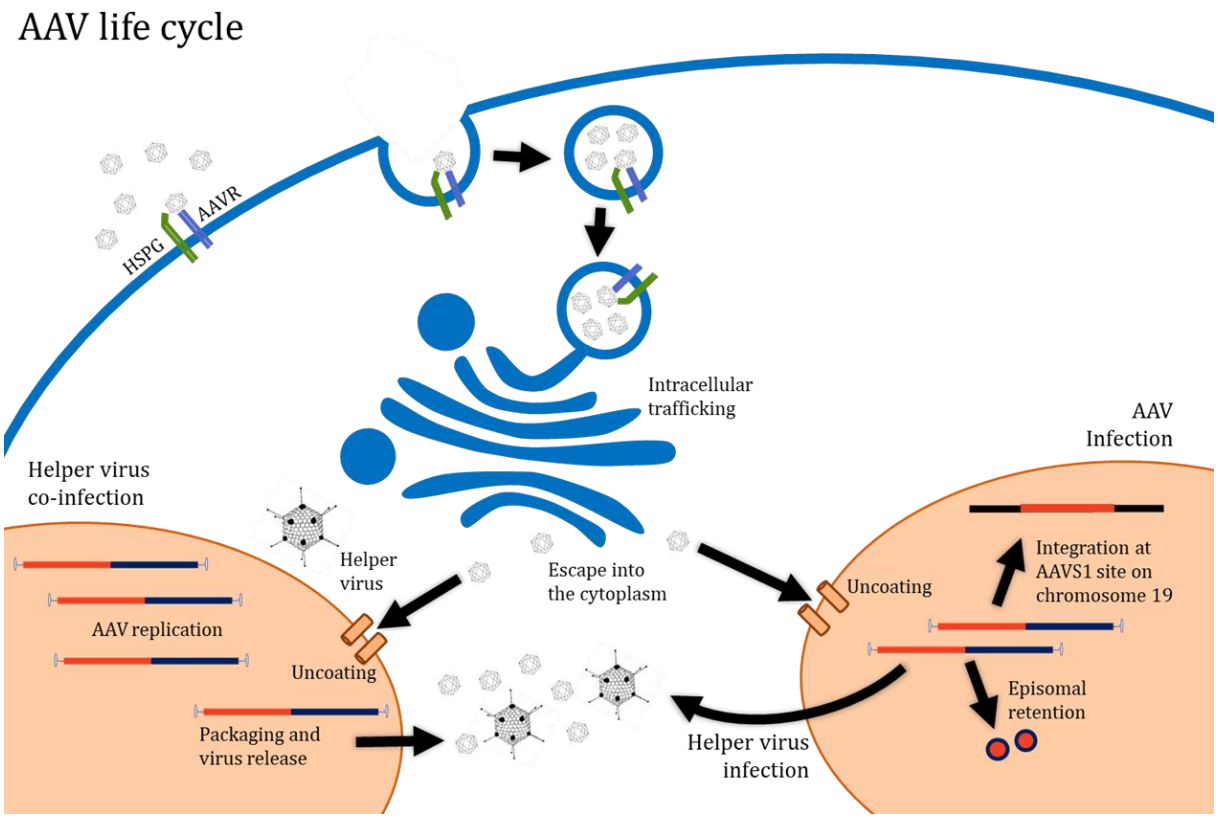

Figure 1.3 AAV life cycle (Adapted from Daya and Berns, 2008; Pillay and Carette,2017 [67], [68]). AAV approaches the cell surface and interacts with its AAVR and HSPG receptors. It becomes internalized and undergoes conformational changes to allow it to escape the endosome and traffic through the intracellular network before release into the cytoplasm and into the nucleus where it uncoats. At this point it can enter either the lytic or latent phase. In the presence of a helper virus it undergoes replication, gene expression, packaging and release. In the absence of a helper virus it either undergoes site-specific integration into AAVS1 on chromosome 19 or is retained in episomes. Super infection with a helper virus (or cellular stress) can rescue the virus from latency. All stages of the life cycle involve complex interactions between the AAV genome, the proteins it produces, the helper virus and the host cell machinery.

The viral DNA is released but is in a transcriptionally inactive state. From here it can enter either the lytic or latent phase. In the lytic phase, helper virus genes are expressed aiding AAV gene expression. For adenovirus these are E2a, E4 and VA RNA, while other helper viruses act in different means [69]. The single stranded (ss) DNA is then transformed into double stranded (ds) DNA through either the ligation of plus and minus DNA strands via a co-infection in the same cell or de novo synthesis of the second DNA strand using the 3' hydroxyl group of the ITR as a primer and relying on the host cell polymerases. The larger rep proteins-

Rep68 and Rep78 play a specific role in catalyzing endonucleolytic cleavage at the terminal resolution site (trs) in a strand-specific manner. The single strand to double strand conversion is considered a rate-limiting step of transduction [70]–[73]. The smaller rep proteins-Rep40 and Rep52 play a role in generating and accumulating ss-viral genomes from ds-replicative intermediates [74].

Transcription and translation of the AAV genome is regulated by helper virus factors. Firstly the Rep proteins are produced, due to their regulatory role on other parts of the life cycle then the capsid proteins (VP1, 2 and 3) and AAP are produced [75]–[77]. The assembly-activating protein is thought to act as a scaffold for capsid assembly in the nucleolus [23]. The newly synthesized DNA is then inserted into the pre-formed capsids through the 5-fold symmetry axis, by the helicase activity of the small rep proteins [78], [79]. The helper virus then aids the release of newly synthesized capsids [80].

In the absence of a helper virus the AAV genome can remain episomally (in the case of AAV vectors) or be integrated into the host genome. For the latter, the concerted actions of Rep 68, Rep 78 and the ITRs direct the integration into the long q arm of human 19 chromosome, 19q13.3-qter (AAVS1) [81], [82]. The virus can re-enter the lytic phase by super-infection or induction of cellular stress [83].

1.1.4 The engineering of Adeno associated virus vectors

AAVs simple biology, its non-pathogenic nature and ability to establish latency were the original factors that drove the engineering of the virus for gene therapy [1]. Coupled to the subsequent finding that the ITRs worked in *cis*, and were the only sequences required to drive replication, packaging and genome rescue of the transgene of interest [25]. This allowed for the *rep* and *cap* to be supplied in *trans* together with the co-infection of a helper virus in order to drive the synthesis of the transgene and have it inserted into AAV capsids. When the helper virus genes critical to AAV were identified, they were subsequently cloned into a plasmid and provided in *trans* eliminating the need for helper virus co-infection [84]–[86]. The next issue was how to scale-up transfections, as high vector titers were needed for use in animal experiments and clinical trials, thus efforts were put into producing cell lines with stable *rep* and *cap* expression to allow the production with high vector yields [87]–[89]. The baculovirus-insect cell system was also developed as an transfection-alternative, scale up method [90]. Insights in receptor usage have also allowed for the development of new purification technologies by affinity chromatography and ion-exchange chromatography, which can also be readily scaled-up [91]–[93].

Since the capsid structure determines tissue and cell specificity through the interaction with various cellular receptors and host cell proteins during transduction, huge amounts of efforts have been put into modifying the capsids. This strategy could be used to engineer capsids to

target specific tissues/cells of interest, but also has the additional benefit of delivering transgenes without immune activation caused by previous exposure- either through original vector administration or natural infection. These include immunological, genetic or chemical modifications. One approach is by using capsid sequences from non-human AAVs [94], [95]. *Directed evolution* via high-throughput screening methods and AAV capsid libraries, with *in vivo* selection has also been used to identify the best capsid variants for different cell types [96]–[98].

A big limitation of AAV is the 4.7kb genome capacity. To circumvent this issue various developments have been made such as dual AAV vectors. This involves the co-transduction of two halves of a larger gene, allowing for reassembly either through intermolecular recombination mediated by the ITRs that forms concatamers (dual trans-splicing vectors; homologous recombination of the 5' and 3' genomes (dual AAV overlapping vectors) or a combination of both mechanisms (dual AAV hybrid vectors) [99]–[102]. *In vivo*, dual vectors produce full-length proteins and show therapeutic efficiency, but require high vector doses [102]. Another approach includes protein transplicing, whereby separate protein domains/polypeptides are encoded in two different expression cassettes. Upon AAV vector administration the polypeptides are produced independently and re-assemble to form a full length protein [103], [104].

The single strand to double strand conversion presents another bottleneck in AAV infection. Self-complementary AAV vectors (scAAV) eliminate the rate limiting step, by unfolding into double stranded DNA, and initiating replication and transcription directly [105]. scAAVs have been successfully developed into gene therapy vectors that have been used in clinical trials to treat Hemophilia B and spinal muscular atrophy [106], [107].

Continual vector optimization combined with a deeper understanding of AAV biology has led to the better AAV vector-based therapies against several different gene-deficiencies. This has resulted in over 100 clinical trials and the successful EMA and FDA approval of 2-3 therapies against Leber's congenital disease (Luxturna), lipoprotein lipase deficiency (Glybera) and spinal muscular atrophy (Zolgensma-pending EU approval) [108]–[111]. That notwithstanding, some open issues in developing better vectors remain such as AAV vector immunogenicity and persistence. These challenges can be tackled by developing new technologies, but also by also filling the gaps of knowledge that remain open in the AAV life cycle such as the consequence of interactions with different cellular host factors.

1.2 The Ubiquitin-Proteasome System (UPS)

The UPS is a means of quality control, playing a role in various cellular processes including-histone modification, DNA repair, cell cycle progression and in the pathogenesis of various diseases. The UPS exists both in the nucleus and the cytoplasm of cells [112]. It involves the addition of a 76 amino acid (~8 kDa) ubiquitin tag -that is conserved in all eukaryotes- to targeted substrates, via a cascade of three enzymes (Figure 1.4a). The process of protein ubiquitination begins with the activation of a conserved glycine residue on the C-terminus of ubiquitin, which is catalyzed by E1, a ubiquitin-activating enzyme ($n \geq 2$ in humans). PPi is displaced from ATP to form the ubiquitin adenylate intermediate which is transferred to E1 at its thiol site, releasing AMP. Thereafter the ubiquitin is transferred to the thiol site of the E2- ubiquitin-conjugating enzyme ($n > 50$). In the final step E3, a ubiquitin ligase ($n > 500$ in humans) facilitates the transfer of ubiquitin to a lysine residue on the target protein through an isopeptide linkage [113].

The different combinations of E2 and E3 regulate the biological specificity of the process. The addition of poly-ubiquitin to Lys_{48} or branched Lys_{48}-Lys_{11} chains signal for proteasomal degradation while monoubiquitination facilitates non-proteolytic functions such as altering the localization or activity of a protein. There are three major families of E3 enzymes based on the functional class of substrates they interact with, similarities in structure and mechanism in which they transfer ubiquitin; namely: Really Interesting New Gene (RING), Homologous to E6AP C-terminus (HECT), and RING-between-RING (RBR) domain-containing E3 ligase families [114]–[121]. RING E3 ligases bind both the E2 enzyme and the substrate catalysing the ubiquitin transfer in a direct manner [122]. Contrastingly, the activated ubiquitin is transferred from the E2 enzyme to a cysteine residue in the HECT E3 enzyme before it is conjugated to the substrate [123]. The RBR E3 ligases share similarity with RING E3s in that they contain 2 RINGs linked via an in-between-RING (IBR) domain, but the mode of action is similar to HECT E3s, in that the activated ubiquitin is first transferred to the E3 then to the substrate (Figure1.4a) [124], [125].

Deubiquitnating enzymes (DUBs) can edit or completely remove conjugated ubiquitin from the proteins of interest. They are important in modifying the fate of substrates and can disassemble poly-ubiquitin chains in order to recycle the ubiquitin monomers (Figure 1.4b) (see [126] for review).

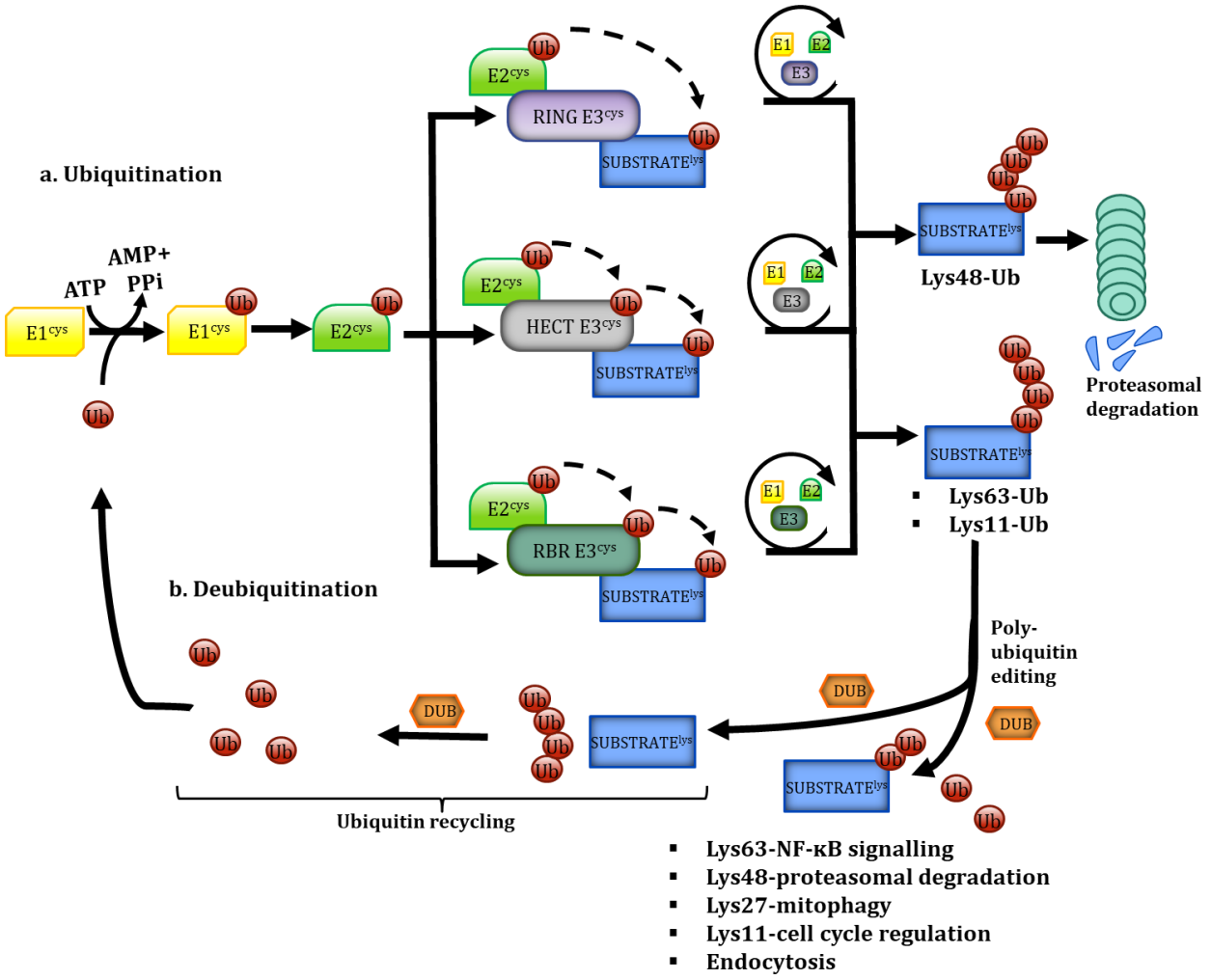

Figure 1.4 The UPS system and deubiquitination (adapted from Zheng et al., 2016 [127])
a. Ubiquitination- Ubiquitin is attached to a cysteine residue of ubiquitin activating enzyme-E1, 10 catalyzed by ATP, then transferred to the active site cysteine of the ubiquitin-conjugating enzyme- E2. E2 thereafter transfers the ubiquitin to the lysine residue on the substrate through a specific E3 enzyme. For E3 RING ligases, the ubiquitin is transferred directly from E2 to the substrate. While for HECT and RBR E3 ligases, the ubiquitin is initially conjugated to a cysteine residue in the E3 enzyme before transfer to the substrate, resulting in different ubiquitin linkages that serve other purposes.
b. Deubiquitination- Deubiquitinating enzymes (DUBs) edit and/or reverse ubiquitination of substrates, thus determining their cellular fate. DUBs can modify the type or length of polyubiquitin chains and can disassemble ubiquitins attached in order to recycle the ubiquitin monomers. PPi, inorganic pyrophosphate.

1.2.1 The Cullin-RING 3 Ubiquitin ligase complex

The Cullin-RING ubiquitin ligases (CRLs) are the most common E3 ligases to date. They form multimeric complexes based on a cullin scaffold with a catalytic center and are highly conserved among different species [128], [129]. Eight different cullins have been classified in mammals (Cul1, 2, 3, 4A, 4B, 5, 7 and 9/PARC). Each CRL complex is composed of different adaptors and/or substrate recognition subunits (srs) (Table 1.2). All CRLs act by bringing the substrate into close proximity to the E2-conjugating enzyme, thus facilitating the transfer of activated ubiquitin to the substrate [130]. Nedd8 acts as a modulator of CRL activation by triggering a conformational change at the carboxy-terminal domain (closed form) that results in the freeing of the RING domain (open active form) [131].

Table 1.2 CRL complex components and adaptors[132]

Cullin	E3 complex components	Adapter
1	Skp1-Cul1-F-box-Rbx1	Skp1
2	Elongin BC-Cul2-Protein SOCS-Rbx1	ElonginC/ElonginB
3	BTB-Cul3-Rbx1 Protein	-
4A, 4B	DDB1-Cul4A/4B-DDB2 o CSA-Rbx1	DDB1
5	Elongin BC-Cul5-Protein SOCS-Rbx1	ElonginC/ElonginB
7	Skp1-Cul7-Fbx29-Rbx1	Skp1
9/PARC	?-Cul9-Rbx1	?

Skp1: S-phase kinase-associated protein 1; F-box: motif that acts as a site of protein–protein interaction; Rbx1: RING-box protein (also known as ROC1); BTB: bric-a-brac/tramtrack/broad-complex; DDB1: damage-specific DNA binding protein 1; SOCS: suppressors of cytokine signalling protein; CSA: cockayne syndrome group A protein.

The Cullin 3 Ubiquitin ligase complex (CRL3) differs from other CRLs because it does not employ an adaptor protein but instead recognizes proteins with a bric-a-brac, tram-track and broad complex (BTB) domain that binds at the Cul3 N-terminus [133], [134]. The BTB domain was originally discovered in *Drosophila melanogaster* transcription factors, but since then over 200 BTB proteins have been found encoded in the human genome [135], [136]. The BTB-containing proteins serve as substrate recognition subunits (srs) to facilitate substrate binding and have different domains that facilitate the recognition of an array of substrates including – Kelch, Zinc finger, Ras and MATH domains[137]. The RING-domain protein (Rbx1) binds to the C-terminus and facilitates the recruitment of the E2-conjugating enzyme [138], [139].

The CRL3 complex plays important roles in regulating key cellular processes including cell migration, oxidative stress, retrograde trafficking and cell cycle progression [140]–[144]. The absence of Cul3 has been demonstrated to inhibit cell migration in drosophila and human cells, via the stabilization of RhoA, a Cul3 substrate, that controls stress fiber development in

the actin cytoskeleton [144]. The absence of Cul3 also causes embryonic lethality in mice, thus highlighting its critical role in the cell [145]. A well-studied substrate recognition subunit of CRL3 is the Speckle-type POZ protein (SPOP) [139].

1.2.2 Speckle-type Poxvirus and zinc finger domain (POZ) Protein (SPOP)

SPOP is a 42kDa protein that was discovered when serum from a scleroderma patient stained a novel antigen that was expressed in nuclear speckles in an immunostaining assay. A BLAST search revealed that the protein contained a POZ domain thus prompting the scientists to name it the Speckle-type Poxvirus and zinc finger domain (POZ) Protein. In addition, the protein appeared to be ubiquitously expressed in tissues of different origin [146]. Mammalian SPOP substrates include Macro2A-which is involved in the silencing of one of the two X chromosomes in a stable manner (X inactivation) through regulating X-chromosome deposition; and DAXX- a protein that plays various roles in the life cycle including apoptosis, transcriptional regulation and controlling the expression of the vascular endothelial cell growth factor receptor 2 (VEGFR2) [147]–[149].

SPOP is a substrate recognition subunit of the Cullin-RING 3 Ubiquitin ligase complex. It has an internal bric-a-brac, Tram-track and Broad Complex/Pox virus and Zinc finger (BTB/POZ) domain that binds to Cul3, a N-terminal Meprin and TRAF homology (MATH) domain that binds to the substrate and a C-terminal domain that contains a nuclear localization signal (NLS)- also referred to as the BTB and C-terminal Kelch (BACK) domain (Figure 1.5). These domains are flexible, allowing for the formation of multimeric complexes, such that SPOP can interact with different motifs on a given substrate [139]. The structure of dimeric SPOP has been resolved and Tyr353 was pinpointed as a critical residue in the formation of high-order SPOP oligomers [150]. The multimeric complexes are dynamic as dimers readily disassociate and re-associate thus giving the speckles a liquid assembly character. These liquid (membrane-less) nuclear speckles have been postulated to increase the efficiency of ubiquitination through the concentration of functional components. A report by Marzahn and colleagues, showed that the BTB and BACK domains in SPOP are crucial for the assembly of high order complexes as mutations in either domain impeded multimerization [151]. The same group recently demonstrated that SPOP undergoes phase separation when co-expressed with DAXX *in vitro* and leaves its nuclear speckles to localize with DAXX in other liquid organelles -so called SPOP-DAXX bodies- *in cells.* Further suggesting that phase separation of SPOP -in a substrate-mediated manner- is essential to its function [152].

The substrates share a SPOP binding consensus sequence (SBC) that is φ-π-S-S/T-S/T (φ-nonpolar; π-polar). When the crystal structure of the SBCs from different substrates were analyzed they displayed similar binding affinities, virtually identical structures and could be super-imposed on each other [139]. However, this has been recently challenged, as the transcription factor Pdx1 lacks two Ser/Thr residues at position 4 and 5 of the SBC sequence,

yet is still able to bind to SPOP. This observation suggests an extended ligand motif for SPOP substrates, thus a less stringent- φ-π-S-π-π, (φ: nonpolar; π: polar) SBC was proposed [153]. Mutations in key hydrophobic dimerization residues in the BTB domain impaired its ability to ubiquitinate target proteins, proving that in its active form SPOP forms homodimers via the BTB domains and as a result- two CRL3s [139]. The same phenomenon has been seen with TRAF6 and Siah, which are simple RING E3s that contain MATH-domains [154], [155].

Mutations of SPOP have also been proven to play significant roles in several different cancers. It exerts tumor-promoting effects by ubiquitinating and degrading several regulators, e.g ERK phosphatases, DAXX, tumor suppressor PTEN, and transcription factor Gli2 in renal clear cell carcinoma [156]. On the other hand, SPOP plays tumor-suppressing roles by regulating Gli2 in gastric and colorectral cancer, progesterone receptors in breast cancer; BET proteins, Cyclin-E1, ERG, and EglN2 in prostate cancer and SIRT2 in non-small cell lung cancer [157]–[164]. These contrasting data have prevented the classification SPOP wholly as a tumor suppressor or a tumor promoter. SPOP also interacts with other regulatory pathways such as the SUMOylation. For example, it plays a role in the degradation of a Sentrin/SUMO-specific protease 7 (SENP7) deSUMOylase which results in cellular senescence [165].

1.2.3 Speckle-type Poxvirus and zinc finger domain (POZ) Protein-Like (SPOPL)

A paralog of SPOP and the only other human protein to contain a MATH-BTB domain is the Speckle-type POZ Protein-Like (SPOPL). It shares 85% sequence identity with SPOP save for an extra 18 amino acids, thus increasing its molecular weight to 45kDa (Figure 1.5) [166]. It is also widely expressed in different human tissues and is highly conserved within different species of vertebrates. But unlike SPOP, SPOPL is localized in endosomes. The endocytic adaptor EPS15 has been identified as a substrate of the CRL3 complex with SPOPL, which plays a role in the efficient formation of intraluminal vesicles and uncoating of the Influenza A virus (IAV) [167].

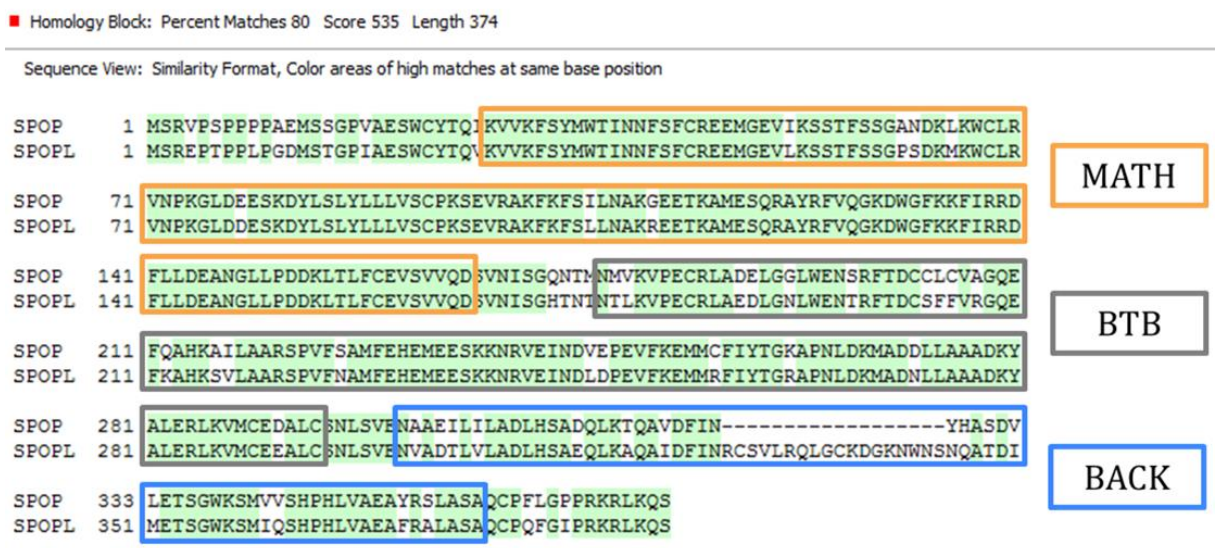

Figure 1.5 Differences between SPOP and SPOPL (Adapted from Errington et al., 2012 [166]) Protein alignment of the two proteins. SPOP and SPOPL share the same N-terminal MATH (orange), and central BTB domains (grey), but SPOPL contains an 18 amino acid insert in the BACK domain (blue). Green highlight shows matching amino acids. Alignment was done using Clone Manager. MATH- Meprin and TRAF homology, BTB-bric-a-brac, Tram-track and Broad domain, BACK- BTB and C-terminal Kelch domain.

SPOPL forms heterodimers with SPOP, however they are less efficient at ubiquitinating target proteins. Therefore the SPOP-SPOPL heterodimers are deemed as a 'molecular rheostat', regulating the way in which SPOP ubiquitinates its targets [166]. When the BACK insert of SPOPL (Figure 1.5) was deleted it was able to oligomerize and ubiquitinate target proteins to the same level observed with SPOP. Thus, it was ascertained as the sequence that causes less efficient heterodimers that disrupt high order oligomers formed by SPOP-SPOP homodimers and form less-active CRL3 complexes (Figure 1.6) [166].

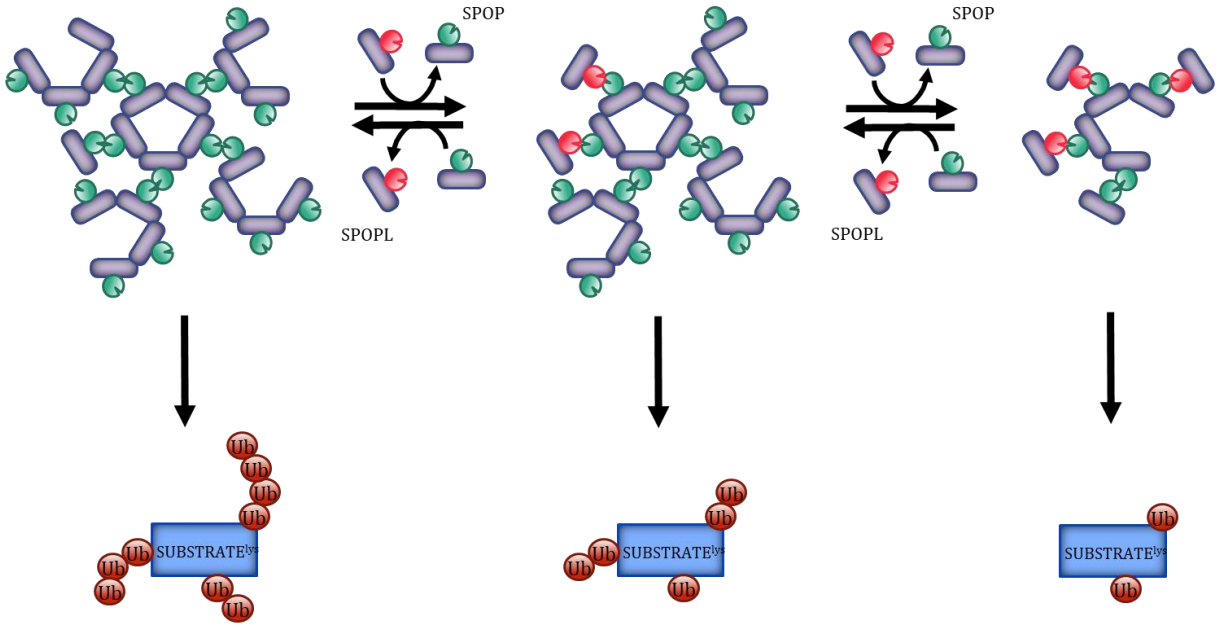

Figure 1.6 The action of SPOPL on SPOP (Adapted from Errington et al., 2012 [166]). A model of how SPOPL modifies the ubiquitination pattern of SPOP.

1.2.4 The ubiquitin-proteasome system and AAV

Post translational modifications are alterations made to amino acids after translation that can result in a change in function or localization. For viruses this could fine tune different aspects to do with infectivity or the response in the host cell. Thus allowing for the virus to co-evolve/adapt to cellular barriers as seen with vaccinia, polyoma and adenoviruses [168]–[170]. In a new study looking at PTMs on the AAV capsids from serotypes AAV1-rh10, Mary and colleagues identified that out of all the PTMs on the AAV capsids, 17% were modifications of a ubiquitin nature, but were serotype-specific [171].

Ubiquitination of the capsids has been long thought of as detrimental to transduction, given that it mostly results in the targeting of capsids to the proteasome for degradation. This was confirmed in the initial studies whereby inhibition of the proteasome resulted in increased transduction efficacies. Proteasome inhibitor (PI) treatment to the apical surface of polarized airway epithelia increased transduction nearly equal level to the level of infection of the basolateral surface (>200-fold) and improved the gene transfer to detectable levels in large bronchial epithelia *in vivo* and was 10 fold higher in the liver [172].

Further studies used different PIs to provide insight into how the proteasome restricts AAV transduction. A second-generation PI- carfilzomib, claimed to reduce the 'promiscuity' seen in other PIs by targeting no other proteases and through the specific inhibition of the chymotrypsin-like activity of the proteasome. Carfilzomib was able to enhance transduction

and gave concrete evidence that proteasome inhibition specifically, with no other off target effects, was able to increase AAV transduction. It was proposed to be through the accumulation of ubiquitinated capsids that positively affected the late steps in AAV transduction [173].

Newer approaches involve targeting the capsid residues that are presumed to undergo ubiquitination. In one study of AAV2 vectors, the modification of 3 out of 7 capsid lysines (K532, K544 and double mutant K490+532) resulted in higher transduction efficacies (82–70%) compared to AAV2-WT vectors (30%) *in vitro* and reported up to 4.9-fold increase in copy numbers and up 12.7-fold higher transgene expression *in vivo* [174]. Baozheng and colleagues, corroborated these findings as changing 4 out of 10 exposed lysines on the AAV2 capsid surface (K490, K544, K549, and K556) resulted in up to a 5-fold higher efficiency than AAV2-WT vectors *in vitro* and *in vivo*. However, when they exchanged these conserved lysines on AAV8 (which is better suited to transduce murine hepatocytes) there was no change in the transduction efficacy, which pointed to a serotype specific effect [175]. Another study exchanged K137 on the AAV8 capsid, resulting in a 40-fold increase in GFP transcripts, demonstrated lower capsid ubiquitination; and significantly reduced the activation of the innate immune response and the formation of neutralizing antibodies in mice [176].

Phosphorylation has also been proven as a pre-requisite for ubiquitination. In one study, 7 exposed tyrosine residues on the AAV2 capsid-that were hypothesized to undergo phosphorylation via the epidermal growth factor receptor protein tyrosine kinase (EGFR-PTK)- were modified to phenylalanine and resulted in a 10-fold higher efficiency *in vitro* and nearly 30 fold higher efficiency *in vivo* with 10-fold lower vector doses. In the same study they showed that this was due to better trafficking to the nucleus and escape from ubiquitination [177]. Another study showed that changes in 11 serines/threonines on AAV2 vectors (S/T→A) resulted in higher transduction efficacies (63–97%) compared to AAV2-WT vectors (41%) *in vitro* and reported up to 4.5-fold increase in copy numbers and up 14-fold higher transgene expression *in vivo* [174]. In a study that relied on a systematic computational analysis to identify possible serine, threonine and lysine residues of interest on the capsid, Sen and colleagues showed that mutations of two serines on the AAV8 capsids resulted in up to 20-fold increase in transcripts in mice [176].

1.3 Aim of the Study

By and large, efforts aimed at modifying specific capsids ubiquitination sites have proven successful. Although deeper insight into the relations with the E3-ubiquitin ligase complex would further enrich our understanding of AAV biology and could additionally provide additional targets that could be used to improve AAV vectors. A yeast-2-hybrid screen and a tandem-affinity purification (TAP-tag) experiment identified Speckle-type POZ Protein (SPOP) as an interaction factor of the AAV capsid protein VP1 [178]. The same study also identified the Cullin-RING 3 Ubiquitin ligase (Cul3). This study aims to validate and characterize the consequence of this interaction, along with evaluating the contribution of other members of the ubiquitin-proteasome pathway- SPOPL and the proteasome. It is hypothesized, that SPOP plays a role by possibly regulating the ubiquitination of AAV capsids during entry or of *de novo* synthesized capsid proteins. Therefore, this study evaluates the effect on incoming capsids during AAV entry (Figure 1.7a) and of newly synthesized capsids (Figure 1.7b).

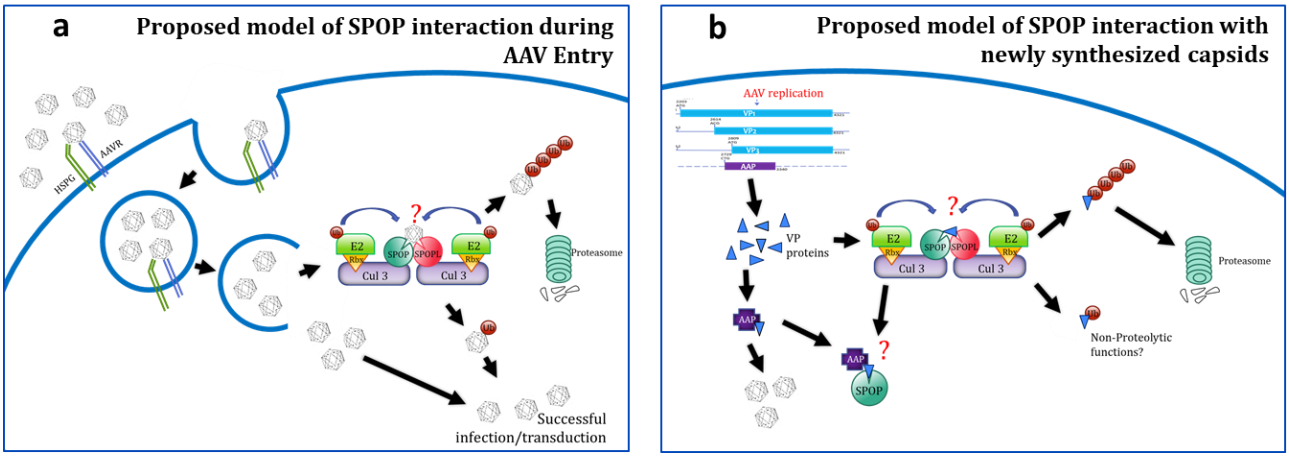

Figure 1.7 Proposed models for the interaction between AAV and SPOP. a. SPOP interacts with incoming capsids either leading to proteasomal targeting or culminates in successful infection. **b.** SPOP interacts with newly synthesized capsid proteins before they are assembled into capsids (via the interaction with AAP) either for proteasomal targeting or for other non-proteolytic functions.

The specific aims include-

1. **To determine the role of ubiquitination/degradation during AAV infection**
    a) Investigate the impact of SPOP, SPOPL, Cul3 and the proteasome on the transduction of AAV.

b) Study the state of capsid proteins during the infection cycle:
   i. Inspect the degradation state of capsid proteins over time (via dot blot).
   ii. Observe the localization of AAV particles via immunofluorescence.
   iii. Determine the effect of the factors on capsid protein degradation.

2. To determine the role of ubiquitination/degradation on *de novo* capsid proteins

a) Determine the effect of SPOP, Cul3 and the proteasome on newly synthesized capsids.
b) Verify the role of AAP and its interplay with SPOP on the stabilization of capsid proteins.

2 Materials

2.1 Biological Materials

2.1.1 Mammalian Cell Culture

HEK 293TT cells
HEK 293TT cells are a human embryonic kidney cells containing two copies of the simian virus T-antigen. The HEK 293TT cells were cultured in supplemented low glucose Dulbecco's modified Eagle's Medium (DMEM) with Hygromycin B (62.5 µM) for selection.

HeLa cells
HeLa cells are human epithelial cervix adenocarcinoma cells containing the HPV 18- genome, cultured in supplemented low glucose DMEM.

HEK 293T SPOP K/O and Parental cells
Wild type Cas9 expressing HEK 293T cells and SPOP Knock out cells (HEK 293T Cas9-Puro SPOP-KO) were kindly obtained from Dr. Luca Busino, University of Pennsylvania, Philadelphia, USA. The HEK 293T Cas9 cells were transfected with a lentivirus CRISPR targeting hSPOP with GFP expression and puromycin resistance. The cells were cultured in supplemented high glucose DMEM.

HeLa SPOP K/O and Parental cells
Wild type HeLa cells and a SPOP Knock out HeLa cell line was obtained from Canopy Biosciences Missouri, USA. The cells were cultured in supplemented high glucose DMEM.

HCT 116 cells
HCT116 are human cells derived from a colon carcinoma with a mutation in codon 13 of Ras. The cells were cultured in supplemented low glucose DMEM.

A549 cells
A549 cells are human epithelial cells derived from a lung carcinoma. The cells were cultured in supplemented low glucose DMEM.

Caski cells
Caski cells are human epithelial cells derived from a metastatic tumor in the small intestine. The cells were cultured in supplemented Roswell Park Memorial Institute (RPMI) medium.

MCF7 cells

MCF7 cells are human epithelial cells derived from adenocarcinoma in the mammary glands. The cells were cultured in supplemented low glucose DMEM.

2.1.2 Bacterial strains

Strain	Genotype
E. coli MegaX DH10 (Invitrogen)	*F-mcrA Δ(mrr-hsdRMS-mcrBC) Φ80lacZΔM15 ΔlacX74 recA1 endA1 araD139Δ(ara,leu)7697 galU galK λ-rpsL nupG*
E. coli XL-Blue supercompetent cells (Agilent Technologies)	*recA1 endA1 gyrA96 thi-1 hsdR17 supE44 relA1 lac [F´ proAB lacIq ZΔM15 Tn10 (Tetr)]*
E. coli SoloPack (Agilent Technologies)	*Tetr Δ (mcrA)183 Δ(mcrCB-hsdSMR-mrr)173 endA1 supE44 thi-1 recA1 gyrA96 relA1 lac Hte [F′ proAB lacIq ZΔM15 Tn10 (Tetr) Amy Camr]*

2.1.2.1 Bacterial culture

LB agar plates

98.5% LB medium

1.5% bacto-agar

Autoclaved, supplemented with appropriate antibiotics

LB medium

10 g Tryptone

5 g yeast extract

5 g NaCl

Adjust final volume to 1 l with Millipore H_2O, pH 7.5, autoclaved

SOC Media (Invitrogen, California, USA)

Antibiotics

Ampicillin final concentration: 100 µg/mL

Kanamycin final concentration: 25 µg/mL

Spectinomycin final concentration: 100 µg/ml

Chloramphenicol final concentration: 20 µg/ml

2.1.3 Viruses

Viruses were produced by transfection of HEK293T(T) cells with the respective plasmids

Virus	Plasmids
AAV2-firefly luciferase	#2772 + #1814 + #1995
AAV2 Wildtype	#3668 + #1814 + #3541
AAV2 Wildtype (stop in AAP)	#3622 + #1814 + #2958
AAV2 Wildtype (stop in AAP + AAP in trans)	#3622 + #1814 + #3651
AAV2 Wildtype (no AAP ORF)	#3623 + #1814 + #2958
AAV2 Wildtype (no AAP ORF + AAP in trans)	#3623 + #1814 + #3651

2.2 Molecular Biology Materials

2.2.1 Plasmids

Plasmid Number	Plasmid description	Reference
1814	pDGΔVP, AAV2/Ad-helper plasmid without cap-gene	A. Sacher
1995	Firefly luciferase reporter construct	M. Müller
2772	pDP2-> AAV2 wt cap without ITRs, with helper functions	M. Müller
2951	SPOP cDNA (closed) in pENTR221 (Gateway compatible)	GPCF, DKFZ
2958	N-Myc, Gateway compatible vector (DEST)	GPCF, DKFZ
2976	N-Myc-SPOP (#2951 in MycDEST #2958/Gateway)	F. Burkart
3104	pKEX-VP1	J. Kleinschmidt
3172	pKEX VP1 N-terminus (until start of VP3); CMV Promotor	F. Burkart
3263	pKEX VP3; CMV Promotor	J. Kleinschmidt
3440	pKEX VP1 N-terminus (until start of VP2); CMV Promotor	This thesis
3441	pKEX VP2 and VP3; CMV Promotor	This thesis
3510	AAP from AAV2 WT	J. Kleinschmidt
3520	Dominant negative SPOP mutant: Amino acid mutation on position 133 from F->V) on (#2976 N-Myc-SPOP)	This Thesis
3521	AAV2 (#2772) with mutation on AAP start codon	This Thesis

3522	pKEX-VP1 (#3104) with mutation on AAP start codon	This Thesis
3531	AAP in pENTR221 (Gateway compatible)	GPCF, DKFZ
3532	VP2 in pENTR221 (Gateway compatible)	GPCF, DKFZ
3541	VP2 in N-eGFP Destination Vector (3512+3532, Gateway)	Q. Chen
3542	VP2 in N-HA Destination Vector (3513+3532, Gateway)	Q. Chen
3543	VP2 in N-RFP Destination Vector (3514+3532, Gateway)	Q. Chen
3623	pTAVORF1cm- AAV2 WT w/o 2nd ORF	J. Kleinschmidt
3622	pTAVORF2stopB- AAV2 w/ STOP in AAP	J. Kleinschmidt
3668	pTAV 2.0- AAV-2 genome WT	J. Kleinschmidt
3669	pDEST24 C-GST	GPCF, DKFZ
3670	SPOP-L (open construct)	GPCF, DKFZ
3708	His-Padre-Trx-SPOPL	This thesis
3716	psPAX2 (2nd generation lentivirus packaging plasmid)	C. Odenwald
3717	pMD2.G (2nd generation lentivirus packaging plasmid)	C. Odenwald
3731	SPOPL-GST I	This thesis
3651	AAP entry clone in pDEST N-Myc vector	This thesis
3854	SPOPL in C-Myc construct	This thesis
3855	SPOPL in pDEST without a tag	This thesis
3888	eGFP-VP2 only (Stop codon added to 3542 to silence VP3)	Q. Chen
3889	eGFP-VP2 only (Stop codon added to 3542 to silence VP3)	Q. Chen
3891	VP2 until VP3 (Gateway clone of #3887+#2960)	Q. Chen
4013	SPOP-pWpI- Lentiviral construct with Blasticidin resistance	This Thesis

2.2.2 Oligonucleotides

2.2.2.1 Site-Directed Mutagenesis (QuikChange)

Primer to stop generate VP-1 unique N-terminus
Fwd.: 5’ – TTGAGGAACCTGTTAAGTAGGCTCCG– 3’
Rev.: 5’ – TTCCCGGAGCCTACTTAACAGGTTCC– 3’

Primer to silence the VP1 start codon
Fwd.: 5’ – GATCCCAAATCAGGTGCGGCTGC– 3’
Rev.: 5’ – AACCATCGGCAGCCGCACCTGATTTG– 3’

Primer to introduce a Stop codon to AAP
Fwd.: 5’ – TACAGGCAGTGGCGCACTAATGGCAGAC– 3’
Rev.: 5’ – GTCTGCCATTAGTGCGCCACTGCCTGTA– 3’

2.2.2.2 qPCR primers

SPOP:
Fwd.: 5’ – GAGAATTCCCGGTTCACAGA– 3’
Rev.: 5’ – GCACTAAAAACCGGAGAACG– 3’

SPOPL:
Fwd.: 5’ – ATTAATAGGTGCAGTGTACTTCG– 3’
Rev.: 5’ – TGCTTGGTTGCTGTTCCAGTT– 3’

Sae2 primers:
Fwd.: 5’ – AAAAAGGGTGTGACCGAGTG– 3’
Rev.: 5’ – GCATCTTCTTCCCCAAACAA– 3’

Cul3 primers:
Fwd.: 5’ – TCCAGGGCTTATTGGATCTG– 3’
Rev.: 5’ – CAGGAGACCTGGAGTTGAGG– 3’

2.2.2.3 siRNA sequences (Eurofins, Ebersberg, Germany)

siSPOP1
TCAGTTTATCATTTGCTCC

siSPOP2
GGCTCACAAGGCTATCTTATT

siSPOP3
GGAGGAAAUGGGUGAAGUCAU

siCUL3
AACAACTTTCTTCAAACGCTA

siSPOPL
CAGTTTGGCATTCCACGCAAA

2.2.2.4 CRISPR crRNAs

SPOP crRNA1
ATTGCTTCAGGCGTTTGCGT

SPOP crRNA2
AGAGTCAACGGGCATAT

SPOP crRNA5
GTTACTGGTCAGCTGTCCAA

2.3 Media and Supplements

2.3.1 General mammalian cell culture

Media
Dulbecco's modified Eagle's Medium-low and high glucose (Sigma Aldrich, Deisenhofen, Germany)
RPMI medium- growth medium developed at Roswell Park Memorial Institute (Sigma Aldrich, Deisenhofen, Germany)

supplemented with 10% fetal calf serum, 1% penicillin/streptomycin, 1% L-Glutamine

Cell culture antibiotics
Hygromycin B- final concentration of 62.5 µM
Blasticidin-final concentration of 5µg/mL in HeLa and 20µg/mL in HEK 293T cells

Cryomedium
60% DMEM, non-supplemented
30% FCS
10% DMSO

Supplements
FCS (PAN Biotech, Aidenbach and Gibco, Pawasleyy, UK)
penicillin/streptomycin (GIBCO, Eggenstein, Germany)
L-glutamine (Sigma-Aldrich, Deisenhofen, Germany)

Disassociation media
0.05% and 0.25% Trypsin-EDTA (Gibco, Eggenstein, Germany)

Transfection reagent
HiPerFect® transfection reagent (Qiagen, Hilden, Germany)

2.3.2 Fusion – Hybridoma Generation

HAT-Media
45ml inactivated FCS
3ml pen/strep
1ml 1M Hepes pH 7.2 + 0,2% β-mercaptoethanol
0.5ml 50x HFCS (Roche, Mannheim, Germany)
9ml HAT media supplement (50x) HybriMax™ (Sigma, St. Louis, USA)
Adjust to final volume of 300ml with non-supplemented RPMI

Feeder-Medium
45 ml inactivated FCS
3ml pen/strep
1ml of HFCS
splenocytes of entire spleen of a mouse
Adjust to final volume of 300 ml with non-supplemented RPMI

PEG
Poly (ethylene glycol) solution 50%(w/v) (Sigma, Taufkirchen, Germany)

2.3.3 Molecular Biology reagents

2.3.3.1 **Quantitative PCR**

SsoAdvanced© Universal SYBR® Green Supermix (Bio-Rad Laboratories, California, USA)

2.3.3.2 Agarose gel-Electrophoresis

1% Agarose gel
1g agarose dissolved in 100 mL TAE running buffer by heating and 7µL ethidium bromide (Roth, Karlsruhe, Germany) was added.

1x TAE running buffer
40 mM Tris
5.71% acetic acid
10% 0.5 M EDTA, pH 8

In Millipore H_2O

Loading buffers and markers
6x loading buffer (ThermoFisher Scientific, Waltham, USA)
1kb DNA ladder plus (NEB, Schwalbach, Germany)
100 bp DNA ladder plus (NEB, Schwalbach, Germany)
Lambd/HindIII DNA ladder (NEB Biolabs, Schwalbach, Germany)

2.3.3.3 Enyzmes

Topoisomerase I (NEB Biolabs, Schwalbach, Germany)
Q5® High-Fidelity DNA Polymerase (NEB Biolabs, Schwalbach, Germany)
T4 Ligase (NEB Biolabs, Schwalbach, Germany)
Clonase™ II enzyme mix (ThermoFisher Scientific, Waltham, USA)
Multiscribe™ Reverse Transcriptase (ThermoFisher Scientific, Waltham, USA)
PfuUltra HF DNA Polymerase (Agilent Technologies, La Jolla, USA)
all restriction enzymes (NEB Biolabs, Schwalbach, Germany)

2.3.4 Materials for virological methods

2.3.4.1 Solutions for vector production

AAV Lysis Buffer
50 mM Tris, pH 8.5
150 mM NaCl
In Millipore H_2O, pH 8.5, autoclave

PBS-MK/NaCl
1 M NaCl in PBS-MK, filter-sterilized

PBS-MK
1 mM $MgCl_2$
2.5 mM KCl
In PBS, filter-sterilized

Iodixanol
60% iodixanol (Sigma-Aldrich, Taufkirchen, Germany)

Opti-MEM (ThermoFisher Scientific, Waltham, USA)

2.3.4.2 Proteasome and Cul3 inhibitors

Pevonedistat (MLN4924)- (Biozol, Eching, Germany)
(S)-MG-132 (Cayman chemicals, Ann Arbor, Michigan, USA)
Bortezomib (Focus Biomolecules, Plymouth, Pennsylvania, USA)

2.3.5 Protein analysis materials

2.3.5.1 Determination of protein concentration

Bradford reagent (BioRad, Munich, Germany)
BSA standard (2 µg/µl) (ThermoFisher Scientific, Waltham, USA)

2.3.5.2 SDS-polyacrylamide gel Electrophoresis

Preparation of SDS-polyacrylamide gels

Tris buffer, pH 8.8
1M Tris
In H_2O, pH 6.8

Tris buffer, pH 6.8
1 M Tris
0.03% bromophenol blue
In H_2O, pH 6.8

acrylamide solution (Roth, Karlsruhe, Germany)
ammonium persulfate (Serva Electrophoresis GmbH, Heidelberg)
TEMED (Sigma-Aldrich, Deisenhofen Germany)

Recipe for five mini SDS-gels

Component	3% Stacking gel	12.5% Running gel
30% acrylamide	1 mL	18.75 mL
1 M Tris buffer	1.3 mL (pH 6.8)	16.88 mL (pH 8.8)
H2O	7.5 mL	8.48 mL
10% SDS	100 µL	450 µL
10% APS	100 µL	450 µL
TEMED	15µL	22.5µL

Sample preparation

3x protein loading buffer
30% glycerol
6% SDS
15% β-mercaptoethanol
0.03% bromophenol blue
187.5 mM Tris
In H_2O, pH 6.8

Electrophoresis

1x TGS buffer (running buffer)
2.5 mM Tris
1.45% glycine
0.1% SDS
In H_2O, pH 8.3

Prestained protein ladder color plus (NEB Biolabs, Schwalbach, Germany)

2.3.5.3 Dot Blot analysis

Stratagene's dot blot chamber (Stratagene, California, USA)
Laboratory pumps (BioRad, Munich, Germany)
Silicone vacuum grease (Beckman Coulter GmbH, Krefeld, Germany)

2.3.5.4 Western Blot analysis

1x NuPAGE® Wet blot transfer (Invitrogen, California, USA)
10mL NuPAGE® wet blot transfer
0.1mL NuPAGE® antioxidant
10mL Methanol
79.9mL Millipore H_2O

1xPBS-T (wash buffer)
0.03% Tween 20
In 1xPBS

Blocking solution
5% milk in PBS-T

2.4 Immunological materials

2.4.1 Antibodies

Type	Description	Reference
A20	Mouse monoclonal antibody raised against VP1 capsid of various AAV serotypes	J. Kleinschmidt
A69	Mouse monoclonal antibody raised against VP1 and VP2 capsid proteins of various AAV serotypes	J. Kleinschmidt
B1	Mouse monoclonal antibody raised against VP1, VP2 and VP3 capsid proteins of various AAV serotypes	J. Kleinschmidt
LN6	Mouse monoclonal antibody raised against GST-SPOP	G. Jaschkowitz
Anti-SPOP polyclonal sera	Guinea pig sera raised against the SPOP protein	This thesis
Anti-SPOPL polyclonal sera	Guinea pig sera raised against the 18aa insert of SPOPL	This thesis
SPOP	Rabbit polyclonal, binds to a synthetic peptide corresponding a region of human SPOP	ProSci
Cul 3	Rabbit polyclonal antibodies produced against a synthetic peptide corresponding to residues surrounding Leu750 of human Cullin-3	Cell Signaling Technologies
Anti-PML	The epitope recognized by PLA0172 maps to a region between residue 375 and 425 of promyelocytic leukaemia using the numbering given in entry NP_150241.2 (GeneID 5371).	Sigma Aldrich
Anti-actin (clone C4)	Mouse monoclonal antibody against residue 18-40 of chicken gizzard skeletal muscle actin	MP Biomedicals
Anti-Histone H3 (di methyl k4) [EPR17707]	Rabbit monoclonal antibody against Human Histone H3 (di methyl K4)	Abcam
GAMPO	HRP-coupled Goat-anti-mouse antibody	Dianova
GARPO	HRP-coupled Goat-anti-Rabbit antibody	Dianova
DAGPO	HRP-coupled Donkey-anti-goat antibody	Santa Cruz
Alexa Flour 488	Alexa Flour 488-coupled Goat-anti-mouse antibody	Life Technologies
Alexa Flour 488	Alexa Flour 488-coupled Goat-anti-rabbit antibody	Life Technologies

Alexa Flour 594	Alexa Flour 594-coupled Goat-anti-mouse antibody	Life Technologies
Alexa Flour 594	Alexa Flour 549-coupled Goat-anti-rabbit antibody	Life Technologies

2.4.2 Immunofluorescence

Fixation
4% PFA in 200 mM HEPES, pH 7.4

Quenching
50 mM ammonium chloride

Permeabilization
0.2% triton-X 100 in PBS

Blocking solution
1% BSA in PBS

DAPI
100 mg/ml in PBS

Mounting medium (Dianova, Hamburg, Germany)

1xPBS
140 mM NaCl
2.7 mM KCl
8.1 mM Na_2HPO_4
1.5 mM KH_2PO4
In Millipore H_2O, pH 7.4, autoclave

Methanol (Sigma-Aldrich, Deisenhofen, Germany)
Ethanol (VWR, Darmstadt, Germany)
Butanol (Applichem, Darmstadt, Germany)
Isopropanol (VWR, Darmstadt, Germany)

2.5 Chemicals

All chemicals were purchased from Sigma-Aldrich (Taufkirchen), AppliChem (Darmstadt), Merck (Darmstadt), Roth (Karlsruhe), Serva (Heidelberg), Fluka (Neu Ulm), Gerbu (Gaiberg), VWR (Darmstadt) and Life Technologies (Karlsruhe).

Kits

Item	**Company**
Gateway® LR Clonase™ II Enzyme mix	Life Technologies, Karlsruhe, Germany
Beetle-Juice	PJK, Kleinbittersdorf, Germany
Chemiluminescence kit	AppliChem, Darmstadt, Germany
Qiagen Maxi Kit	Qiagen, Hilden, Germany
QIAprep Spin Miniprep kit	Qiagen, Hilden, Germany
QIAquick Gel extraction kit	Qiagen, Hilden, Germany
QIAquick PCR Purification Kit	Qiagen, Hilden, Germany
QuikChange® II Site-directed mutagenesis Kit	Agilent Technologies, La Jolla, USA
High capacity cDNA Reverse Transcription kits	ThermoFisher Scientific, Waltham, USA
Rneasy© Mini Kit	Qiagen, Hilden, Germany.
Gateway® LR Clonase™ II Enzyme mix	Life Technologies, Karlsruhe, Germany

2.6 Electrical equipment

Cell culture hoods

Item	**Company**
Bio GARD cell culture hood	The Baker Company, Sanford, USA
Steril GARD III Advance cell culture hood	The Baker Company, Sanford, USA

Centrifuges

Item	**Company**
Refrigerated Sorvall RC6+ centrifuge	ThermoFisher Scientific, Waltham, USA
Refrigerated table-top centrifuge 5417R	Eppendorf, Hamburg, Germany
Table top centrifuge 5415C	Eppendorf, Hamburg, Germany
Ultracentrifuge Sorvall Discovery 90 SE	ThermoFisher Scientific, Waltham, USA
Megafuge 1.0	Heraeus, Hanau, Germany

Centrifuge rotors

Item	**Company**
Fiberlite™ F12-6 x 500 LEX Fixed Angle Rotor	ThermoFisher Scientific, Waltham, USA
Fiberlite™ F13-14 x 50cy Fixed Angle Rotor	ThermoFisher Scientific, Waltham, USA
TFT65 Fixed Angle Rotor	ThermoFisher Scientific, Waltham, USA

Freezer and fridges

Item	**Company**
Liebherr Comfort	Liebherr, Biberach, Germany
Liebherr MedLine	Liebherr, Biberach, Germany
Liebherr Premium	Liebherr, Biberach, Germany
Liebherr ProfiLine	Liebherr, Biberach, Germany
Ultra-low freezer	Heraeus, Hanau, Germany

Incubators

Item	**Company**
Function Line incubator	Heraeus, Hanau, Germany
Sanyo CO_2 incubator	Sanyo/Panasonic Healthcare Company, Wood Dale, USA

Microscopes

Item	**Company**
Leitz Diavert	Diavert Leitz, Wetzlar, Germany
Will Wilovert	Wilovert Hund, Wetzlar, Germany
Zeiss Cell Observer	Zeiss, Jena, Germany
FV3000, Confocal Laser Scanning Microscope	Olympus, Hamburg, Germany

Electrophoresis

Item	**Company**
Polyacrylamide Gel Electrophoresis Chamber	Hoefer, San Francisco, USA
Xcell SureLock™ MiniCell Electrophoresis System	ThermoFisher Scientific, Waltham, USA
Transblot SD chamber	BioRad, Munich, Germany
Agarose Electrophoresis chamber	BioRad, Munich, Germany
Electrophoresis power supply ST PS 305	Gibco BRL, Eggenstein, Germany

Plate reading equipment

Item	**Company**
1420 Multilabel Counter Viktor3	Perkin Elmer, Norwalk, USA
Multiskan Go microplate spectrophotometer	ThermoFisher Scientific, Waltham, USA
PreCision 50-1200 µL-multichannel	Biozym, Hesswasch-Oldendorf, Germany

Shakers, Mixers and water baths

Item	**Company**
Bacterial culture shaker	Informs AG, Bottmingen, Switzerland
Combimage Red/RET magnetic stirrer	IKA, Staufen, Germany
Test-tube-rotator	Snijders Scientific, Tilburg, Netherlands
Thermomixer 5436	Eppendorf, Hamburg, Germany
Thermomixer comfort	Eppendorf, Hamburg, Germany
Duomax 1030 shaker	Heidolph, Schwabach, Germany
Table-top Shaker	GFL, Burgwedel, Germany
Vibramax-VXR	IKA, Staufen, Germany
Vortex Genie 2TM	Bender and Hobein, Wasmaning, Germany
GFC Waterbaths	Grant Instruments, Cambridge, UK
UC water bath	Julabo, Seelbach, Germany

Others

Item	**Company**
Integra pipetboy	Integra Biosciences GmbH, Fernwald, Germany
800 W microwave	Bosch, Gerlingen-Schillerhöhe, Germany
C1000 Touch Thermal Cycler	BioRad, Munich, Germany
CFX96 Touch™ thermocycler	BioRad, Munich, Germany
Electrophoresis power supply ST PS 305	Gibco BRL, Eggenstein, Germany
Gel Doc EZ Imager	BioRad, Munich, Germany
Ice maker	Hoshizaki, Willich-Munchheide, Germany
Impulse Sealer	RNS Corp., Taipei, Taiwan
MicroPulser™ Electroporator	BioRad, Munich, Germany
MilliQ ultra-pure water unit Millipore	Merck, Darmstadt, Germany
Nanodrop spectrophotometer	PegLab, Erlangen, Germany
Nitrogen tank	Chrono Messer, Krefeld, Germany
pH meter	Sartorius, Göttingen, Germany
Sartorius scale	Sartorius AG, Göttingen, Germany
Transblot SD chamber	BioRad, Munich, Germany

Western Blot developing machine	Agfa, Mortsel, Belgium
X-Ray cassette	Kodak, Stuttgart, Germany

Common use utensils

Item	**Company**
1.5 mL and 2.0 mL microcentrifuge tubes	Eppendorf, Hamburg, Germany
10 mm cover slips	ThermoFisher Scientific, Waltham, USA
10 cm culture plates	Greiner, Frickenhausen, Germany
15 mL reaction tubes	TPP, Klettgau, Switzerland
14mL BD falcon round-bottom tube	BD biosciences, 2 Oak Park, Bedford, USA
25, 75 and 150 cm^2 Tissue culture flasks	TPP, Klettgau, Switzerland
50 mL reaction tubes	Greiner, Frickenhausen, Germany
6, 10 and 15 cm cell culture dishes	Sarstedt Inc., Newton, USA
6-, 12-, and 24-well test plates	TPP, Klettgau, Switzerland
96-well LIA plate	Greiner, Frickenhausen, Germany
96-well plate	Costar Corning, USA
Ultracentrifuge tubes	Beckman Coulter GmbH, Krefeld, Germany
Cell lifter	Costar Corning
Chemiluminescence films	GE Healthcare Limited, Buckinghamshire, UK
Cryo tubes, 2 ml	Roth, Karlsruhe, Germany
Electroporation cuvettes 25 x 2 mm	Peqlab, Erlangen, Germany
Glass slides	ThermoFisher Scientific, Waltham, USA
Inoculating loop	Greiner, Frickenhausen, Germany
Nitrocellulose membrane	Schleicher & Schuell, Dassel, Germany
One-time use filter, 0.2/0.4 µm	Renner, Darmstadt, Germany
Parafilm “M”	American National Can, Chicago, USA
Pipette tips	Nerbe plus GmbH, Winsen/Luhe, Germany
Pipettes 1000, 200, 100, 20, 10 and 2 µL	Gilson, Middleton, USA
Syringes and needles	BD Franklin Lakes, USA
Whatman filter paper 3MM paper	Schleicher & Schuell, Dassel, Germany

Software

Software	**Company**
Adobe CS4/CS6	Adobe, San Jose, USA
Clone Manager 9.0 for Windows	Scientific & Educational Software, Cary, USA
Mendeley	Elsevier, Amsterdam, Netherlands

GraphPad Prism 5.0	GraphPad Software, La Jolla, USA
ImageJ 1.40	NIH, Bethesda, USA
Microsoft Office 2003, 2010	Microsoft, Redmont, USA
Microsoft Windows XP, 8.1	Microsoft, Redmont, USA
Wallac 1420 Workstation	Perkin Elmer, Norwalk, USA
ZEN Black	Zeiss, Jena, Germany
Multiskan Go 3.2	ThermoFisher Scientific, Waltham, USA
CFX Manager™ Software	Bio-Rad Laboratories, California, USA

3 Methods

3.1 Cell culture methods

3.1.1 Cell culture maintenance

Cells were grown in 175cm^2 flasks and split when they reached 75-90% confluency. To do so, the media was aspirated off the cells and they were washed with 1xPBS and then treated with 0.05-0.25% trypsin-EDTA for 5 minutes at 37°C to detach the cells. The trypsin was neutralized with supplemented media and the cells were split according to the needs of future experiments. The appropriate amount of media was then added to the flask and the cells were grown at 37°C, 5% CO_2 and 90% humidity. For the experiments, the cells were harvested and counted using a Neubauer chamber and diluted according to the appropriate need.

3.1.2 Cryopreservation

Cells from a confluent 175cm^2 flask were frozen as follows. The media was aspirated off the cells and they were washed with 1xPBS and then treated with 3mL trypsin for 5 minutes at 37°C. 7mL of supplemented media was added to the cells and they were collected in a 15mL tube. The cells were pelleted at 1500rpm for 10minutes, supernatant was aspirated, and the cells were re-suspended in 1mL cryomedium and transferred to a labeled cryovial. The vial was placed in an isopropanol tank overnight at -80°C and the cells were thereafter transferred to liquid nitrogen for long term storage.

3.1.3 siRNA transfections

8x10^4 cells were seeded on 24-well plates a day prior to the experiment to allow for stable growth. The next day the cells were treated with a transfection mix made of 40nM siRNA, 3µL Hiperfect and 100µL un-supplemented DMEM per well that was incubated for 7 minutes then added to the cells in a drop-wise fashion before incubation for 48 hours at 37°C 5% CO_2 and 90% humidity. After the knockdown the cells were either harvested for western blot, qPCR or were transduced with virus.

3.1.4 Transfection with PEI

The appropriate number of cells was seeded on a plate/dish and transfected as follows:

Table 3.1- Overview of cells amounts and transfection mixes for different plate formats

Tissue culture plate	Number of cells	Volume of H_2O (µL)	Amount of DNA (µg)	Volume of un-supplemented DMEM (mL)	Volume of PEI (µL)	Volume of supplemented DMEM (mL)
24-well plate	7 x 10^4	2.5	0.375	0.07	1.25	0.2
12-well plate	1 x 10^5	5	0.75	0.13	2.5	0.4
6-well plate	2.5 x 10^5	10	1.5	0.25	5	0.75
10 cm dish	3.5 x 10^6	61.5	10	1.6	31	4.6
15 cm dish	7 x 10^6	185	27	4.6	92.5	13.8

According to the plate format chosen for the experiment the appropriate volumes of water, DNA, un-supplemented DMEM and PEI were mixed thoroughly and incubated for 10 minutes before adding the supplemented DMEM. Media was aspirated from the cells and the transfection mix was added to the cells for 4 hours before it was replaced by 5% supplemented DMEM and incubated at 37°C 5% CO_2 and 90% humidity for 6-72 hours.

3.1.5 CRISPR-Cas9 transfection

All materials were obtained, and procedures followed according to manufacturer's protocols (GE Healthcare). Briefly, 1x10^5 HEK 293TT cells that were stably transduced with a Cas9 lentivirus (by Dr. Caroline Odenwald) were seeded on a 24-well plate a day prior to allow for stable growth overnight. The next day a transfection mixture made of 1.25µL 10µM tracrRNA and 1.25µL 10µM crRNA (designed to target the gene of interest) in 47.5µL un-supplemented media; and 1µL of dharmaFECT 1 reagent in 49µL un-supplemented media, were incubated separately for 5 minutes before being mixed together by gently pipetting up and down; and incubated for 20 minutes at room temperature. The transfection mix was then diluted in 400µL antibiotic-free supplemented media, added to the cells and then incubated for 48-72 hours at 37°C 5% CO_2 and 90% humidity. All wells (except A1) of a 96-well plate were filled with 100µL of supplemented media. After the transfection, the cells were counted, with the help of a 37Neubauer chamber, 200µL 2x10^4 cells were placed in the well A1 and 100µL was transferred down the wells of the first column from A-H with gentle pipetting up and down. The same procedure was repeated from column 1-12 with a multichannel pipette ensuring a 1:2 dilution across the plate. 100µL of supplemented media was then added to all wells and they are incubated at 37°C 5% CO_2 for 7-10 days. Single colonies were isolated, grown out and tested for a successful knock out using western blot methods.

3.1.6 Hybridoma production

HAT Media and 1.5mL PEG were pre-heated in a water bath. SP2/0 cells were harvested and centrifuged at 2000rpm for 5 minutes then washed twice in un-supplemented RPMI. The cells were counted with the help of a 38Neubauer chamber and $3x10^8$ cells were resuspended in 30mL RPMI. The spleens of immunized and naïve mice were removed and added to a 10mL tube on ice. It was thereafter homogenized on a sterile net using the stump of a 5mL syringe, the spleenocytes were transferred back to the tube, centrifuged at 2000rpm for 5 minutes and washed two times with un-supplemented RPMI. This resulted in the fusion and feeder cells respectively. The fusion cells were mixed with the SP2/0 cells and centrifuged once more at 2000rpm for 5 minutes and the feeder cells were added to the pre-warmed HAT-media. The Fusion cell-SP2/0 cell mix was submerged a beaker was filled with warm water and the pellet was gently stirred with a sealed glass pipette. 1.5mL of PEG was added under continuous stirring for 90 seconds then 1mL of un-supplemented RPMI in 1 minute, 3mL in 1 minute and 16mL in 2 minutes. The cell mixture was centrifuged at 2500rpm for 10 minutes and then incubated at room temperature for 5 minutes. The supernatant was carefully removed, and the pellet was mixed with HAT-medium before 150µL was spread onto 96-well plates using a multichannel pipette, then the plates were incubated for 7-10 days at 37°C 5% CO_2 and 90% humidity. Single colonies were isolated, grown out and tested for a successful monoclonal antibody against the protein of interest.

3.2 Virological methods

3.2.1 AAV2 Virus production

AAV2-reporter vectors were produced from a set of five 15cm dishes seeded with cells. The cells were transfected as described above (PEI transfection) with: 3.22µg pDGΔVP (#1814), 27.74µg Cap construct and 24µg Reporter construct (often firefly luciferase) for 48-72 hours. The cells were dislodged using a cell scraper and transferred to two 50mL tubes and spun down at 1500rpm for 10-15 minutes. The suspensions were discarded, and the pellets washed once with 1xPBS and transferred into a single tube. After a second centrifugation round, the pellet was resuspended in AAV lysis buffer and cells were subjected to 5 freeze-thaw cycles before Benzonase was added at 50U/mL lysate and incubated at 37°C for 30 minutes. The lysate was thereafter centrifuged at 5000rpm for 10 minutes then added to base of the Iodixanol gradient, followed by 1.5mL of 15% Iodixanol in PBS-MK+1M NaCl, then 1.5mL 25% Iodixanol in PBS-MK+3µL Phenol red, then 1.5mL 40% Iodixanol in PBS-MK and finally 3.8mL of 60% Iodixanol + 5µL phenol red. The gradients are carefully balanced to 0.00g, sealed then placed in an ultracentrifuge at 50,000rpm at 10°C for two hours. After the run, the virus was harvested in the 40% Iodixanol phase, aliquoted and stored at -20°C. An aliquot was also sent for qPCR for the titer determination.

3.2.2 AAV2 quantification

The AAV genome titer was quantified using quantitative real time PCR. The procedure was conducted by the group of Barbara Leuchs (DKFZ, Heidelberg).

3.2.3 AAV2 transduction assays

The appropriate number of cells were seeded on a plate/dish and were infected with MOI=10^3 for transduction experiments, MOI= 10^4 for characterization by western blot and MOI= 10^5 for immunofluorescence experiments. The AAV2-firefly luciferase vectors were transduced either alone or in the concert with proteasome inhibitors for 4 hours then substituted with supplemented media and incubated at 37°C, 5% CO_2 and 90% humidity for 6-72 hours. Thereafter the cells were either harvested for immunofluorescence, western blot or luciferase assays. For the detection of the transduction of luciferase the media was aspirated from the cells and incubated with 100µL 1x lysis buffer (PJK) for 15 minutes. Thereafter the lysate was transferred to white bottom 96-well plates in triplicate and incubated with beetle juice for 1 minute before readout.

3.2.4 Lentivirus production

Low passage HEK 293TT cells were cultures in a 75cm flask until fully confluent then trypsinized and a third of the cells were seeded onto three 10cm dishes and allowed to grow for 48 hours. On the day of transfection, in the first tube- 4ug pMD2.G (#3716), 4ug pSPAX (#3717) and 8ug SPOP-pWpI- Lentiviral construct (#4013) were diluted in Opti-MEM, up to a total volume of 250µL. In a second tube- 48µL PEI was diluted in 202µL of Opti-MEM and both tubes were combined and incubated for 20 minutes at room temperature. The media on the cells was replaced with DMEM 10%FCS w/o antibiotics and the transfection mix was added dropwise to the dish, while shaking and the dishes were incubated at 37°C, 5% CO_2 and 90% humidity. The following day, the media was changed and on the second and third day after transfection the media on the cells (containing released lentivirus) was collected and pulled. The media was filtered and centrifuged at 19,400rpm for 2 hours at 20°C. The supernatant was thereafter discarded and 150µL Opti-MEM was added to the tube, sealed with parafilm and incubated overnight at 4°C. The next day 20µL aliquots were prepared and stored at -80°C for long term storage.

3.2.5 Lentivirus infection

In order to infect cells with the SPOP lentivirus, 3x10^6 SPOP Knock out cells were plated on a 10cm dish a day prior to allow for stable growth. The next day, the cell medium was replaced with fresh supplemented DMEM containing 4µg/ml of Polybrene. The plate was swirled gently and 20µL lentivirus was added in a dropwise fashion. The cells were incubated at 37°C, 5% CO_2 and 90% humidity overnight. The following day the media was changed, the cells were observed for the next two days and underwent blasticidin selection on the third day after infection (at a final concentration of 5µg/mL in HeLa and 20µg/mL in HEK 293T cells). The cells were further observed for cell death and the media containing the antibiotic was

changed two days later. The cells surviving thereafter were considered stably- lentivirus infected and tested for the recovery of SPOP, via western blot. After this was confirmed the cells were expanded further and cryopreserved for future use.

3.3 Molecular Biology methods

3.3.1 DNA purification

All DNA was obtained from 250mL or 2mL of bacterial cultures harboring the plasmid of interest that were purified using the Qiagen Maxiprep and miniprep kits respectively according to manufacturing instructions.

3.3.2 Determination of the DNA concentration

The concentration of purified DNA was determined using a Nanodrop against a blank of the buffer that the DNA was dissolved in. This was determined by comparing the absorption at 260 nm (DNA) and 280 nm (protein). When the ratio (Abs 260 nm/ Abs 280 nm) was between 1.8 and 2.0 it was considered pure. A ratio of < 1.8 represented a contamination with other organic compounds or proteins, while a ratio of > 2.0 indicated an RNA contamination.

3.3.3 Gateway cloning

The cDNA of genes of interest contained in Gateway-compatible entry-vectors in were obtained from the GPCF, DKFZ and were transferred to the appropriate destination vector using the LR reaction according to the manufacturer's instructions. Briefly, the LR reaction mix was made as follows:

Table 3.2- Gateway cloning reaction mix

Component	**Volume (µL)**
Entry clone 50-150ng)	1-7
Destination vector 150ng/µL)	1
TE Buffer	Up to 8µL
LR Clonase™ II enzyme mix	2

The reaction was incubated at 25°C for 1 hour then stopped by the addition of 1µL proteinase K, mixed and incubated at 37°C for 10 minutes. Bacteria was transformed by mixing 1µL of the LR reaction then electroporation, followed by the addition of 500µL LB and shaking at 225-250rpm for 1 hour at 37°C before being spread on an agar plate with the appropriate antibiotics and incubated overnight at 37°C. Colonies that grew on the plate were picked, grown, DNA was isolated and digested with restriction enzymes to confirm that the insertion was successful. Glycerol stocks of the verified constructs were made and stored at -80°C.

3.3.4 Polymerase chain reaction (PCR)

PCR was used to amplify genes of interest for different cloning procedures. The reaction mix was composed of the following:

Table 3.3 – Q5 PCR reaction mix

Component	**Volume (µL)**
Q5 reaction buffer	5
dNTPs	2
Forward primer	1.25
Reverse primer	1.25
DNA	1ng
Q5® High-Fidelity DNA Polymerase	0.25
GC enhancer	5
ddH_2O	9.25

The reactions ran under the following program:

Table 3.4- Parameters set for the PCR program

Number of cycles	**Temperature (°C)**	**Time (sec)**	**Step**
1 x	98	30	Denaturation
30x	98	10	Denaturation
	58	30	Annealing
	72	30	Extension
1x	72	120	Final extension

The PCR product was purified using the QIAquick PCR Purification Kit according to manufacturer's instructions and thereafter either visualized on a 1% agarose gel or used in other cloning procedures.

3.3.5 DNA Ligation

In order to ligate an insert into a vector a ratio of 1:3 was set up as follows and incubated overnight at 16°C.

Table 3.5- DNA ligation reaction mix

Component	**Volume (µL)**
10x T4 DNA Ligase Buffer	2
Vector DNA	0.02pmol
Insert DNA	0.06pmol
T4 DNA Ligase 400,000U/mL)	1

ddH_2O	up to 20µL

3.3.6 RNA purification

All mRNA was obtained from cultured cells grown in a 12-24 well format and purified using the Rneasy Mini Kit according to manufacturing instructions and the concentration was determined using a Nanodrop.

3.3.7 Reverse Transcription

In order to perform quantitative PCR, cDNA was generated from extracted RNA. All materials were obtained, and procedures followed according to manufacturer's protocols (ThermoFisher Scientific, Waltham, USA). Briefly, the basic master mix for one reaction as follows:

Table 3.6- Reverse transcription reaction mix

Component	Volume (µL)
10x RT buffer	2
25x dNTP mix 100mM)	0.8
Random primers	2
Multiscribe™ Reverse Transcriptase	1
ddH_2O	4.2

10µL of 2X RT master mix was added to 10µL RNA in a PCR tube and mixed by gently pipetting up and down. After a brief centrifugation the samples are placed in a thermocycler and run under the following program:

Table 3.7- Parameters set for the PCR program

Temperature (°C)	Time (min)
25	10
35	120
85	5
4	∞

3.3.8 Quantitative PCR (qPCR)

In order to quantify the amount of (reverse transcribed) mRNA transcripts are in a sample the following qPCR mix was prepared on ice:

Table 3.8- qPCR reaction mix

Component	Volume (µL)
SsoAdvanced© Universal SYBR® Green Supermix	5
Forward primer	350nM
Reverse primer	350nM
cDNA	3
Nuclease free ddH_2O	Up to 10 µL

The samples were mixed thoroughly and pipetted into a 96-well PCR plate in duplicates, sealed and run in the CFX96 Touch™ thermocycler under the following program:

Table 3.9- Parameters set for the qPCR program

Process stage	**Temperature (°C)**	**Acquisition Mode**	**Hold (mm:ss)**	**Ramp Rate (°C/s)**	**Acquisitions per (°C)**
Pre-incubation	95	None	05:00	4.4	
Amplification	95	None	00:20	4.4	
	60	None	00:15	2.2	
	72	None	00:15	4.4	
Melting Curve	95	None	00:05	4.4	
	70	None	01:00	2.2	
	72	Continuous	-	-	2
Cooling	40	None	00:30	1.5	

The data obtained was analyzed with the CFX Manager™ Software.

3.3.9 CPO I cloning

4µL 100pMol of each oligonucleotide was mixed with 32µL annealing buffer (10mM Tris-Cl, 150mM NaCl pH7.6) and was run in a thermocycler under the following program:

Table 3.10- Parameters set for the PCR program

Temperature (°C)	**Time (min)**
95	5
72	20
37	20

The ligation reaction was set up as follows: 1µL of the vector cleaved with CPOI and dephosphorylated was mixed with 1µL of the annealed primers, together with 2µL of 10x T4 DNA ligase buffer, 1µL T4 DNA ligase(400,000 cohesive end units/ml) and 15µL water. The mixture was incubated at room temperature for 40 minutes, 1µL was used to transform electrocompetent bacteria before being spread on an agar plate with the appropriate antibiotics and incubated overnight at 37°C. Colonies that grew on the plate were picked, grown, DNA was isolated and digested with restriction enzymes to confirm that the insertion was successful. Glycerol stocks of the verified constructs were made and stored at -80°C.

3.3.10 QuikChange II Site-Directed Mutagenesis

The QuikChange II Site-Directed Mutagenesis kit (Agilent technologies) was used to mutate single nucleotides or amino acids according to manufacturer's instructions. Briefly, the reaction mix was made as follows:

Table 3.11- QuikChange II reaction mix

Component	**Volume (µL)**
10x reaction buffer	5
Forward primer	125ng
Reverse primer	125ng
dNTP mix	1
Nuclease free ddH_2O	Up to 50 µL
PfuUltra HF DNA Polymerase (2.5U/µL)	1

The samples were subjected to the following PCR program:

Table 3.12- Parameters set for the PCR program

Number of cycles	**Temperature (°C)**	**Time (sec)**	**Step**
1 x	98	30	Denaturation
12-18x*	98	30	Denaturation
	55	60	Annealing
	68	7-10 min.	Extension
1x	72	120	Final extension

**12 cycles for point mutations, 16 for single amino acid changes and 18 for multiple amino acid changes.*

1µL of *Dpn* I restriction enzyme (10 U/µl) was added to the reaction to digest the parental dsDNA, mixed gently but thoroughly and then spun down and incubated at 37°C for 1 hour. 1µL of the reaction was used to transform XL-1 Blue supercompetent cells via heat shock before being spread on an agar plate with the appropriate antibiotics and incubated overnight at 37°C. Colonies that grew on the plate were picked, grown, DNA was isolated and

confirmed via sequencing. Glycerol stocks of the verified constructs were made and stored at -80°C.

3.3.11 Restriction digests

To check whether a sequence was cloned correctly, restriction digests were performed. A test digest consisted of 1x respective buffer, ~1µg DNA, water bringing the total volume up to 20µL and the restriction enzyme(s). The reactions were then incubated at 37°C for 1 hour before analysis on an agarose gel.

3.3.12 Agarose gel electrophoresis

1% Agarose gels were used to analyze DNA. This consisted of 1g agarose in 100mL TAE buffer with 7µL Ethidium bromide. After the gel polymerized it was placed in the running chamber filled with TAE buffer, 6x DNA loading buffer was mixed with the samples and loaded alongside a DNA marker (of the appropriate size range). Gels were run at 100V for 30 minutes and visualized at 254nm for analysis. In order to purify DNA from bands excised from the gels, the QIAquick Gel extraction kit was used according to manufacturer's instructions

3.3.13 Transformation of E.coli bacteria

3.3.13.1 Transformation of E.coli bacteria via electroporation

Mega X (MXDH10) is an electrocompetent strain of E. coli. To transform this bacterium, a vial of frozen cells was thawed on ice and transferred to an electroporation cuvette. 1µL of the construct of interest was mixed with the bacteria and the cuvette was placed in the electroporator and pulsed at 2.5 kV for 5ms. 0.5mL LB Medium was added to the cells and they were shaken at 225-250rpm for 1 hour at 37°C before being spread on an agar plate with the appropriate antibiotics and incubated overnight at 37°C. Colonies that grew on the plate were picked, grown, DNA isolated and confirmed via sequencing. Glycerol stocks of the verified constructs were made and stored at -80°C.

3.3.13.2 Transformation of E.coli bacteria via heat shock

XL-1 Blue supercompetent cells were transformed via heat shock. To do so 1µL of the construct of interest was mixed with the cells which were gently swirled and incubated on ice for 30 minutes before being subjected to 45 second heat shock pulse at 42°C, then placed on ice again for a further 2 minutes. 0.5mL SOC Medium was added to the cells and they were shaken at 225-250rpm for 1 hour at 37°C before being spread on an agar plate with the appropriate antibiotics and incubated overnight at 37°C. Colonies that grew on the plate were picked, grown, DNA isolated and confirmed via sequencing. Glycerol stocks of the verified constructs were made and stored at -80°C.

3.3.14 Verification of DNA via sequencing

To determine that the correct DNA sequence was successfully cloned, an aliquot was sent to Eurofins, Ebersberg, Germany. Whereby the appropriate sequencing primer was selected. The results were analyzed using Clone Manager.

3.3.15 Preparation of glycerol stocks

In order to prepare glycerol stocks for the long-term storage of constructs, 1mL of an overnight culture of the construct of interest was mixed in a cryovial with 300µL of pre-warmed sterile glycerol and stored at -80°C.

3.4 Protein analysis methods

3.4.1 Immunofluorescence

Cells for immunofluorescence were seeded on coverslips in a 12-well plate format. They underwent either transfection or infection and were incubated at 37°C 5% CO_2. The media on the cells was aspirated and they were washed with 1xPBS for 10 minutes. The cells were then fixed with 2% PFA for 15 minutes and incubated two times for 10 minutes with 50mM Ammonium Chloride to quench artifacts of the dyes, then the cells were incubated with 0.2% Triton-X for permeabilization. The cover slips were thereafter washed three times with 1xPBS and incubated with 1%BSA for 1 hour at 37°C for blocking. The cells were incubated with the appropriate primary antibody diluted in blocking buffer for 1 hour at 37°C or overnight at 4°C. Then washed three times with 1xPBS and incubated with the corresponding Alexa-conjugated antibody (also diluted in blocking buffer) for 1 hour at 37°C. After three more washes the coverslips are transferred onto microscopy slides using mounting medium and are sealed with nail polish. The slides were thereafter viewed under the Zeiss Cell Observer or Olympus confocal microscope.

3.4.2 Protein concentration determination

The concentration of the proteins was determined by the comparison to a BSA standard as follows: 2µg/ml of BSA was titrated in a 2-fold manner in the first 10 wells of a 96-well plate in duplicate followed by a blank. The protein of interest was diluted 3 times in a two-fold manner and the Bradford reagent was diluted 1:5 and was added to the plate. The concentration of the protein was then measured on the Multiskan Go microplate spectrophotometer and protein amounts were adjusted accordingly.

3.4.3 Dot Blot

For the analysis of native proteins, a Dot blot was performed. Either a nitrocellulose or PVDF membrane (pre-soaked in methanol for activation) were briefly soaked in transfer buffer before being placed on top of 3 filter papers on the bottom module of the dot blot apparatus. The 96 well top portion of the apparatus was fixed on top of the bottom half, sealed with parafilm and connected to a vacuum pump. The pump was switched on and after a few minutes 5-10µL of the protein sample was loaded into the wells. After the loading was completed, the pump was run for a bit longer to ensure that the sample was pulled through efficiently, then the apparatus was disassembled, and the blot was placed in 5% blocking milk. After 30 minutes-1 hour the blot was diluted in the appropriate concentration of primary antibody diluted in blocking buffer and incubated overnight at 4°C with shaking. The

next day the blot was washed with 1xPBS-T (0.03% Tween), three times and then incubated with the appropriate HRP-conjugated secondary antibody for 1 hour at room temperature with shaking. After three more washing rounds, the blot was incubated with chemiluminescent detection reagent and developed using the developing machine.

3.4.4 SDS-PAGE

SDS-PAGE was performed to separate proteins according to their molecular weights. The cells were harvested in lysis buffer, mixed with 3x SDS loading buffer and were boiled at 95°C for 5 minutes. 10-15µL of the samples were added to the SDS-gel set up in the chamber and filled with 1x TGS buffer. The stacking gel was run at 80 V for 30min and the resolving gel at 100- 120 V.

3.4.5 Western Blot

If the samples were needed for western blot analyses the SDS gel was transferred by wet blot transfer. Blotting pads were soaked in wet blot transfer buffer and placed in the X Cell II™ Blot Module. Blotting papers were soaked in the same fashion and placed on the pads, the gel was carefully removed from the chamber and placed up-side-down onto the papers and smoothened over to remove bubbles. A PVDF membrane, pre-soaked in methanol for activation was placed in the transfer buffer, then placed on top of the gel, followed by more blotting papers and pads. The chamber was placed into the running chamber and filled on the inside with wet blot transfer buffer and on the outside with distilled water. The chamber was run at 30V for 1 hour and the resulting membrane was placed in 5% blocking milk. After 30 minutes-1 hour the blot was diluted in the appropriate concentration of primary antibody and incubated overnight at 4°C with shaking. The next day the blot was washed with 1xPBS-T, three times and then incubated with the appropriate HRP-conjugated secondary antibody for 1 hour at room temperature with shaking. After three more washing rounds, the blot was incubated with chemiluminescent detection reagent and developed using the developing machine.

4 Results

4.1 The intracellular localization of SPOP and SPOPL

A yeast-2-hybrid screen and TAP-tag experiment previously performed in the lab identified the Speckle-type POZ protein (SPOP) as an interaction partner of AAV capsid protein VP1. In order to visualize the cellular localization of SPOP, monoclonal antibodies were produced for use in an indirect immunofluorescence assay (Figure 4.1a). Across different cells lines, endogenous SPOP was expressed in its characteristic speckled pattern in the cell nucleus. The Speckle-type POZ protein-like (SPOPL), the paralog of SPOP which bares the same protein sequence save for an extra 18 amino acids, also exhibits a speckled pattern but in stark contrast to SPOP, SPOPL is localized in endosomes (Figure 4.1b).

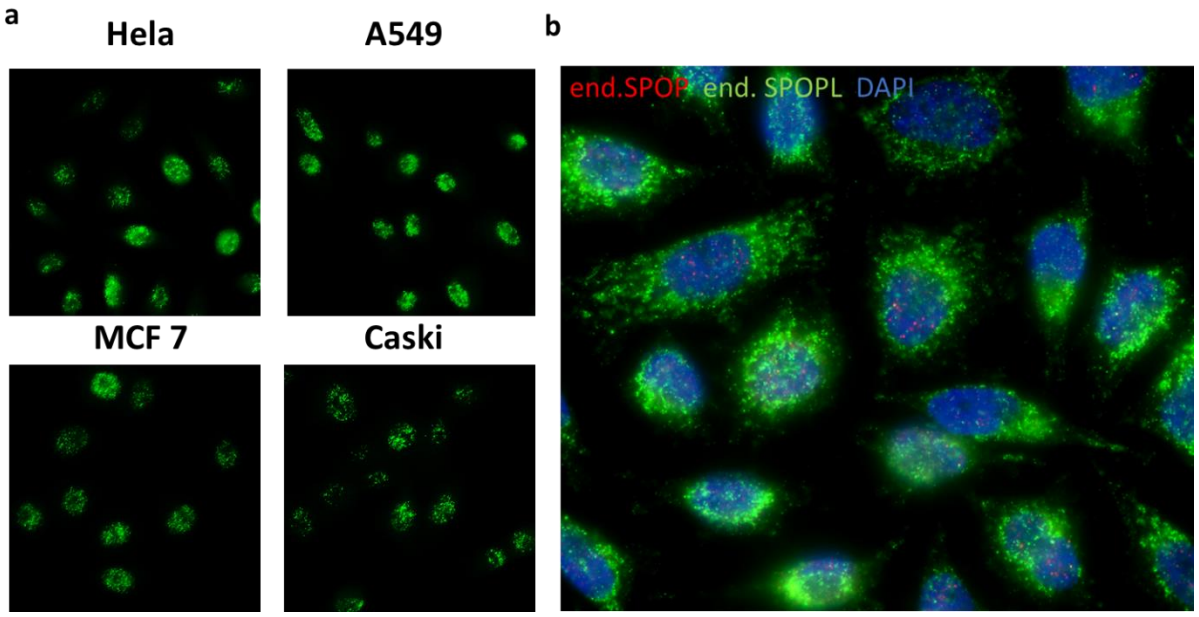

Figure 4.1 SPOP localizes in the nucleus while SPOPL localizes in endosomes. a. Endogenous SPOP was visualized in different cell lines. SPOP is expressed in nuclear speckles. **b.** The localization of SPOP and SPOPL in HeLa cells was visualized. SPOP is present in nuclear speckles (stained in red), while SPOPL is localized in endosomes (stained in green). SPOP was visualized with LN6 (anti-SPOP mouse monoclonal antibody), SPOPL with polyclonal guinea pig serum raised against SPOPL, DAPI (blue) was used to stain the nucleus.

The co-staining of SPOP and SPOPL shows the contrasting localization. SPOPL (stained in green) is expressed outside the nucleus (in endosomes) while SPOP (stained in red) can be seen in distinct dots inside the nucleus. It appears that SPOPL is expressed in a much higher

level in comparison to SPOP, provided that the antibodies detect both proteins with similar sensitivity. This may be due to regulatory role that SPOPL is thought to play on SPOP.

4.2 SPOP co-localizes with different AAV2 capsid proteins

As mentioned above, previous experiments identified the interaction of SPOP with AAV2 capsid protein VP1. In order to visualize this, SPOP was co-stained alongside the AAV2 capsid proteins (Figure 4.2).

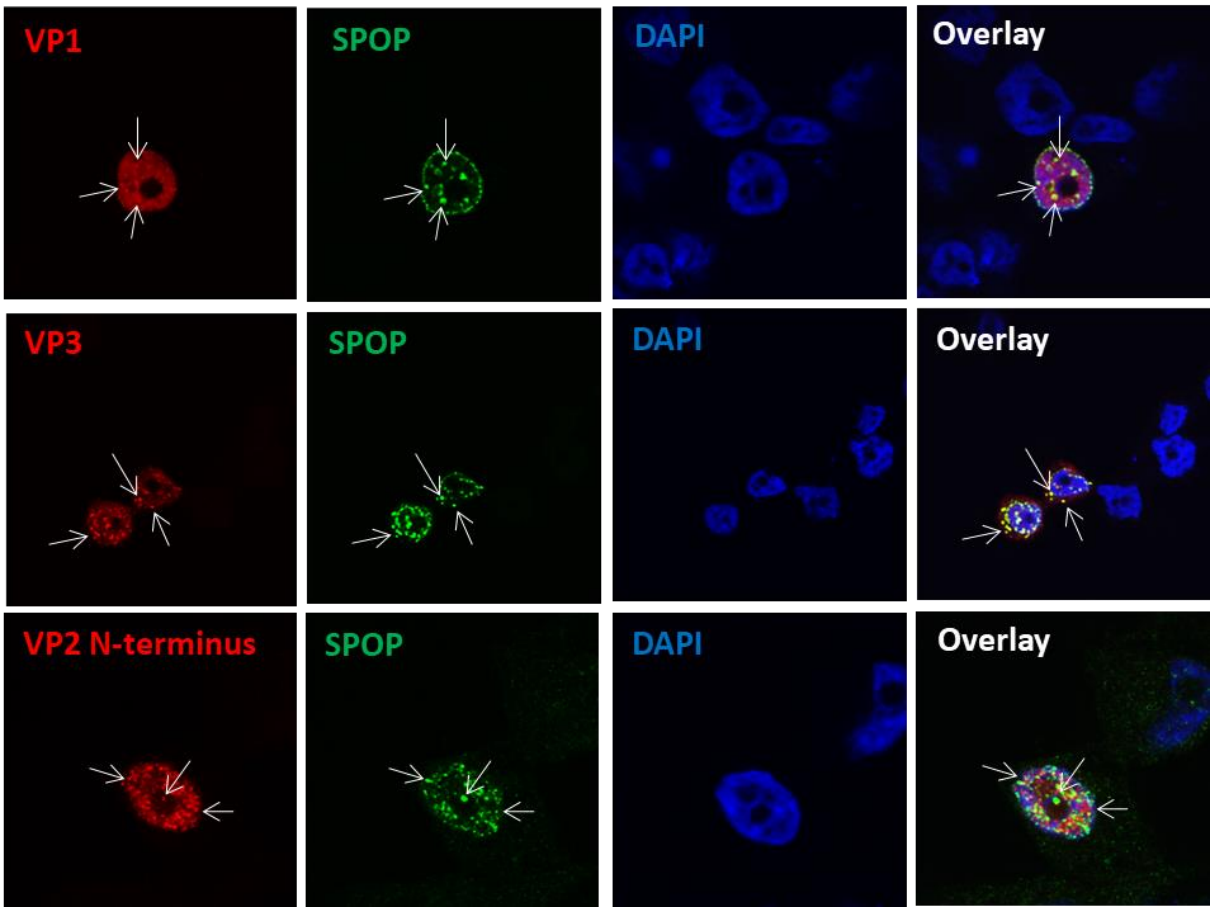

Figure 4.2 SPOP co-localizes with different capsid proteins. SPOP was visualized alongside the overexpressed AAV2 capsid proteins. Top panel shows a construct expressing VP1 only (VP2 and 3 start codons are silenced). Middle panel shows a construct expressing VP3 only and the lower panel shows a construct expressing the VP2 N-terminus (the region between VP2 and VP3). Endogenous SPOP was visualized with LN6 (anti-SPOP antibody), VPs were visualized with B1 (top and middle panel) and A69 (lower panel), DAPI was used to stain the nucleus. Arrows indicate areas of signal overlap.

VP1 (upper panel) is expressed ubiquitously throughout the nucleus, however some distinct dots can be seen. These appear to overlap with the nuclear speckles in which SPOP is

expressed. The VP3 (middle panel) and VP2 N-terminus (lower panel) proteins appear to be expressed in a more punctuated pattern in the nucleus. As with VP1, the proteins appear to overlap with SPOP speckles, seen by the yellow signal in the overlay (indicated by the arrows). Even though co-localization is not direct proof of interaction, it gives an indication that there could be several SPOP-binding motifs along the sequences of the AAV2 capsid proteins.

4.3 Investigating the effect of SPOP on AAV2 transduction

4.3.1 The effects of SPOP knockdown with various siRNAs was inconclusive

In order to characterize the interaction between SPOP and AAV, at first the influence on transduction was investigated. This was done by a protein knockdown using different siRNAs targeting SPOP mRNA in two different cell lines, followed by the transduction of AAV2-firefly luciferase (Figure 4.3).

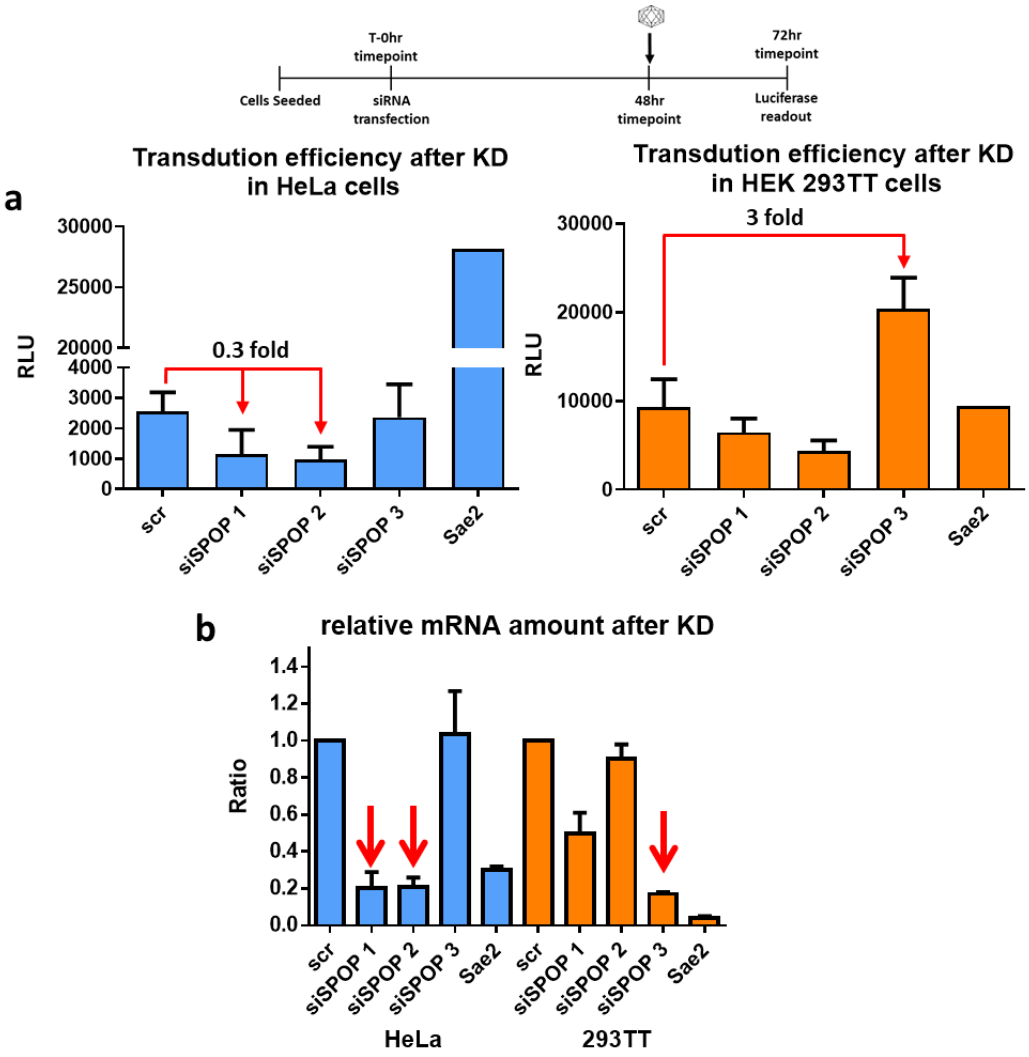

Figure 4.3 The effects of SPOP knockdown with various siRNAs was inconclusive. HeLa and HEK 293TT Cells were transfected with siRNAs against SPOP mRNA (siSPOP1,2,3) or SUMO 1 enzyme mRNA (Sae2) as a control, then transduced with AAV2-firefly luciferase vectors at a MOI= 10^3 (see scheme). **a.** Transduction efficiency when compared to the negative control (scr). **b.** qPCR analysis of the amount of mRNA after knockdown. Note, data displayed represents the mean and standard deviation of 3 independent experiments.

The amounts of mRNA after the knockdown were quantified using qPCR (Figure 4.3b). Different effects were seen between the siRNAs in the various cell lines. According to the qPCR, the only conditions where a down regulation of SPOP could be confirmed was by siSPOP1 and siSPOP2 treatment in HeLa cells and siSPOP3 in HEK 293TT cells. However, this downregulation culminated in opposing effects. The knockdown by siSPOP1 and siSPOP2 in HeLa resulted in a 0.3 fold change in transduction, while siSPOP3 caused a 3 fold increase. Sae 2 served as a positive control, as its knockdown resulted in a significant increase in transduction in HeLa cells and could be verified via qPCR.

4.3.2 A knockout of SPOP resulted in a 2 fold increase in AAV2 transduction efficiency

Given the diverging effects seen with the siRNAs, we investigated the consequence of the total exclusion of SPOP to the system using CRISPR-Cas9 technology (Figure 4.4).

I attempted to produce CRISPR-Cas9 knockouts in the lab, with varying levels of success (Figure 4.4a). In one clone SPOP was completely knocked out (cl 1a) while the other had reduced expression in comparison to the control (cl 1b). The resultant effect was a 2-fold increase in AAV2 transduction. However, this effect levelled out over time.

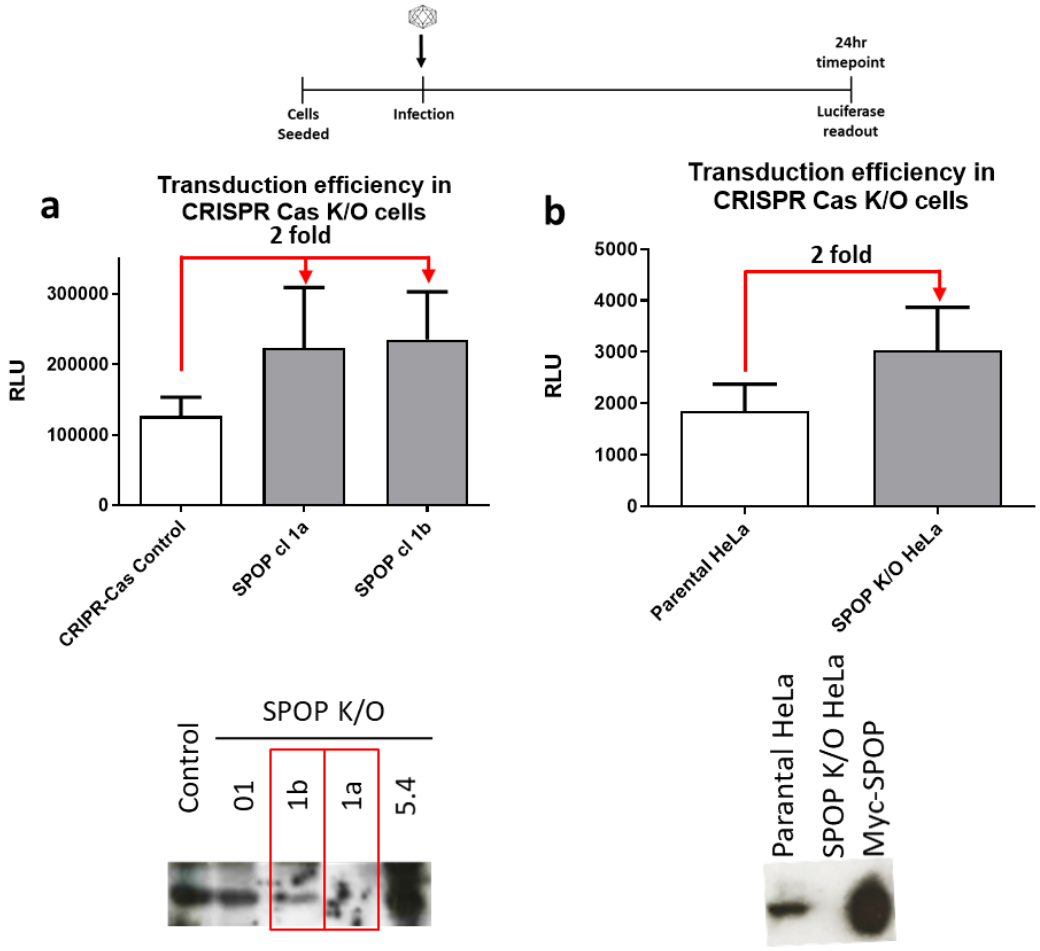

Figure 4.4 SPOP has a 2 fold effect on AAV2 transduction efficiency, as confirmed in a knockout model. CRISPR-Cas9 knockout cells were transduced with AAV2-firefly luciferase vectors and compared to control cells (see scheme). Western blot analysis revealed the status SPOP in the clones, using guinea sera raised against SPOP. **a.** Self-made HEK 293TT Cells with clones that have down-regulated protein (SPOP K/O cl. 1b) or complete knockout (SPOP K/O cl. 1a) were transduced with MOI= 10^3. **b.** Commercially obtained SPOP knockout HeLa were transduced with MOI= 10^4. Note, data displayed represents the mean and standard deviation of 3 independent experiments.

To confirm the above observation, commercially produced SPOP knockout HeLa cells were obtained and tested. These cells were less permissive to AAV2, but the 2-fold effect was verified, likewise, this also levelled out over time.

4.4 Investigating the effect of SPOPL, Cullin 3 and the proteasome on AAV2 transduction

SPOP acts as substrate recognition subunit (SRS), on a Cullin 3 scaffold. The E3-ubiquitin ligase complex is involved in the ubiquitination and targeting of proteins primarily to the proteasome for degradation. To do so, SPOP forms active homodimers. Nonetheless, the pattern of ubiquitination can also alter the consequence for the cargo, e.g. by mediating the targeting to different compartments, SPOPL forms less-active heterodimers that are believed to regulate SPOP in this manner. For this reason, the role that the other complex factors play on the transduction of AAV2 was also investigated.

4.4.1 SPOPL and Cullin 3 do not affect AAV2 transduction efficiency

Along with SPOP, Cullin 3 was also identified via the TAP-tag experiments as an interacting protein of AAV capsid protein VP1. Thus, the effect on transduction efficiency after a downregulation of the protein was investigated (Figure 4.5).

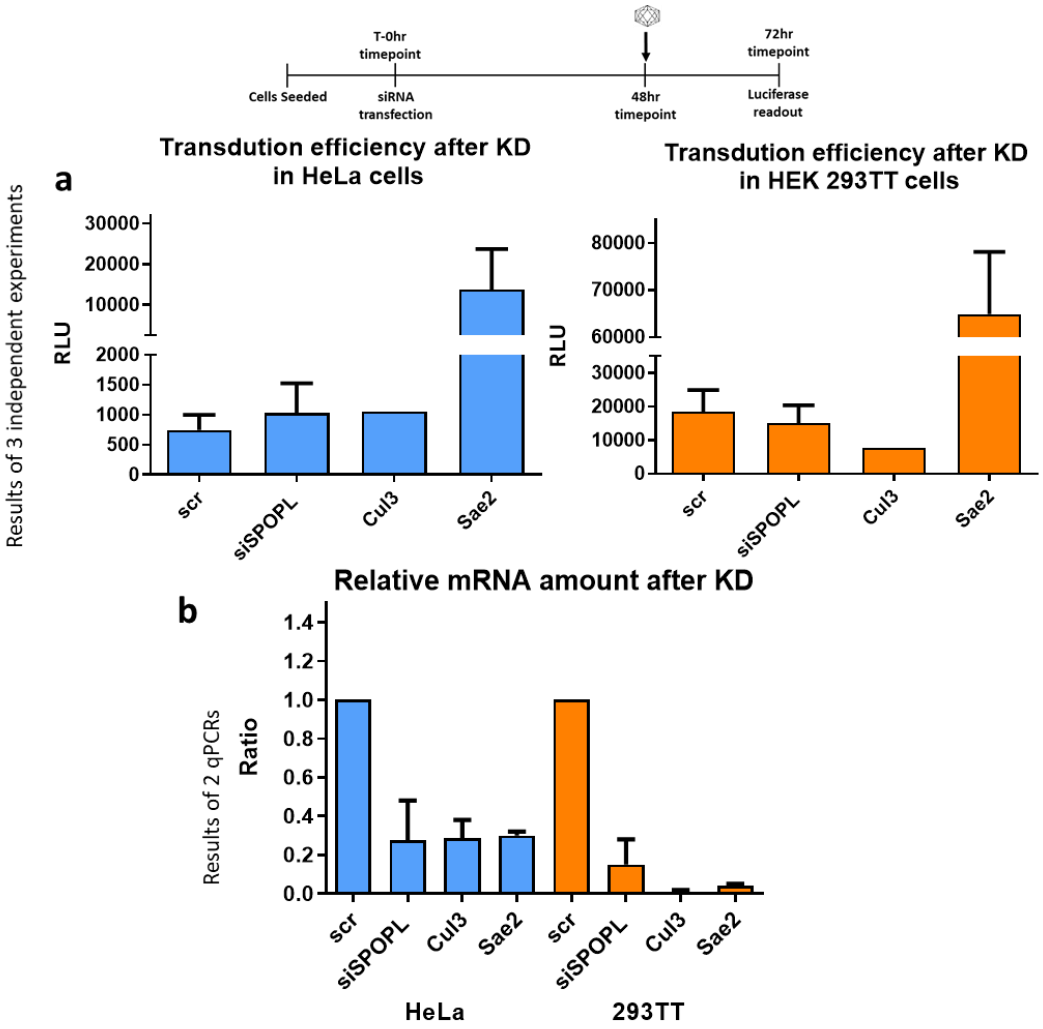

Figure 4.5 SPOPL and Cullin 3 have minor effects on AAV2 transduction. HeLa and HEK 293TT cells were transfected with siRNAs against SPOPL (siSPOPL), Cullin 3 (Cul3) or SUMO 1 enzyme (Sae2) mRNA as a control, then transduced with AAV2-firefly luciferase vectors at a MOI= 10^3 (see scheme). **a.** Transduction efficiency when compared to the negative control (scr). **b.** qPCR analysis of the amount of mRNA after knockdown. Note, data displayed represents the mean and standard deviation of 3 independent experiments.

The downregulation of SPOPL and Cullin 3 did not have a significant effect on AAV2 transduction in both the cells lines (Figure 4.5a). Especially in comparison to knockdown of the SUMOylation enzyme Sae2 which resulted in an up to a 3-11-fold increase in transduction in HEK 293TT and HeLa cells respectively. Moreover, the knockdown of all proteins could be confirmed by a significant reduction of mRNA copies.

4.4.2 Proteasome inhibition increases AAV2 transduction, even in SPOP-deficient cells

If the ubiquitination of AAV leads to the degradation, then the inhibition of the proteasome should result in increased transduction. This has been previously shown in literature and was confirmed in our system (Figure 4.6)[179].

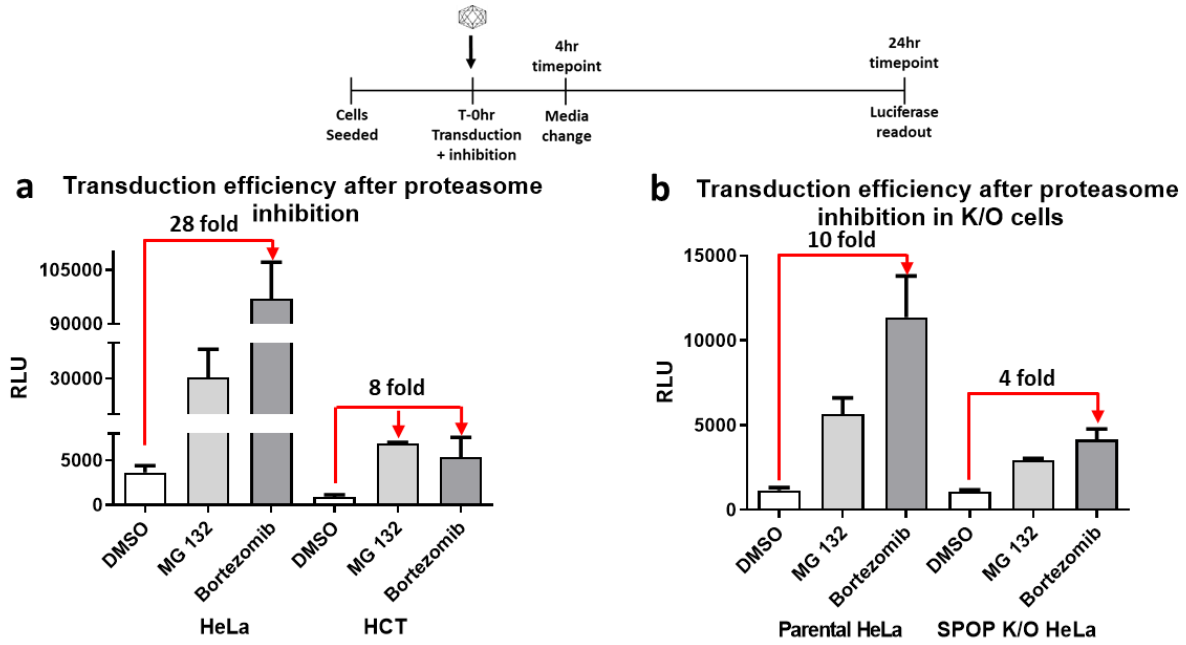

Figure 4.6 Proteasome inhibition increases AAV2 transduction even after SPOP knockout. Cells were treated with proteasome inhibitors (MG-132 and bortezomib) or DMSO as a control and transduced with AAV2-firefly luciferase vectors at MOI= 10^3 for 4 hours (see scheme). **a.** Transduction efficiency in HeLa and HCT cells. **b.** Transduction efficiency in commercially obtained SPOP knockout HeLa and parental HeLa controls. Note, data displayed represents the mean and standard deviation of 3 independent experiments.

The cells exhibited different transduction efficacies, for example HeLa cells were more permissive to AAV transduction, and proteasome inhibition had a more pronounced effect in comparison to HCT cells. Nonetheless, an 8-fold increase in transduction upon proteasome inhibition was observed in these cells (Figure 4.6a). Even between batches of HeLa cells there appeared to be differences, the commercially obtained parental HeLa cells only showed a 10-fold increase upon bortezomib treatment compared to the 28-fold increase in HeLa cells from the lab. Surprisingly, there was still an increase in transduction in the absence of SPOP, albeit less than that in the parental cells. This points to the involvement of other E3-ubiquitin ligases in the restriction of AAV via the proteasome.

4.4.3 Proteasome and Cul3 complex inhibition increases transduction of AAV2 specifically, even in SPOP-deficient cells

Next, the question beckoned if the restriction was AAV-specific or if this could be seen also for other viruses. Therefore, the effect of AAV2 vector transduction was compared to that of HPV16 vectors upon inhibition of the proteasome, or of the cullin-3 complex, or both (Figure

4.7).

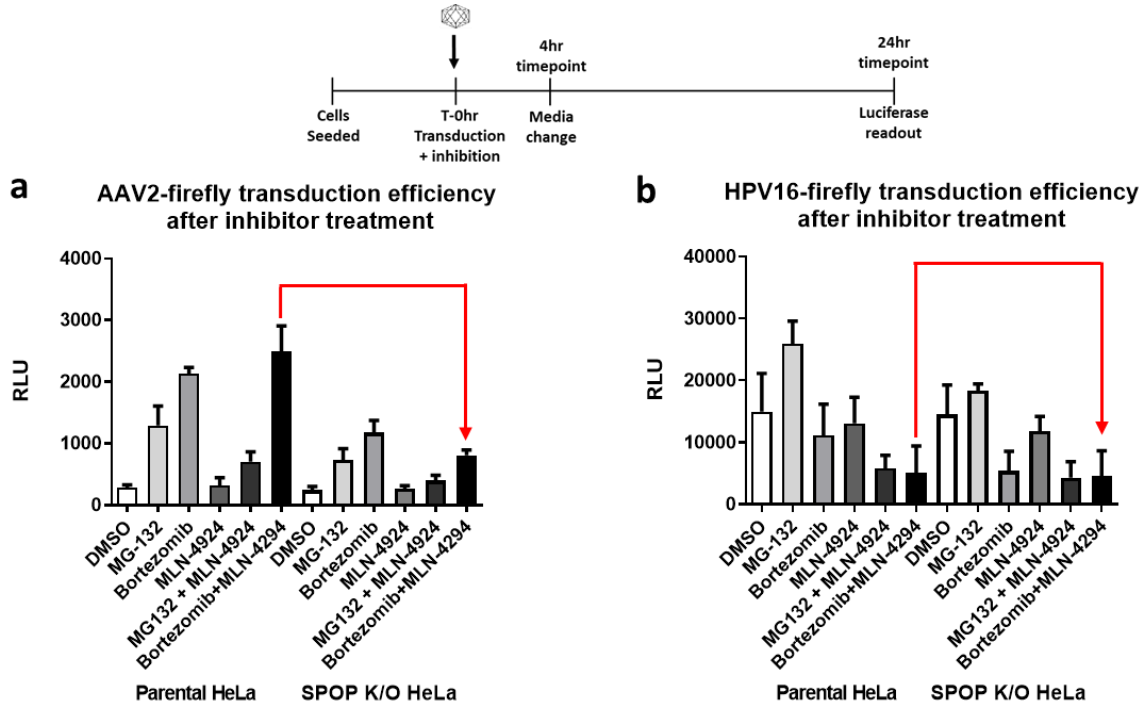

Figure 4.7 Proteasome and Cul3 complex inhibition increases transduction of AAV2 specifically even after SPOP knockout. Parental HeLa cells and SPOP knockout HeLa cells were treated with proteasome inhibitors (MG-132 and bortezomib) or cullin 3 complex inhibitor (MLN-4924) either with DMSO as a control or in concert; and transduced with viruses encoding firefly luciferase for 4 hours (see scheme). **a.** Transduction efficiency of AAV2-firefly luciferase vectors at a MOI= 10^3. **b.** Transduction efficiency of HPV-16 firefly luciferase vectors at 1:1000. Note, data displayed represents the mean and standard deviation of 3 independent experiments. Red lines indicate the AAV-specific effect when comparing proteasome + CRL3 inhibition in both cell lines.

As seen before, inhibition of the proteasome resulted in an increase in transduction. On the other hand, the inhibition of the cullin-3 complex did not influence transduction, which is consistent with the cullin-3 knockdown experiments (see Figure 4.5). The increment upon proteasome inhibition was also seen in the SPOP knockout cells, but 3 times less than in the parental cells (see red bars, Figure 4.7a). The effect was confirmed to be AAV-specific (see red bars, Figure 4.7b).

4.5 Investigating the effect of SPOP on stability of incoming capsids

Given the mild effect that SPOP has on AAV2 transduction, we sought to investigate whether the interaction of SPOP and AAV might have a consequence on the stability of the capsids. To do this, cells were transduced with AAV2 firefly luciferase vectors and were collected over

time to see if there were differences in the presence or absence of SPOP. At first the intact capsids were probed over time via dot blot analyses (Figure 4.8).

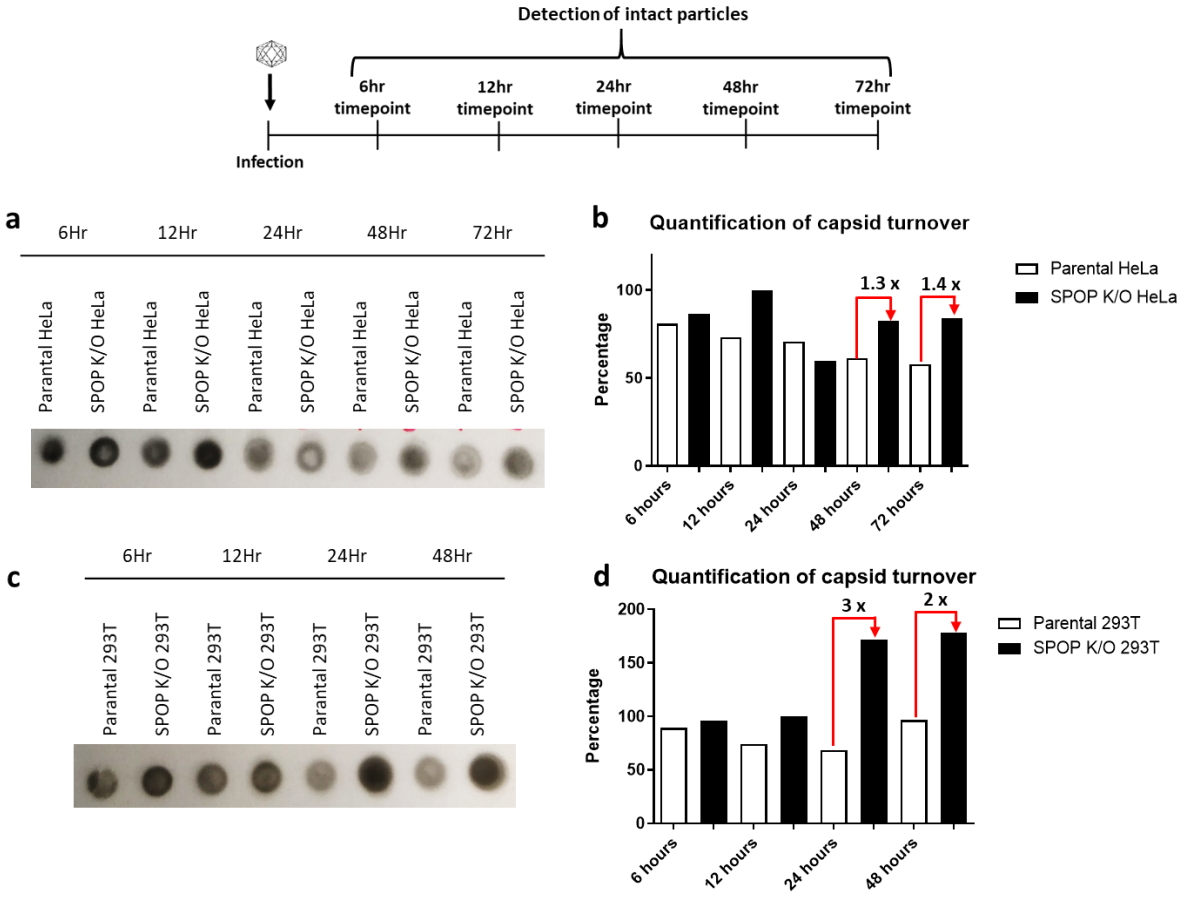

Figure 4.8 The AAV2 particles are stabilized in the absence of SPOP. Parental cells and SPOP knockout cells were transduced with AAV2-firefly luciferase vectors at a MOI= 10^4. The cell lysates were harvested at different timepoints, spotted on a dot blot and capsids were visualized with anti-capsid antibody A20. (see scheme). **a.** Capsid turnover in HeLa cells. **b.** The quantification of capsids in HeLa cells set relative to capsids at 12hours in SPOP K/O cells. **c.** Capsid turnover in HEK 293T cells. **d.** The quantification of capsids in HEK 293T cells set relative to capsids at 12hours in SPOP K/O cells.

The number of capsids of the incoming virus should reduce overtime given that the virus completes its infection cycle, this steady decrease is seen in the parental cells (see parental HeLa, Figure 4.8 a, b). However, the absence of SPOP appeared to stabilize capsids in both cell lines. The effect was more pronounced in HEK 293T cells with 2 times more capsids at 48 hours (Figure 4.8 c, d). The lower capsid amount quantified at 24 hours in the SPOP knockout cells is due to a blotting artefact.

Next we investigated if the stability seen on a protein level could also be visualized via indirect immunofluorescence. Consequently, cells were infected as above and stained for capsids at different timepoints (Figure 4.9).

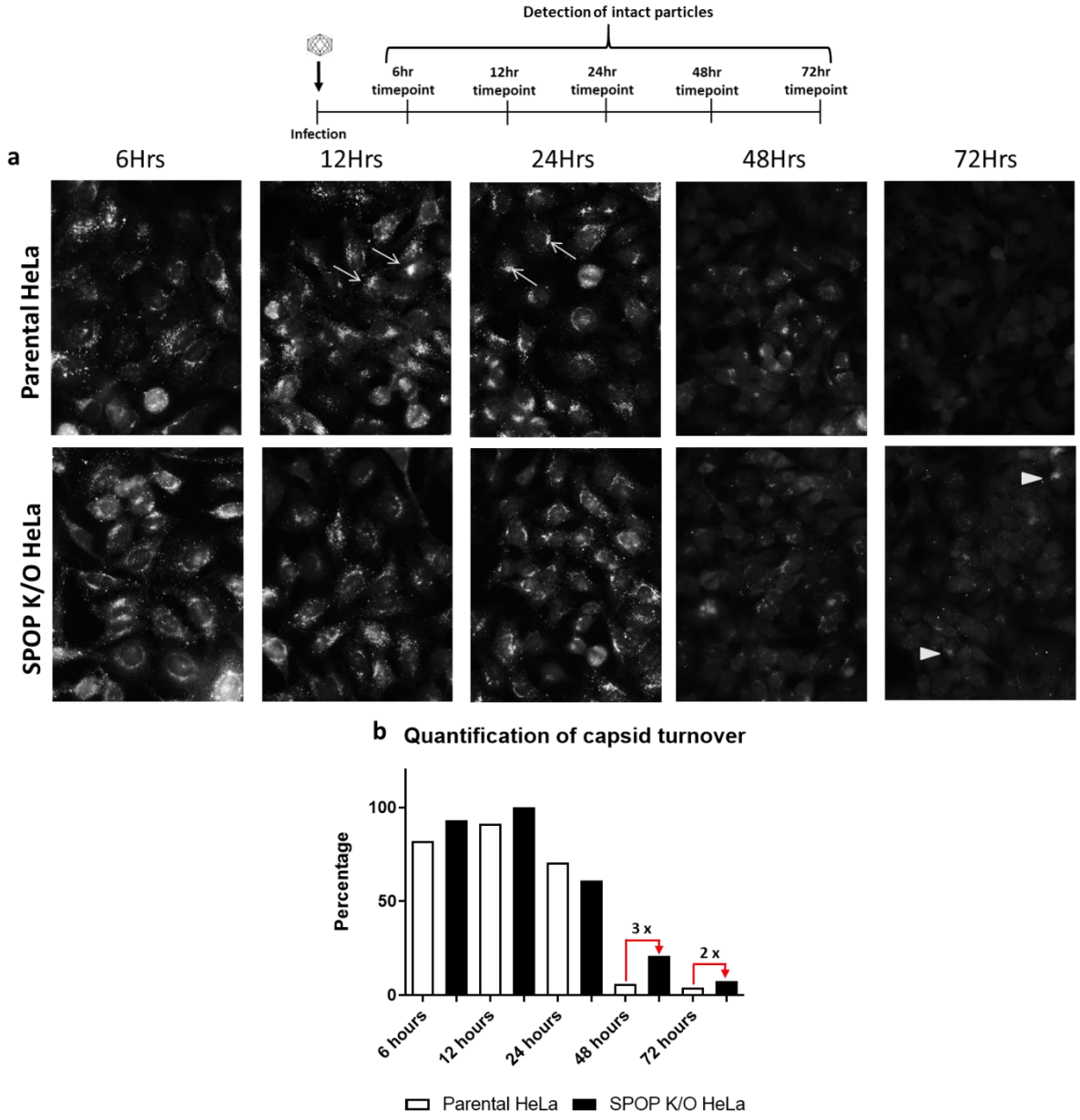

Figure 4.9 The AAV2 particles persist for longer in the absence of SPOP. Parental and SPOP knockout HeLa cells were transduced with AAV2-firefly luciferase vectors at a MOI= 10^5. The cells were fixed and stained for capsids using the anti-capsid antibody A20 (see scheme). **a.** Capsids in the parental (upper panel) and SPOP knockout HeLa cells (lower panel) are visualized. **b.** The capsids from 6 different fields of view, were quantified and set

relative to capsids at 12 hours in SPOP K/O HeLa cells. Arrows indicate a point accumulation of capsids; arrowheads indicate capsids that are still visible after 48 hours.

From 12 hours on in the parental cells the capsids are seen to accumulate close to the nucleus (arrows, Figure 4.9a). However, this accumulation could not be seen in the SPOP knockout cells. Moreover, the number of capsids reduced over time in the parental cells but appeared to be stabilized in the absence of SPOP and could be seen at 72 hours (arrowheads, Figure 4.9a). A quantification of capsids from different sections of the microscopy slides revealed that there were 3 times as many capsid-specific signals in the SPOP knockout cells at 48 hours and 2 times as many after 72 hours. Hence, the interaction with SPOP appeared to reduce the stability of incoming capsids.

4.6 Investigating the effect of SPOP on stability of newly synthesized capsid proteins

Given the interaction with SPOP affected the stability of incoming capsids, we wanted to investigate whether the interaction also influenced newly synthesized capsids proteins and intact capsids. The assembly activating protein (AAP) plays a crucial role in most AAV serotypes. It is thought to act as a scaffold for the assembly of capsids[23]. Therefore, we explored the role of SPOP on newly synthesized capsid proteins before assembly (by expressing AAV2 WT constructs that lack AAP), after assembly (by supplying AAP in *trans*) and with the addition of SPOP.

4.6.1 SPOP regulates stability of newly assembled capsids

As mentioned above AAV2 capsids only assemble in the presence of AAP. Therefore, AAP was supplied in *trans* and the assembly capabilities in the presence and absence of SPOP were evaluated (Figure 4.10).

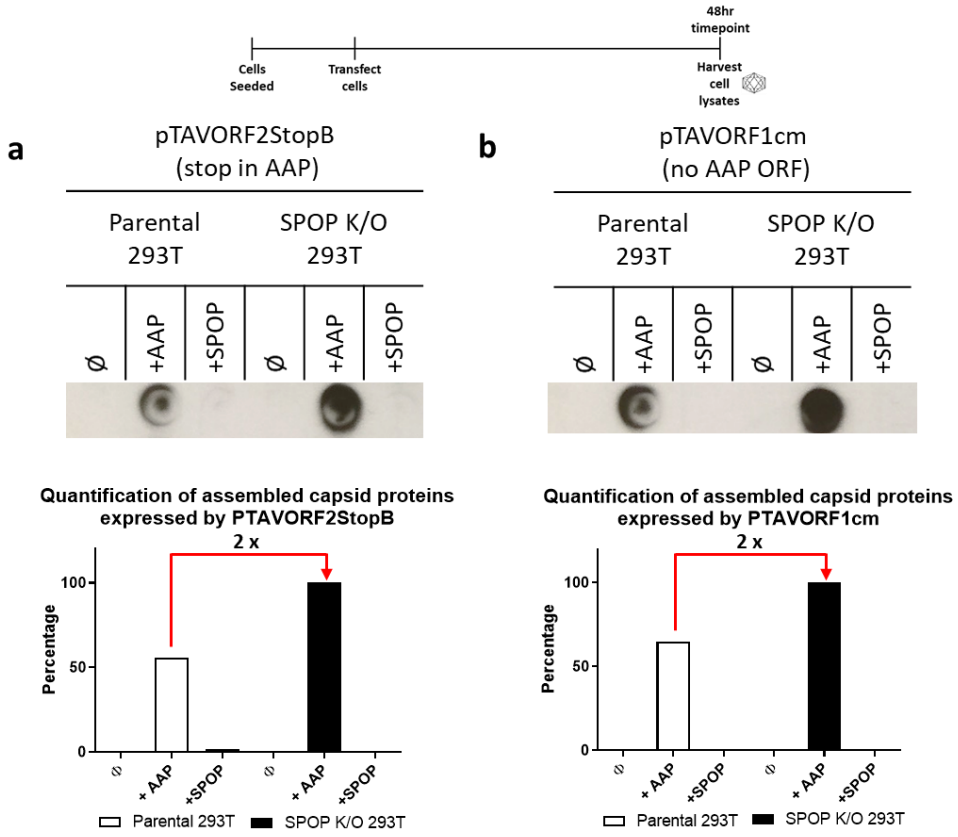

Figure 4.10 SPOP affects the stability of newly assembled capsids. The state of the *de novo* synthesized capsids was analysed by dot blot and quantified relative to capsids of pTAVORF2stopB + AAP and pTAVORF1cm + AAP in the SPOP K/O cells, respectively. The capsid proteins were expressed from constructs that do not contain AAP either alone(Ø) or in *trans* with a construct expressing AAP (+AAP) or SPOP (+SPOP). **a.** Dot blot displaying the expression from a construct that has a stop in the second ORF that expresses AAP (pTAVORF2stopB). **b.** Dot blot displaying the expression from a construct that has been codon modified and does not contain the second ORF expressing AAP (pTAVORF1cm). A20 antibody visualized intact capsids. The results displayed are representative of three experimental replicates.

As seen with the stability of incoming capsids, SPOP is also able to regulate newly synthesized capsids. An evaluation of the dot blot shows that 2-fold more capsids are produced in the absence of SPOP with either construct. This eludes to the ability of SPOP to restrict different parts of the AAV life cycle.

4.6.2 SPOP regulates newly synthesized unassembled capsid proteins

The effect of SPOP on the state of unassembled capsid proteins was also evaluated. Since AAP assembles capsids, we evaluated the state of unassembled capsid proteins by using the same vector that had a stop in the AAP sequence (pTAVORF2stopB) as above (Figure 4.11).

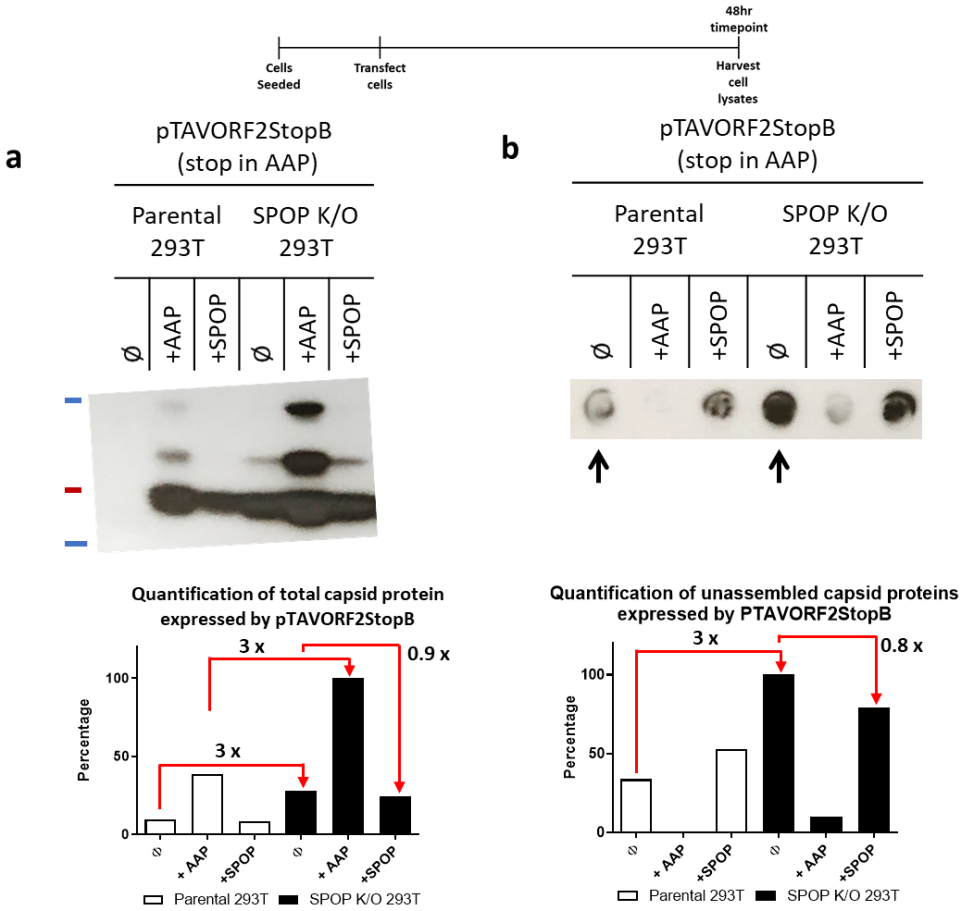

Figure 4.11 SPOP affects the stability of unassembled capsid proteins. The state of the capsid proteins was analysed by western blot (**a**) and via dot blot (**b**); and quantified relative to VP2 of pTAVORF2stopB + AAP in the SPOP K/O cells (**a**); and relative to the unassembled capsids of pTAVORF2stopB Ø in the SPOP K/O cells (**b**), respectively. The capsid proteins were expressed either alone (Ø) or in *trans* with a construct expressing AAP (+AAP) or SPOP (+SPOP). B1 antibody was used to visualize unassembled VP. The black arrows indicate the differences in the expression of unassembled VP in the presence or absence of endogenous SPOP. The results displayed are representative of three experimental replicates.

According to the western blot, the absence of SPOP also appeared to stabilize the unassembled capsid proteins- seen by the 3-fold increase in absence of AAP (Ø) (Figure 4.11a). The same phenomenon was confirmed via the dot blot with a 3-fold increase in comparison to the parental cells (Figure 4.11b). Moreover, the re-expression of SPOP in the knockout cells (via transfection) appeared to reduce the stability of the unassembled capsid proteins (0.8-0.9 fold change). The overexpression of SPOP in the parental cells appeared to partially stabilize the VP protein. This was seen by the appearance of VP3 in the western blot analysis (Figure 4.11a) and the increased signal in the dot blot (Figure 4.11b). The

overexpression of one protein could alter the molecular composition of a complex, possibly leading to its inactivation. This shall be discussed in more detail later.

Furthermore, there was a 3 fold higher expression of capsids proteins (+AAP) in the SPOP knockout cells which supports the effect of SPOP on the intact capsids (see Figure 4.10).

The effects seen above were verified with the other construct that did not contain AAP (Figure 4.12).

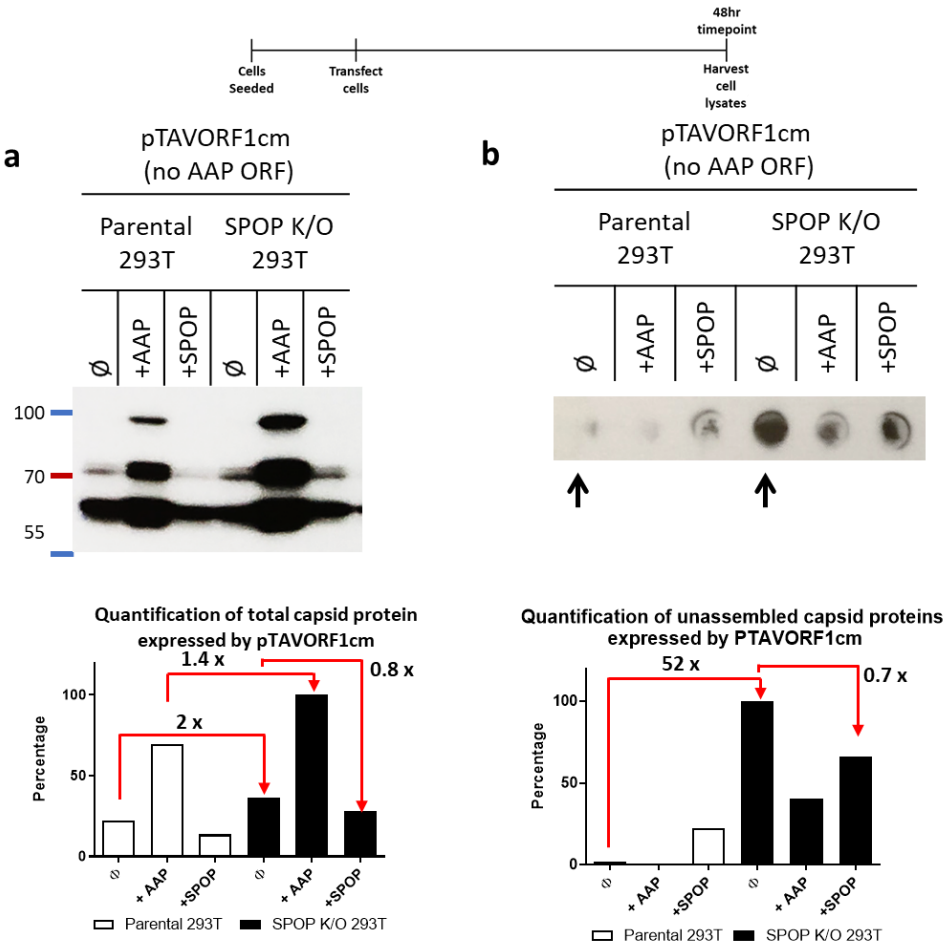

Figure 4.12 SPOP affects the stability of unassembled capsid proteins. The state of the capsid proteins was analysed by western blot (**a**) and via dot blot (**b**); and quantified relative to VP2 of pTAVORF1cm + AAP in the SPOP K/O cells (**a**); and relative to the unassembled capsids of pTAVORF1cm Ø in the SPOP KO cells (**b**), respectively. The capsid proteins were expressed either alone(Ø) or in *trans* with a construct expressing AAP (+AAP) or SPOP (+SPOP). B1 antibody was used to visualize unassembled VP. The black arrows indicate the differences in the expression of unassembled VP in the presence or absence of endogenous SPOP. The results displayed are representative of three experimental replicates.

Both constructs had different levels of expression but showed a similar trend. The absence of SPOP was able to stabilize unassembled capsid proteins, with a 52-fold increase seen in the dot blot (Figure 4.12b). The re-expression of SPOP in the knockout cells (via transfection) had a destabilizing effect on the unassembled capsid proteins seen with the 0.8-fold change in the western blot (Figure 4.12a) and the 0.7-fold change in the dot blot. However, the effect of SPOP overexpression in the parental cells had opposing effects in the western blot and dot blot assays.

Again, the effect of SPOP on assembled capsids is seen as 1.4-fold more capsid proteins were expressed in the SPOP knockout cells upon *trans* expression of AAP.

4.6.3 SPOP rescue via lentiviral infection does not fully restore the parental cell phenotype

Although the transfection of SPOP in the knockout cells had a destabilizing effect on unassembled VP, the expression varied and did not fully reach wild type levels, therefore I restored SPOP expression through the lentiviral infection of the SPOP knockout cells. The restoration of the SPOP protein was verified via western blot and the cells were used in the same assay as described above. The question was whether SPOP rescue would to restore the phenotype seen in the parental cells (Figure 4.13).

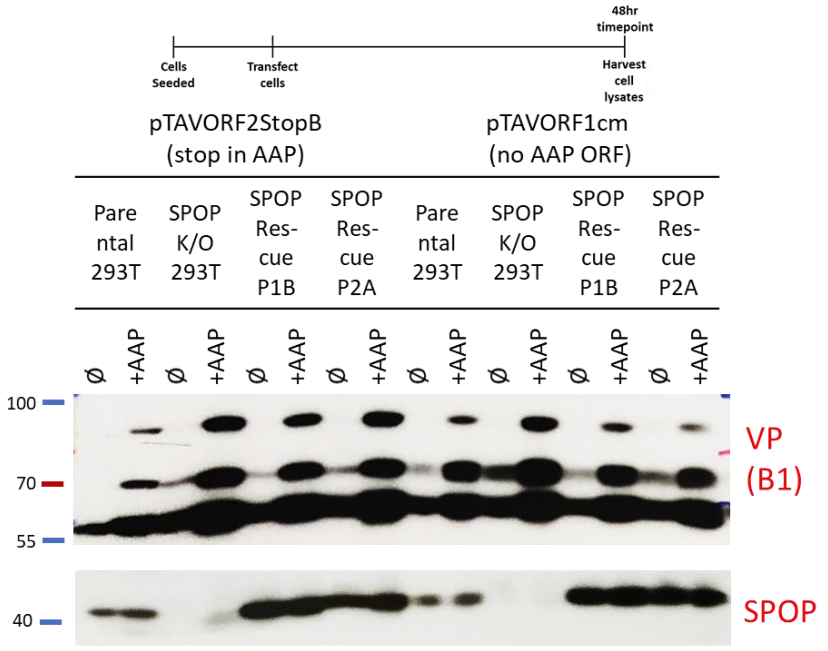
48hr timepoint
Cells Seeded
Transfect cells
Harvest cell lysates
pTAVORF2StopB (stop in AAP)
pTAVORF1cm (no AAP ORF)
Parental 293T
SPOP K/O 293T
SPOP Rescue P1B
SPOP Rescue P2A
Parental 293T
SPOP K/O 293T
SPOP Rescue P1B
SPOP Rescue P2A
Ø
+AAP
100
70
55
40
VP (B1)
SPOP

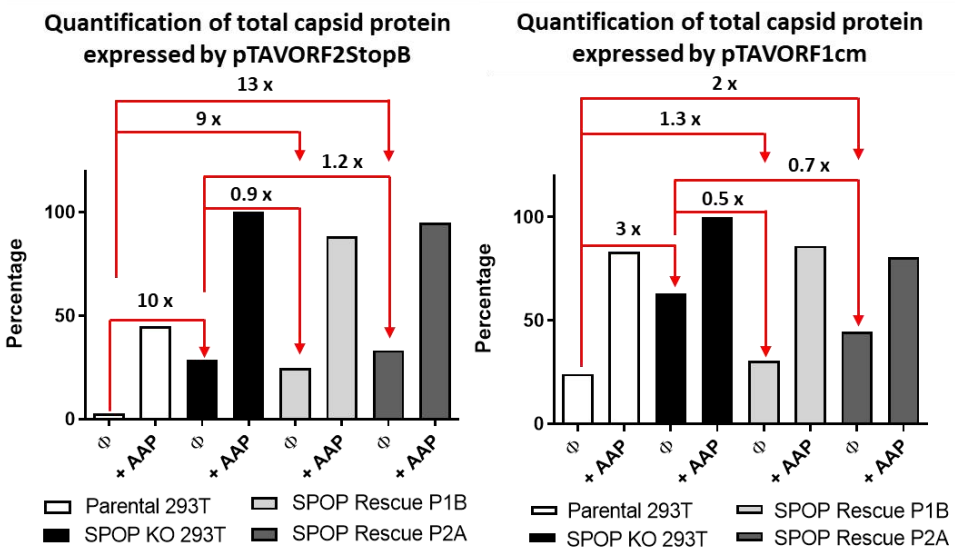
Quantification of total capsid protein expressed by pTAVORF2StopB
13 x
9 x
1.2 x
0.9 x
10 x
Percentage
100
50
0
Ø
+ AAP
Parental 293T
SPOP KO 293T
SPOP Rescue P1B
SPOP Rescue P2A
Quantification of total capsid protein expressed by pTAVORF1cm
2 x
1.3 x
0.7 x
0.5 x
3 x
Percentage
100
50
0
Ø
+ AAP
Parental 293T
SPOP KO 293T
SPOP Rescue P1B
SPOP Rescue P2A

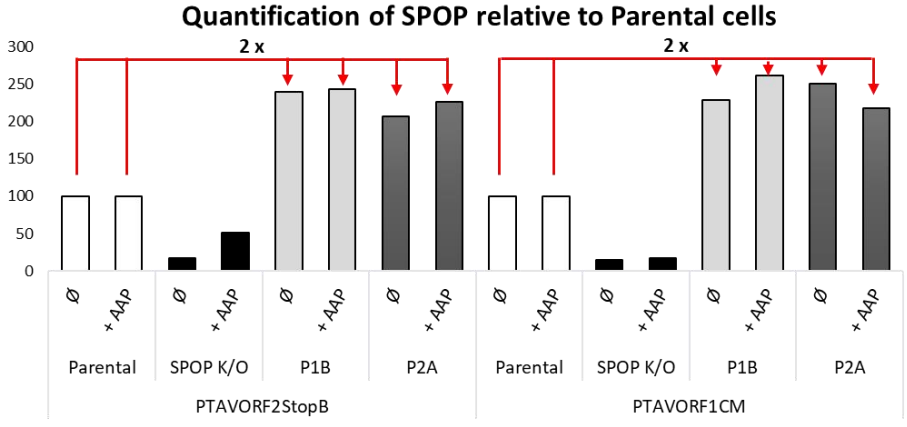
Quantification of SPOP relative to Parental cells
300
250
200
150
100
50
0
2 x
2 x
Ø
+ AAP
Parental
SPOP K/O
P1B
P2A
PTAVORF2StopB
PTAVORF1CM

Figure 4.13 The restoration of SPOP destabilizes unassembled capsid proteins, but not to wild-type levels. The state of the capsid proteins in the presence or absence of SPOP was analysed by western blot. The capsid proteins were expressed via two different constructs that do not contain AAP (pTAVORF2stopB and pTAVORF1cm) either alone(Ø) or in *trans* with a construct expressing AAP (+AAP). B1 was used to visualize the VP proteins. The upper panel of graphs quantify the VP2 bands relative to PTAVORF2stopB + AAP and pTAVORF1cm + AAP, respectively. The graph in the lower panel quantifies the amount of SPOP relative to the levels in the parental cells. Anti-SPOP antibody was used to visualize SPOP. P1B and P2A were SPOP knockout cells infected with lentiviruses that encoded for SPOP, thus restoring the expression of the protein (see SPOP western blot and quantification). The results displayed are representative of three experimental replicates.

The restoration of SPOP was clearly visible in both clones (P1B and P2A, see SPOP western blot) and resulted in similar effects. The SPOP rescue was able to destabilize the unassembled capsid proteins in all cases (0.5-0.9 fold change), as seen previously via transfection, except for the 1.2-fold increase seen upon expression from the pTAVORF2stopB construct in the P2A cells. A quantification of the SPOP amounts (graph in the lower panel) revealed that the rescue cells had twice as much SPOP as the parental cells. One would expect that this would cause double the destabilization, however it was not able to reach the levels observed in the parental levels. In fact, in these cells the unassembled capsid proteins (Ø) were still stabilized to a higher extent than that seen in the parental cells. i.e. 9-13 times more for the pTAVORF2stopB construct and 1.3-2 times more for the pTAVORF1cm construct.

There was also a reduction in the stability of the assembled capsids (+AAP). However, in contrast to unassembled capsids, expression from the pTAVORF1cm construct was able to restore the intact capsid expression back to wild-type levels (Figure 4.13).

These different observations led us to question the functionality of the restored SPOP. Therefore, in order to probe this, we evaluated the endogenous levels of other SPOP substrates, in the parental cells, knockout cells and upon restoration in both HeLa and HEK 293T cells (Figure 4.14).

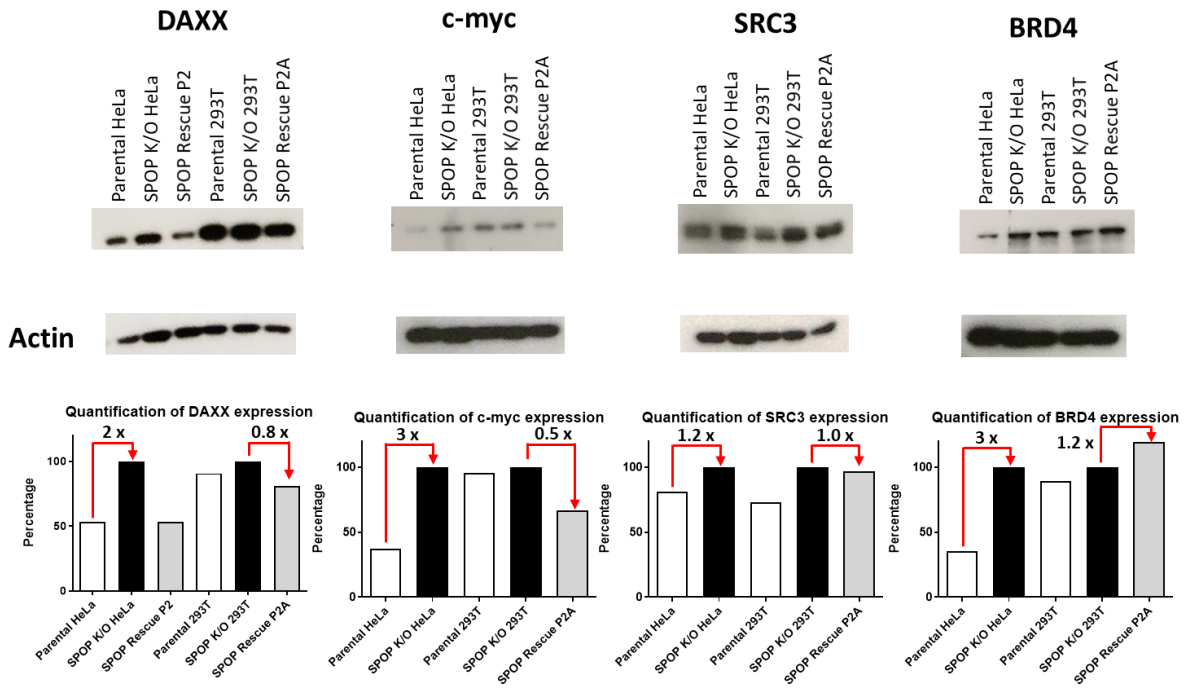

Figure 4.14 Analyses of SPOP binding substrate levels. The levels of endogenous SPOP binding substrates- DAXX, c-myc, SRC3 and BRD4 were evaluated via western blot and quantified relative to the levels of the proteins in the SPOP knockout HeLa or HEK 293T cells, respectively.

In general, a knockout of SPOP resulted in an increase of substrate levels in both HeLa and HEK 293T cells, however this was more evident in the HeLa cells with up to 3-fold increases of c-myc and BRD4. These effects were SPOP-specific given the equal actin signals. The differences in baseline expression could be due to the tissue origin, given that HeLa are from the cervix while HEK 293T are from the kidney. Nevertheless, the amounts of the DAXX and c-myc increased after SPOP knockout and a restoration of SPOP lead to a downregulation, as seen with the unassembled capsid proteins. Interestingly, for these two proteins, the amounts reduced to even lower levels than those seen in the parental cells. The restoration of SPOP had no effect on SRC3 expression and increased BRD4 expression (however this was only 1.2-fold).

4.6.4 The effect of SPOP on newly synthesized unassembled capsid proteins can be visualized

As for the incoming capsids, next we checked if the increase in stability seen on a protein level could also be visualized via indirect immunofluorescence. Therefore, newly synthesized capsid proteins were produced and stained (Figure 4.15).

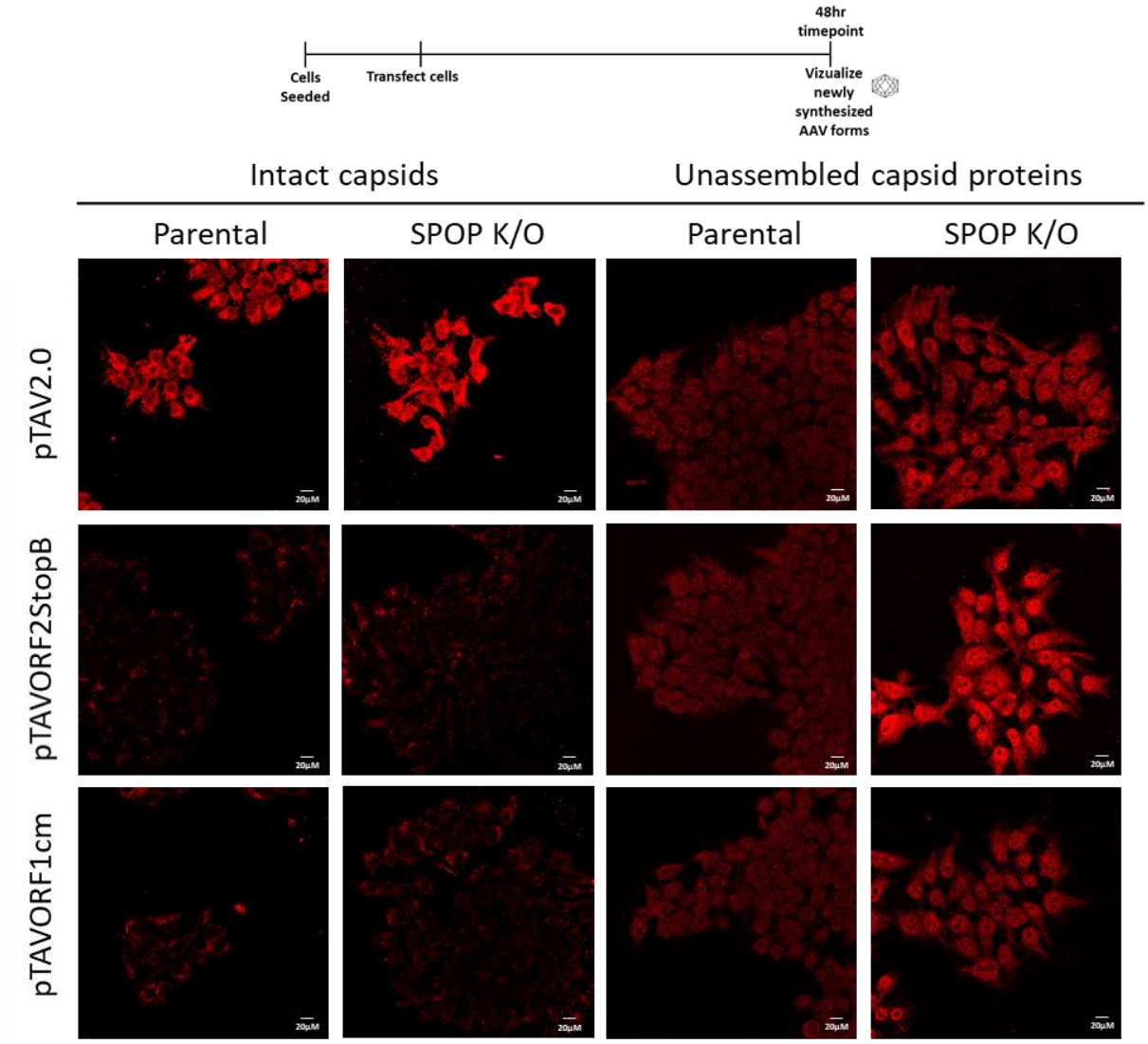

Figure 4.15 The newly synthesized capsid protein stabilization in the absence of SPOP can be visualized. The state of newly synthesized capsids proteins in the presence or absence of SPOP was analysed by immunofluorescence (see scheme). The capsid proteins were expressed via a construct with all capsid proteins intact, including AAP (pTAV2.0), or two different constructs that do not contain AAP (pTAVORF2stopB and pTAVORF1cm). A20 antibody was used to visualize intact capsids, B1 antibody was used to visualize unassembled

capsid proteins and Alexa 594 was used as a secondary antibody. Confocal images were taken at 60x magnification.

The pTAV2.0 construct contains the wildtype AAV2 genome, with *rep, cap* and AAP. The accumulation of intact capsids was much higher in SPOP knockout cells compared to the parental cells (top panel, Figure 4.15). This difference was not obvious with expression via the other two vectors with AAP supplied in *trans*. The expression and stabilization of unassembled capsid proteins in absence of SPOP was most apparent, seen by the higher signal intensity in the knockout cells compared to the parental cells (compare the 3rd and 4th column, Figure 4.15). This was highest for the expression of capsid proteins via the pTAVORF2stopB construct. Furthermore, the immunofluorescence result was consistent with the western blot and dot blot data where 2-3 fold higher protein accumulation is seen in the knockout cells. The unassembled capsid proteins appear to be majorly located in the nucleus, but also present in the cytoplasm.

A closer look into the knockout cells revealed the stabilization of the capsid proteins, expressed in a punctuated pattern in the cell nucleus (see insert, Figure 4.16).

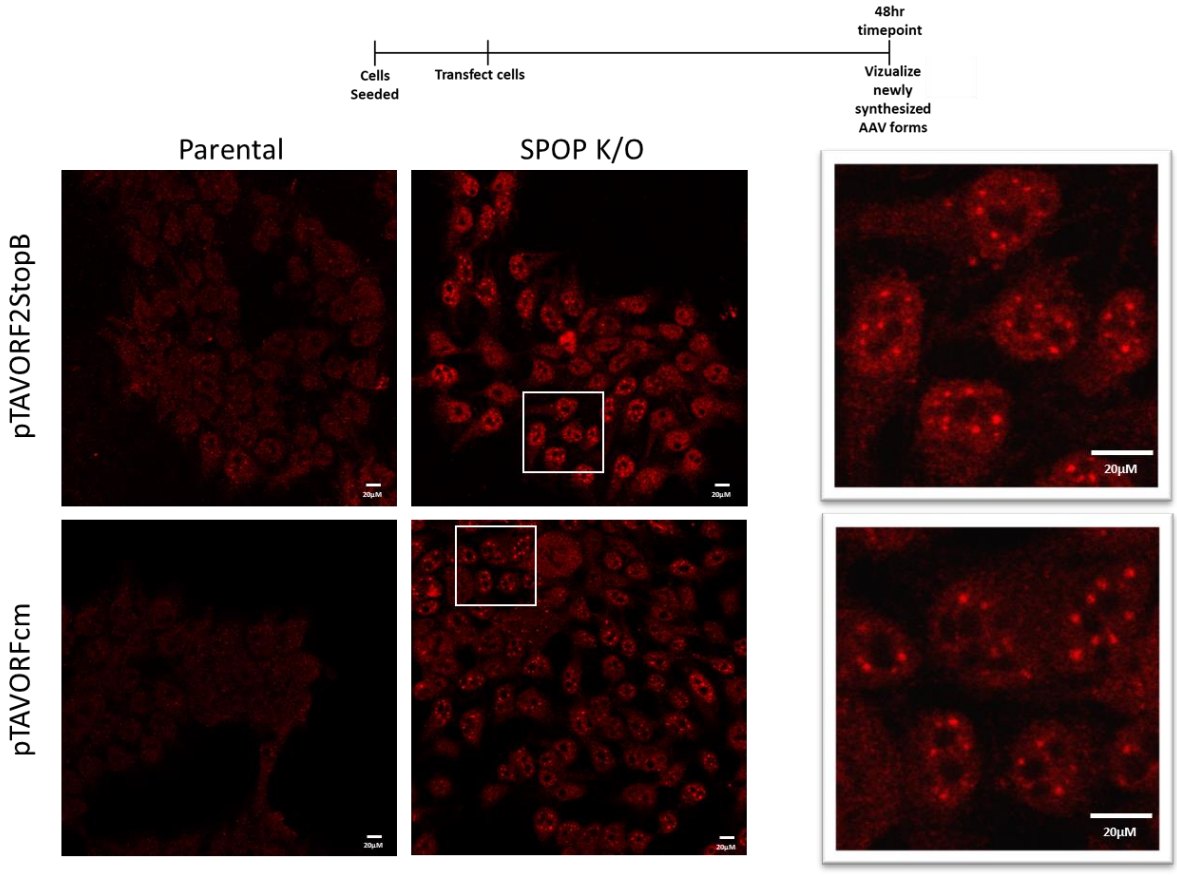

Figure 4.16 Absence of SPOP results in the stabilization of unassembled capsid proteins in nuclear clusters. The state of unassembled capsids proteins in the presence or

absence of SPOP was analysed by immunofluorescence. The capsid proteins were expressed via two different constructs that do not contain AAP (pTAVORF2stopB and pTAVORF1cm). B1 antibody was used to visualize unassembled capsid proteins and Alexa 594 was used as a secondary antibody. The insert is displayed on the right.

Although the unassembled capsid proteins were expressed in the nucleus and the cytoplasm, the accumulations were only observed in the nucleus of the SPOP knock out cells. Which would mean that with functional SPOP, these proteins would be degraded soon after production. This is also seen in the dot blot and western blot assays whereby there is less unassembled VP in the parental cells, compared to the knockouts.

The nucleolus is the site of capsid assembly; however, these clusters appear to be in the nucleoplasm and not in the nucleoli, though this would need confirmation with co-staining of a nucleoli marker. PML has been identified as a restriction factor for AAV, thus we sought to find out if the accumulation of the unassembled capsid proteins was in the PML nuclear bodies (Figure 4.17). Nevertheless, a co-staining revealed that the capsid proteins accumulated outside the PML bodies (see insert, Figure 4.17).

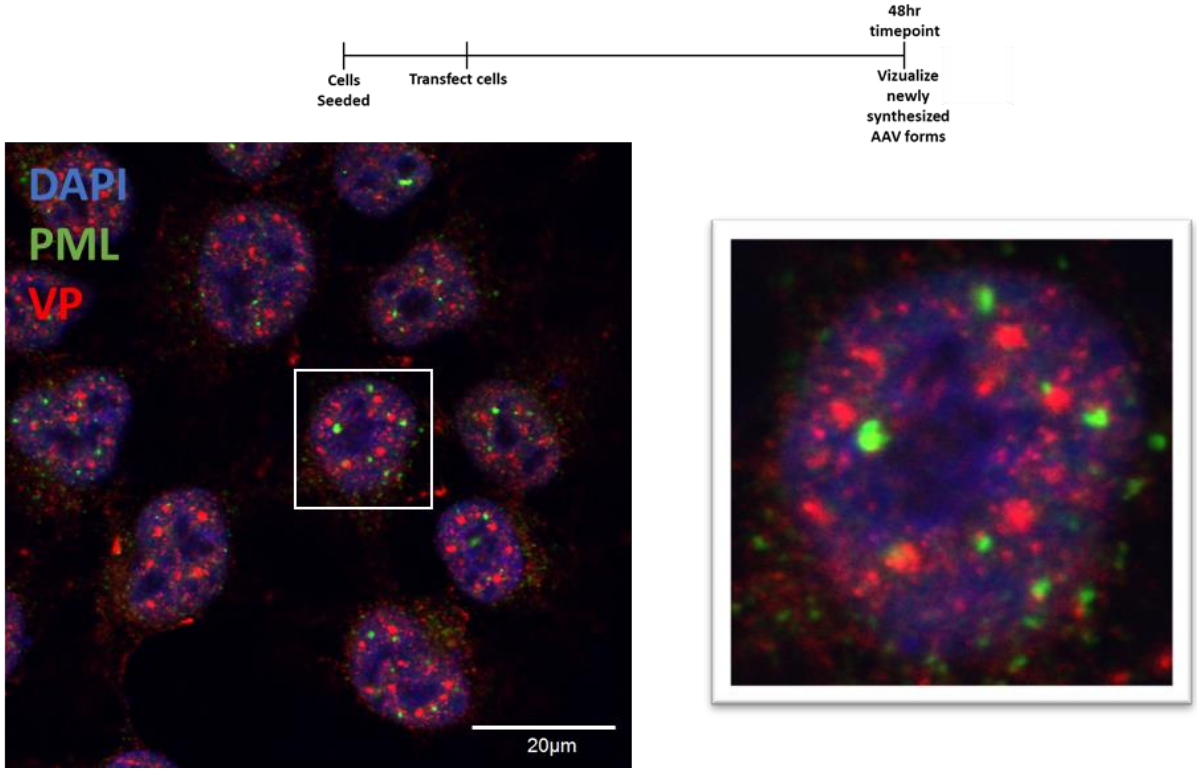

Figure 4.17 Stabilized unassembled capsid proteins do not accumulate in the PML bodies. The compartment in which the unassembled capsids proteins gather was investigated. The capsid proteins were expressed with pTAVORF2stopB, that does not contain AAP. B1 mouse antibody was used to visualize unassembled capsid proteins, Alexa

594 labelled anti-mouse was used as a secondary antibody. PML was stained with an anti-PML rabbit antibody and Alexa 488 labelled anti-rabbit, was used as a secondary antibody. DAPI was used to stain the nucleus. The insert is displayed on the right.

4.7 Investigating the effect of Cullin 3 and the proteasome on newly synthesized capsid proteins

4.7.1 Cullin has a minor effect on the stability of newly synthesized capsid proteins

Cullin 3 was identified as an interacting factor of AAV via the previously performed TAP tag experiments. Given that it acts as the scaffold for SPOP, but had no effect on incoming capsids, the role it plays on the stability of newly synthesized capsid proteins before assembly (by expressing AAV2 WT constructs that lacked AAP), after assembly (by supplying AAP in *trans*) and with the addition of SPOP was investigated in cells that had down regulated Cullin 3 (Figure 4.18).

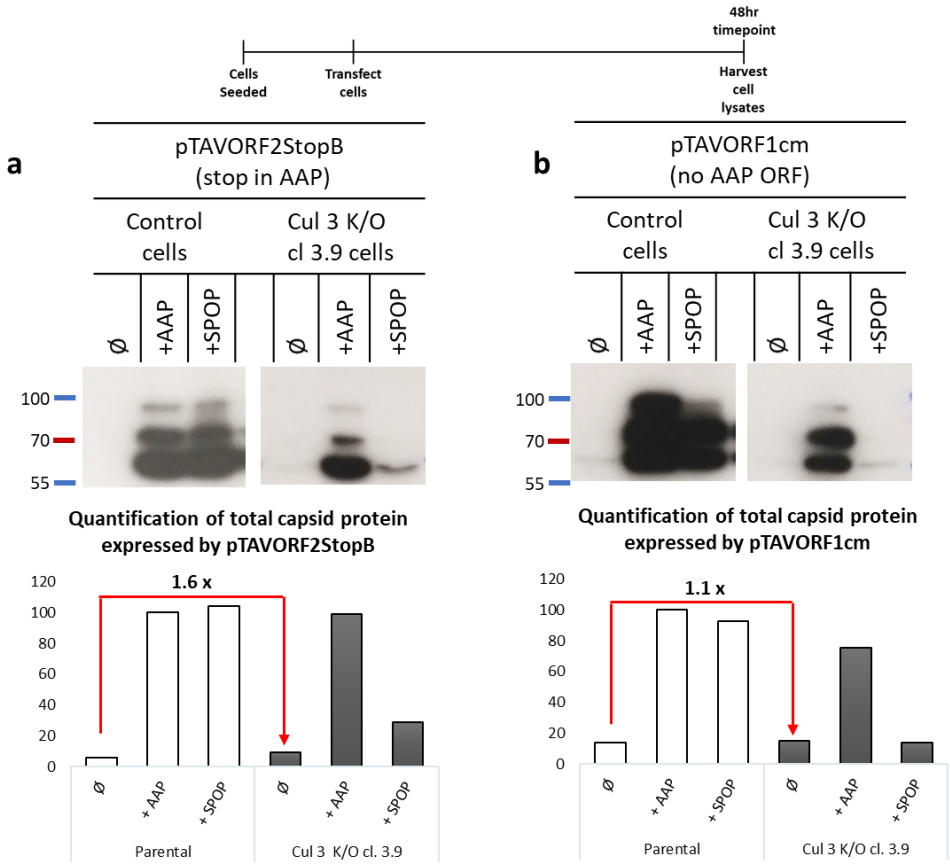

Figure 4.18 Cullin 3 has a minor effect the stability of newly synthesized unassembled capsid proteins. The state of the capsid proteins expressed in the cells with down regulated Cullin 3 was analysed by western blot and quantified relative to VP3 of pTAVORF2stopB + AAP (**a**) and pTAVORF1cm + AAP (**b**), respectively. The capsid proteins were expressed via

constructs that do not contain AAP either alone(Ø) or in *trans* with a construct expressing AAP (+AAP) or SPOP (+SPOP). **a.** Western blot and quantification of capsid proteins expressed from pTAVORF2stopB. **b.** Western blot and quantification of capsid proteins expressed from pTAVORF1cm. B1 was used to visualize the VP proteins. The results displayed are representative of three experimental replicates.

Unlike with SPOP, unassembled capsid proteins (Ø) were affected to a much minor extent by the lack of Cullin 3. i.e. a 1.1-1.6 fold change compared to a 2-10 fold observed in the absence of SPOP. In addition, the lack of Cullin 3 appeared to cause a decrease in the number of intact capsids (+AAP). In line with the parental cells, the over expression of SPOP appeared to cause some stabilization of the capsid proteins.

4.7.2 Proteasome inhibition stabilizes newly synthesized capsid proteins

If the mode of AAV restriction via SPOP is exclusively through the proteasome, then it would be expected that its inhibition in the parental cells would culminate in the same effect as that seen in the absence of SPOP. To test this, newly synthesized capsids were expressed in presence of proteasome inhibitor and probed for changes in stability via western blot (Figure 4.19 and 4.20).

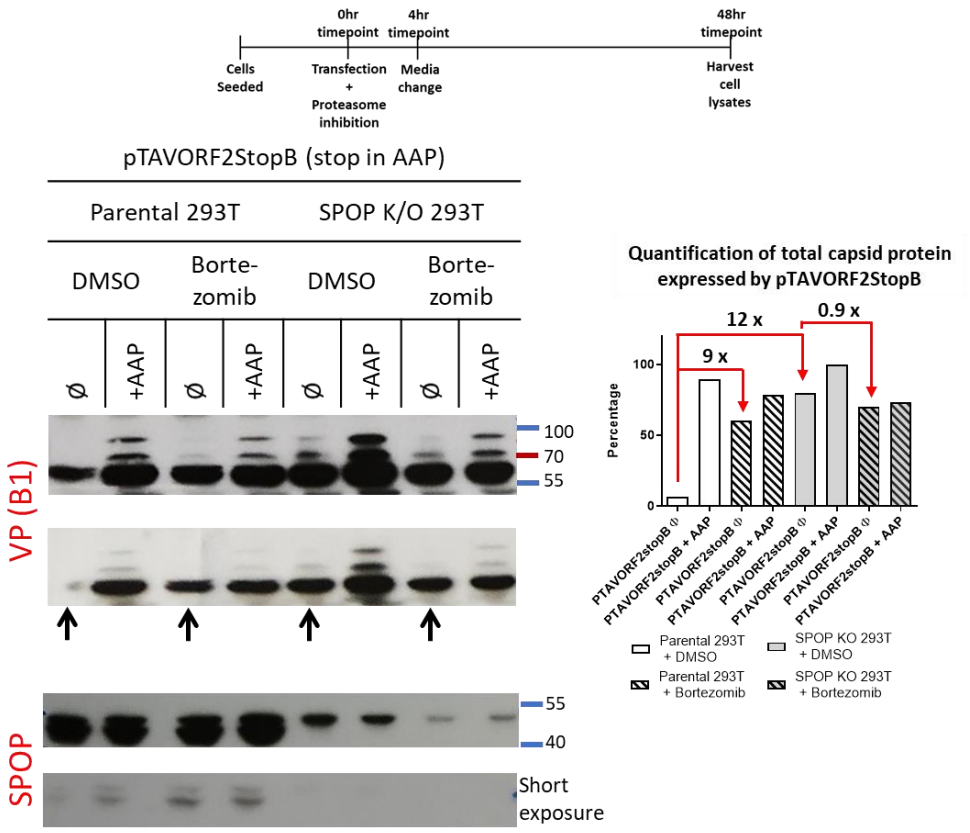

Figure 4.19 Proteasome inhibition stabilizes unassembled capsid proteins. The state of the capsid proteins was analysed by western blot and quantified relative to VP3 of pTAVORF2stopB + AAP in the SPOP K/O cells, under the presence or absence of proteasome inhibitor (bortezomib). The capsid proteins were expressed from pTAVORF2stopB that does not contain AAP either alone(Ø) or in *trans* with a construct expressing AAP (+AAP) or SPOP (+SPOP). B1 was used to visualize the VP proteins while the anti-SPOP antibody was used to visualize SPOP. Lower panels display blots with shorter exposure times. The black arrows indicate the differences in the expression of unassembled VP. The results displayed are representative of three experimental replicates.

Looking at the parental cells, proteasomal inhibition appeared to also stabilize the unassembled capsid proteins- seen by the 9-fold increase when capsid proteins were expressed without AAP (Ø). However, the SPOP effect on the stabilization was stronger, i.e. 12-fold. Interestingly, proteasome inhibition appeared to cause a minor 0.9-fold change in the amount of unassembled VP in the SPOP knock out cells. Furthermore, proteasome inhibition appeared to reduce the stability of intact capsids (+AAP) in both cell lines (Figure 4.19).

The results were verified by looking at the other construct that does not contain AAP, pTAVORF1cm (Figure 4.20).

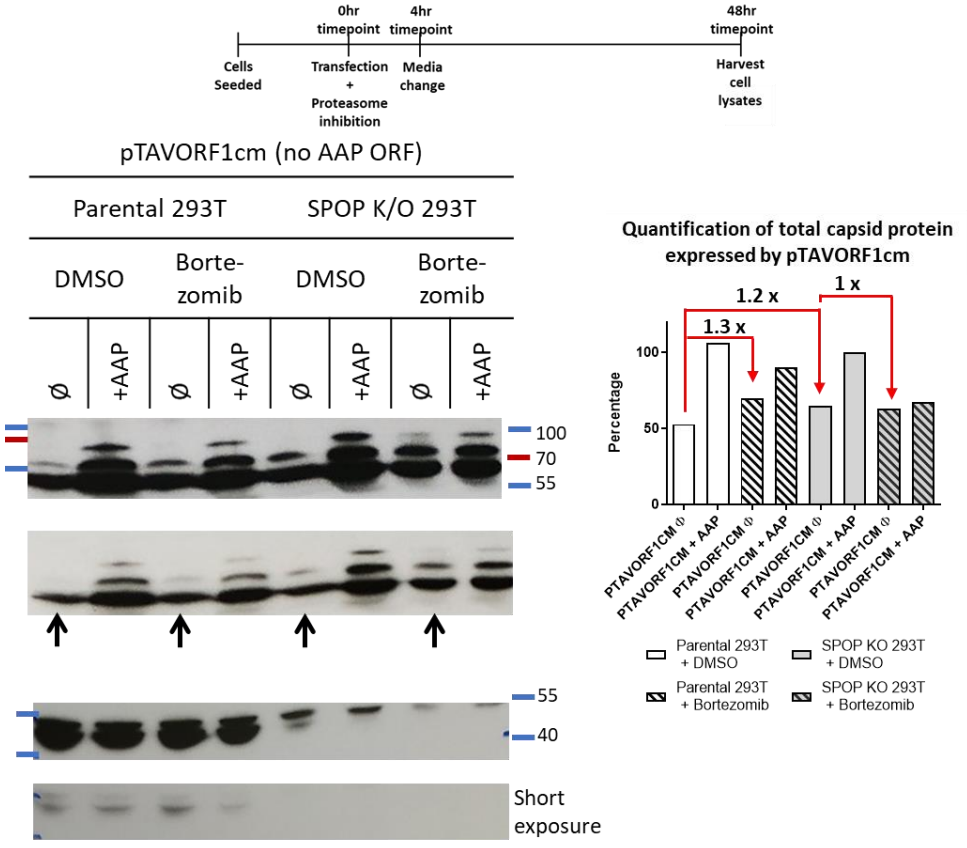

Figure 4.20 Proteasome inhibition stabilizes unassembled capsid proteins. The state of the capsid proteins was analysed by western blot and quantified relative to VP3 of pTAVORF1cm + AAP in the SPOP K/O cells, under the presence or absence of proteasome inhibitor (bortezomib). The capsid proteins were expressed from pTAVORF1cm that does not contain the AAP ORF either alone (Ø) or in *trans* with a construct expressing AAP (+AAP) or SPOP (+SPOP). B1 was used to visualize the VP proteins while the anti-SPOP antibody was used to visualize SPOP. Lower panels display blots with shorter exposure times. The black arrows indicate the differences in the expression of unassembled VP. The results displayed are representative of three experimental replicates.

The e73ffect of proteasome inhibition on unassembled capsid proteins expressed from the pTAVORF1cm construct, paints a comparable picture. In that, bortezomib treatment in the parental cells caused a 1.3-fold increase when capsid proteins were expressed without AAP (Ø). However, the effect of SPOP knock was similar to proteasome inhibition, i.e. 1.2 vs 1.3 fold, respectively. In addition, proteasome inhibition did not affect the stability of unassembled VP in the SPOP knock out cells. As seen above, bortezomib treatment reduced the stability of intact capsids (+AAP) in both cell lines (Figure 4.19 and 4.20).

5 Discussion

5.1 The localization of SPOP, SPOPL and AAV2 capsid proteins

Previously performed tandem affinity purification and yeast 2 hybrid screens identified the speckle-type POZ protein (SPOP) as a putatve interaction partner of AAV capsid protein VP1 [178]. In order to characterize and validate this interaction, first the localization patterns of the individual host factors were investigated. SPOP and its paralog-SPOPL share ~80% sequence homology, are both characterized by a speckled pattern, however they display distinct differences in localization within the cell (Figure 4.1b). SPOP is localized in distinct nuclear speckles while SPOPL is localized in the endosomes. The extra 18 amino acid sequence in the BACK domain of SPOPL is thought to confer this difference in cellular localization [180]. SPOPL is thought to regulate SPOP, as SPOP-SPOPL heterodimers are less active than SPOP-SPOP homodimers.

The AAV2 capsid sequences appear to contain multiple putative SPOP binding sites (SBSs), hinted by the co-localization of SPOP with different capsid proteins. This is a common feature of SPOP substrates, in humans the death-domain-associated protein (DAXX) has been shown to contain multiple SBSs and in drosophila, the transcription factor- Ci and MAPK phosphatase-Puc also contain multiple SBSs for the SPOP ortholog HIB/Roadkill [148], [181], [182]. AAV capsid protein VP2 N-terminus contains a PDSSS amino acid stretch that shares the same characteristics as the originally proposed SPOP binding consensus (SBC) of φ-π-S-S/T-S/T (φ-nonpolar; π-polar) [139]. According to the recently proposed less stringent SBC-φ-π-S-π-π -after Pdx1 was found to bind with SPOP- AHSQS in VP1,2 and 3 and FHSSY in VP1 and 2 would also qualify as SBSs and would be consistent with the pattern observed in Figure 4.2 [153]. Further mutational analyses and pull-down assays could confirm this.

5.2 Investigating the effect of SPOP, SPOPL, Cullin 3 and the proteasome on incoming AAV2 capsids

To investigate the effect of the different factors on AAV2 vector transduction, at first RNAi methods using siRNAs targeting the mRNAs of interest were employed, followed by a transduction assay with AAV2 firefly luciferase vectors. A down regulation of mRNA copies, verified via qPCR gave an indication of knockdown success. The varying effects seen with SPOP knockdown through the different siRNAs could either be seen as the sum total of the divergent effects -which would be equivalent to the phenotype observed in the knockouts- or could be an off target effect of the siRNAs (Figure 4.3). In a previous study using the same set of siRNAs, siSPOP1 also managed to greatly reduce infection of influenza A virus (IAV) in A549 cells, while siSPOP2 little effect. However, in HeLa cells siSPOP2 managed to reduce infection effectively and a qPCR confirmed a reduction of transcripts. These variable effects

could either point towards differences in cell-type specificity or give further evidence to the off target effects of the siRNAs [180].

A blast search of the siRNA sequences revealed that the siSPOP3 sequence has 80% homology to the ATP binding cassette subfamily A member 13 (ABCA13). The ATP-binding cassette (ABC) transporters are transmembrane-spanning proteins that are involved in the transport of different molecules. Although no relation between AAV and the ABCs have been made so far, defects in ABCA (along with other subfamilies) have been associated with Hepatitis C virus (HCV), though the exact mechanisms are not yet fully understood [183], [184]. Perhaps this could also play a role in AAV, culminating in the 3 fold increase seen with siSPOP3 treatment.

The knockout of SPOP via CRISPR-cas9 technology provided a scenario whereby the effects of the specific elimination of SPOP could be studied (Figure 4.4). This revealed a 2 fold increase in transduction. The moderate increment hints at the possible involvement of other players in the ubiquitin proteasome system in the restriction of AAV transduction. For example a recent study found that the Ring Finger Protein 121 (RNF121), a factor that was identified in the same haploid screen as the universal receptor AAVR, is an essential E3-ligase in AAV transduction [10], [185]. In RNF121 knockout cells, transduction of AAV1, 2, 6 and 9 was significantly reduced and this was independent of vector dose or cell line. In addition, an overexpression of RNF121 could restore the transduction [185]. The observation that the SPOP-effect levelled overtime in both scenarios with the self-made knockouts and the commercially obtained ones, points towards the intrinsic ability of the cell to restrict incoming virus via alternative pathways, especially if the SPOP- CRL3 is not the sole pathway that mediates the ubiquitination and degradation of capsids.

If SPOP is not essential in regulating transduction, then the same would hold true for SPOPL and Cullin 3 (Figure 4.5). One would expect a similar increase with Cul3 knockdown as seen with SPOP since it acts as the scaffold. However, Cul3 binds to BTB proteins in general and ~180 are encoded in the human genome. BTBs are involved in a range of functions such as chromatin remodelling and transcriptional regulation, oxidative stress regulation and vesicle trafficking, just to name a few [137], [186], [187]. A down regulation of the above mentioned RNF121, decreases AAV transduction, therefore it is plausible that the phenotype observed in this study is a sum of effects of CRL3s with different BTB proteins. SPOPL is thought to be a regulator of SPOP, that forms less active SPOP-SPOPL CRL3s [188]. Given that a mild effect is seen with SPOP and that SPOPL acts as a negative regulator, the lack of an effect of SPOPL on transduction is expected.

Proteasome inhibition has previously been shown to increase AAV transduction [179]. Although the exact mechanism is poorly understood, it is thought that the accumulation of ubiquitinated capsids form a conducive environment for the late stages of transduction [179].

Proteasome inhibitor treatment was able to increase transduction in all cell lines used in this study (Figure 4.6). The differences observed between HeLa and HCT 116 cells is a reflection of cell-type specific permissiveness to AAV2 infection (Figure 4.6a). HeLa cells are regarded as highly permissive to AAV, as evidence of AAV2 cytoplamic transport was largely obtained in experiments using HeLa cells, [53], [189]. HCT116 cells have been used to a lower extent, while other colon-derived cell lines such as Caco-2 cells show much lower levels of permissiveness [190]. Differences are brought about by the receptors and co-receptors that are present on the cell surface and the roles that they play on AAV entry. A study looking into the best serotypes for the small intestine and the colon revealed that AAV4, 7, 8, 9, and 10 transduce with cells with higher efficiency [191].

A further difference is observed between HeLa batches, denoted by the variation in transduction efficiency and the boost upon proteasomal inhibition, i.e a 28-fold increase in HeLa cells from the lab stocks vs the 10-fold increase in commercially obtained HeLa cells (parental). A study of different batches of HeLa cells found that there were stark differences in genomic and transcriptomic profiles. Some cells gained and others lost genomic material, causing major differences in basal gene expression [192]. Therefore, since the HeLa cells came from different sources, it it plausible that they harbour differences in genetic variation in comparison to each other. However, since the SPOP knockout cells were derived from the commercially obtained parental cells, they serve as the best comparison for differences in phenotype as a result of the loss of SPOP function.

If the SPOP-CRL3 complex was the sole machinery that restricted AAV infection via proteasomal targeting, then it would be expected that there would be no difference between a disruption of SPOP (via knockout) or proteasomal inhibition. However, there was still an observable effect after treatment with PIs in the SPOP knockout cells. Even though this effect was remarkably lower (4-fold, as compared to 10-fold in parental cells), it gives further evidence that along with the SPOP-CRL3 complex, there is other ubiquitin-conjugation machinery involved in restricting AAV transduction.

Neddylation is a process required for cullin activation. It is exerted by the binding of Nedd8 (a ubiquitin-like protein) to a lysine in the c-terminal domain that triggers a conformational change causing the RING domain to free up, thereby reducing the distance between the active site of the E2 enzyme and the lysine on the target. Nedd8 additionally acts by recruiting the E2 enzyme to cullin [130], [193]. MLN-4924 inhibits neddylation and thus the activation of Cul3 [194]. MLN-4924 treatment did not affect AAV2 transduction efficiency, which is consistent with the lacking effect of knocking down Cul3 on AAV transduction (Figure 4.7). However, the combined treatment with proteasome inhibitors was able to boost transduction, with the highest increase seen with ‘Bortezomib + MLN-4924’ in the parental cells. The SPOP knockout cells still exhibited an increase upon combined treatment, albeit to a lesser extent, as previously seen with proteasome treatment alone. For the ‘Bortezomib +

MLN-4924' combined treatment in the context of HPV 16, no increase to transduction was observed in both the parental and SPOP knockout cells (compare red lines in Figure 4.7). This confirmed that the aforementioned effects were specific to AAV2 transduction.

Next, the effect of SPOP on the stability of the incoming capsids was evaluated. In the absence of SPOP, the incoming capsids showed up to 3-fold higher stability according to the results of the dotblot assay (Figure 4.8) and the immunofluorescence analysis (Figure 4.9). These experiments give evidence to the mechanism in which SPOP is able to restrict AAV transduction, i.e through the ubiquitination and subsequent degradation via the proteasome. This is also consistent when looking at the protein accumulation of the other SPOP substrates (Figure 4.14), whereby the absence of SPOP increased their levels up to 3-fold when compared to baseline levels in the parental cells. The variation seen between the substrates could be a result of differences in cell-type specific expression in different tissues. The mechanisms in which SPOP binds and acts on other endogenous substrates- DAXX, c-myc, SRC3 and BRD4 have been well characterized.

The direct interaction between DAXX and SPOP was proven via immunoprecipitation and shown that the interaction was required for proteasomal degradation [148]. This was demonstrated by showing that upon expression of SPOP N- or C- terminal mutants, or by proteasome inhibition, DAXX was stabilized. Furthermore, in an *in vitro* ubiquitination assay WT SPOP was required to ubiquitinate DAXX and the expression of the same SPOP mutants resulted in little to no ubiquitination of DAXX [148]. SPOPs ability to interact with and facilitate the ubiquitination and degradation of the transcription factor (c-myc) was also proven using similar techniques. In this case they showed that SPOP-F102C and SPOP-F133V, which had alterations in the substrate binding pocket, significantly reduced the amount of ubiquitinated c-myc. In addition, the use of cyclohexamide to inhibit new protein synthesis together with doxycyclin-induction of SPOP, was able to reduce the half-life of c-myc from ~50 min to ~25 min [195]. For the steroid receptor co-activator-3 (SRC3), SPOP was proven to interact depending on the phosphorylation of the S101/S102. By using a combined shRNA and chase experiment, *in vitro* ubiquitination and employing SRC3 phosphorylation deficient mutants; it was proven that SPOP mediates the polyubiquitination and degradation of SRC3 [158]. Finally, BRD4 which is a member of the bromodomain family involved in epigenetic reading of lysine acetylation, was identified as in interaction partner in a yeast-2-hybrid screen with full length SPOP as bait. The aforementioned experiments were subsequently carried out and SPOP was shown to specifically ubiquitinate and degrade BRD4 [196], [197].

The results of this study give strong indications that SPOP acts in a similar manner on incoming AAV capsids. A capsid pull down after infection in the different cell lines and an inspection of the ubiquitination status, would provide a more concrete picture to link SPOP to the capsid ubiquitination. It would be expected that in the absence of SPOP the capsids would exhibit less ubiquitination.

5.3 Investigating the effect of SPOP, Cullin 3 and the proteasome on newly synthesized capsid proteins

The same phenomenon is seen on newly synthesized capsids whereby the absence of SPOP led to 2-fold higher production of capsids (Figure 4.10). In a study characterizing the post translational modifications of AAV1-rh10, Mary and colleagues highlighted that the environment in the producer cell line may affect the kind of post translational modifications that the virus receives, rather than solely being affected upon entry/during infection [171]. As hypothesized above, SPOP regulates new capsids via ubiquitination and subsequent proteasomal degradation. *In vitro* ubiquitination assays as performed for the other SPOP substrates would be able to provide more information on this restriction. These results also indicate the ability of SPOP to regulate different parts of the AAV life cycle.

However, given that this is a fold lower than the restriction seen for incoming capsids, it is also conceivable that AAV/Ad proteins co-expressed could be using the SPOP-SPOPL machinery to alter the ubiquitination signal on the newly synthesized capsids, for other non-proteasomal consequences such as trafficking to the cytoplasm for release. For example, E4ORF6 of Adenovirus 5 which is involved in the DNA replication of AAV5 (thus encoded in the helper plasmid that is supplied in *trans*), has been shown to form an E3-ubiquitin ligase complex that degrades *de novo* AAV capsids, but the VA RNA (also encoded in the helper plasmid) is able to overcome these effects, in order to achieve overall efficient production of AAV5 [198]. In addition, other viruses such as coxsackie, herpes and poxviruses also hijack the host cell ubiquitin machinery in their viral replication, transcription, and late stage lytic/latent regulation (reviewed in [199]). This provides a picture of the complex host-viral interactions that might be exploited by the virus for its own benefit.

Apart from the effect of SPOP on assembled capsids, there appeared to be another function of the SPOP interaction with newly synthesized unassembled capsid proteins (Figure 4.11-12 & 4.15-17). These results are consistent with the previous observation via a yeast-2-hybrid screen and a TAP tag experiment that SPOP interacts with the AAV capsid protein VP1. It is evident from the western blot and dot blot assays that SPOP restricts unassembled capsid proteins via facilitating their degradation. This is particularly exemplified by the 52-fold increase in unassembled VP in the SPOP knockout cells compared to the parental controls (Figure 4.12b). The differences seen between the constructs could be attributed to the fact that pTAVorfStopB still encodes for a bit of AAP, which might have an effect on the capsid proteins.

The stabilization of VP proteins could be vizualized distinctly as the capsid proteins formed a punctuated pattern in the nucleus of the cells where AAV transcription and packaging takes place [200] (Figure 4.16). Early experiments on the subcellular compartmentalization of AAV2 assembly, revealed a similar punctuated pattern of VP1 and VP2 in the nucleus while

VP3 was equally distributed between the nucleus and the cytoplasm. In the same study they identified that the capsid proteins colocalized with Rep proteins and AAV2 DNA in these nuclear clusters [200]. It is therefore plausible that the newly synthesized capsid proteins are stabilized in the nucleoplasm when neither AAP is available to facilitate assembly, nor is SPOP present to ubiquitinate and target them to the proteasome for degradation.

The Mittag group postulated that SPOP migrates to form liquid bodies (membrane-less organelles) with its substrates inside the nucleus. These bodies contain high-order SPOP complexes, increasing the concentration of SPOP-CRL3 players, thus thought to facilitate substrate ubiquitination [151]. A recent study by the same group was able to confirm their theory by showing that SPOP phase separates with DAXX *in vitro* and leaves its nuclear speckles to colocalize with DAXX in so called SPOP/DAXX bodies *in cells* [152]. This gives another possible explanation of the nuclear clusters observed, i.e unassembled VP proteins that serve as a substrate for SPOP are localized in liquid bodies, awaiting interaction with SPOP leading to the subsequent degradation. In addition, the aforementioned study showed that these liquid bodies did not co-localize with the nucleoli, polycomb bodies, Cajal bodies, or PML bodies [151]. A co-staining with PML in this study is consistent with that finding (Figure 4.17). The promyelocytic leukemia (PML) nuclear bodies (sometimes refered to as ND-10) were previously shown not to associate with the replication compartment of AAV; and to restrict second-strand DNA synthesis [201][202].

Next, the question of the effect of SPOP rescue was evaluated. The restoration of SPOP did not fully reverse effect on the stability of unassembled capsid proteins (Figure 4.13). The protein levels in the rescue cells was generally lower than those seen in the knockout cells, but was not able to reach base-line levels seen in the parental cells. Although the restoration of SPOP was confirmed through the reappearance of a protein at 42kDa (via western blot), there was no guarantee that the protein expressed had the same functionality as the wildtype SPOP. Therefore, this was tested by checking the levels of other known endogenous SPOP substrates in the rescue cell line (SPOP rescue P2A) (Figure 4.14). The substrates displayed different phenotypes: from reducing to levels even lower than those seen in the parental cells (DAXX and c-myc), displaying no change (SRC3) and even increasing to levels higher than seen in the knockout cells (BRD4). According to the SPOP western blot analysis, the amount in the rescue cell lines was 2-fold more than in the parental cell lines. However, the overexpression of SPOP was previously shown to promote the degradation of all four proteins [148], [195], [197], [203]. Altogether, these variable results were not able to give a clear indication of the functionality of restored SPOP. However, this could also be linked to differences in cell-type-specific expression of the various proteins, as previously discussed.

The lack of effect of cullin on newly synthesized capids is in line with the same phenotype on incoming capsids (Figure 4.5 and 4.18). Given the numerous BTB proteins within a cell that can interact with cullin 3, it is possible that the phenotype observed here is a result of the off-

target effects by the lack of CRL3 formation with a different protein [137]. Interestingly, in this experiment the overexpression of SPOP in the Cul3-downregulated cell lines caused some stabilization of VP3. This is peculiar given that SPOP needs to form the CRL3 in order to perform its ubiquitination function. However, the appearance of baseline VP expression without AAP has also been previously observed [204].

If SPOP acts by targeting new capsids to the proteasome, it would be expected that either proteasome inhibition or a down regulation of SPOP would have the same effect. This is observed in this study, PI use was able to stabilize the unnassembled capsid proteins expressed from both AAP-lacking-constructs to similar extent as the lack of SPOP (Figure 4.19 and 4.20). In line with this, there was little to no effect of PI use in the SPOP knockout cells. Interestingly, PI use led to the reduction in intact capsids in both cell lines. Taken together, these results elude to the need for some level of ubiquitination in order to stabilize the *de novo* synthesized capsids. Further experiments such as the *in vitro* ubiquitination assays as performed with other SPOP substrates would provide insight into the level/type of ubiquitination.

All in all, this study sheds light on the different roles that players of the E3-ubiquitin ligase complex with SPOP and the proteasome plays on various parts of the AAV2 life cycle. Indeed if the SPOP binding motifs were purely detrimental to the virus, it would have evolved to lose them. In line with this fact are the results on the interaction with newly-synthesized capsids, which elude a possible recruitment of the host cell SPOP-CRL3 machinery by AAV to its own benefit. Follow up studies would be needed to verify the type and consequence of the ubiquitination of newly synthesized capsids.

5.4 Future perspectives

In order to zero in on the AAV capsid sequences that bind to SPOP, immunoprecipitations with the different sections of the VP could be carried out. This assay would verify if the capsid sequences are able to bind to SPOP via different sections are in line with co-localization experiments. Thereafter, a mutational analysis could be carried out on the putative SPOP binding sites to pinpoint if they modulate this interaction. In order to confirm the effect of SPOP on transduction, either an overexpression of SPOP in (early passage) knockout cells or a transduction assay could be done comparing the knockouts to the SPOP recovery cells. If the 2-fold effect is negated upon recovery, this would affirm the role of SPOP on transduction. Another option would be to use a cell line that is less permissive to AAV, downregulate SPOP and observe if there is an increase in the AAV transduction efficiency.

In terms of understanding the exact mechanisms in which SPOP regulates the stability of incoming capsids, it would be imperative to pull down the incoming capsids in the parental and SPOP knockout cell lines and probe their ubiquitination status. *In vitro* ubiquitination assays on newly synthesized capsid proteins and assembled capsids with SPOP and several SPOP binding mutants and/or capsid mutants would be able to provide more information on the type of ubiquitination SPOP facilitates on newly synthesized AAV variants.

6 References

[1] R. W. Atchison, B. C. Casto, and W. M. Hammon, “Adenovirus-Associated defective virus particles.,” *Science*, vol. 149, no. 3685, pp. 754–6, Aug. 1965.

[2] J. R. Schlehofer, M. Ehrbar, and H. zur Hausen, “Vaccinia virus, herpes simplex virus, and carcinogens induce DNA amplification in a human cell line and support replication of a helpervirus dependent parvovirus.,” *Virology*, vol. 152, no. 1, pp. 110–7, Jul. 1986.

[3] H. You *et al.*, “Multiple human papillomavirus genes affect the adeno-associated virus life cycle,” *Virology*, vol. 344, no. 2, pp. 532–540, Jan. 2006.

[4] A. K. Cheung, M. D. Hoggan, W. W. Hauswirth, and K. I. Berns, “Integration of the adeno-associated virus genome into cellular DNA in latently infected human Detroit 6 cells.,” *J. Virol.*, vol. 33, no. 2, pp. 739–48, Feb. 1980.

[5] E. A. Rutledge, C. L. Halbert, and D. W. Russell, “Infectious clones and vectors derived from adeno-associated virus (AAV) serotypes other than AAV type 2.,” *J. Virol.*, vol. 72, no. 1, pp. 309–319, Jan. 1998.

[6] G. Gao, L. H. Vandenberghe, and J. M. Wilson, “New recombinant serotypes of AAV vectors.,” *Curr. Gene Ther.*, vol. 5, no. 3, pp. 285–297, Jun. 2005.

[7] G. Gao *et al.*, “Clades of Adeno-Associated Viruses Are Widely Disseminated in Human Tissues,” *J. Virol.*, vol. 78, no. 12, pp. 6381–6388, Jun. 2004.

[8] Z. Yan, R. Zak, G. W. G. Luxton, T. C. Ritchie, U. Bantel-Schaal, and J. F. Engelhardt, “Ubiquitination of both adeno-associated virus type 2 and 5 capsid proteins affects the transduction efficiency of recombinant vectors.,” *J. Virol.*, vol. 76, no. 5, pp. 2043–53, Mar. 2002.

[9] J. A. Chiorini, F. Kim, L. Yang, and R. M. Kotin, “Cloning and characterization of adeno-associated virus type 5.,” *J. Virol.*, vol. 73, no. 2, pp. 1309–1319, Feb. 1999.

[10] S. Pillay *et al.*, “An essential receptor for adeno-associated virus infection,” *Nature*, vol. 530, no. 7588, pp. 108–12, Jan. 2016.

[11] A. M. Dudek *et al.*, “An Alternate Route for Adeno-associated Virus (AAV) Entry Independent of AAV Receptor.,” *J. Virol.*, vol. 92, no. 7, Apr. 2018.

[12] B. Akache, D. Grimm, K. Pandey, S. R. Yant, H. Xu, and M. A. Kay, “The 37/67-kilodalton laminin receptor is a receptor for adeno-associated virus serotypes 8, 2, 3, and 9.,” *J. Virol.*, vol. 80, no. 19, pp. 9831–9836, Oct. 2006.

[13] Y. Kashiwakura *et al.*, “Hepatocyte growth factor receptor is a coreceptor for adeno-associated virus type 2 infection.,” *J. Virol.*, vol. 79, no. 1, pp. 609–14, Jan. 2005.

[14] K. Qing, C. Mah, J. Hansen, S. Zhou, V. Dwarki, and A. Srivastava, “Human fibroblast growth factor receptor 1 is a co-receptor for infection by adeno-associated virus

2," *Nat. Med.*, vol. 5, no. 1, pp. 71–77, 1999.

[15] C. Summerford and R. J. Samulski, "Membrane-associated heparan sulfate proteoglycan is a receptor for adeno-associated virus type 2 virions.," *J. Virol.*, vol. 72, no. 2, pp. 1438–45, Feb. 1998.

[16] M. Mietzsch, F. Broecker, A. Reinhardt, P. H. Seeberger, R. Heilbronn, and M. J. Imperiale, "Differential Adeno-Associated Virus Serotype-Specific Interaction Patterns with Synthetic Heparins and Other Glycans," *J. Virol.*, vol. 88, no. 5, pp. 2991–3003, Mar. 2014.

[17] A. Handa, S. I. Muramatsu, J. Qiu, H. Mizukami, and K. E. Brown, "Adeno-associated virus (AAV)-3-based vectors transduce haematopoietic cells not susceptible to transduction with AAV-2-based vectors," *J. Gen. Virol.*, vol. 81, no. 8, pp. 2077–2084, 2000.

[18] G. Di Pasquale *et al.*, "Identification of PDGFR as a receptor for AAV-5 transduction," *Nat. Med.*, vol. 9, no. 10, pp. 1306–1312, Oct. 2003.

[19] Addgene, "Adeno-associated Virus (AAV) Guide," *https://www.addgene.org/guides/aav/*. .

[20] J. A. Rose, K. I. Berns, M. D. Hoggan, and F. J. Koczot, "Evidence for a single-stranded adenovirus-associated virus genome: formation of a DNA density hybrid on release of viral DNA.," *Proc. Natl. Acad. Sci. U. S. A.*, vol. 64, no. 3, pp. 863–869, Nov. 1969.

[21] B. J. Carter, G. Khoury, and D. T. Denhardt, "Physical map and strand polarity of specific fragments of adenovirus-associated virus DNA produced by endonuclease R-EcoRI.," *J. Virol.*, vol. 16, no. 3, pp. 559–568, Sep. 1975.

[22] F. T. Jay, C. A. Laughlin, and B. J. Carter, "Eukaryotic translational control: adeno-associated virus protein synthesis is affected by a mutation in the adenovirus DNA-binding protein.," *Proc. Natl. Acad. Sci. U. S. A.*, vol. 78, no. 5, pp. 2927–2931, May 1981.

[23] F. Sonntag, K. Schmidt, and J. A. Kleinschmidt, "A viral assembly factor promotes AAV2 capsid formation in the nucleolus.," *Proc. Natl. Acad. Sci. U. S. A.*, vol. 107, no. 22, pp. 10220–5, Jun. 2010.

[24] S. E. Straus, E. D. Sebring, and J. A. Rose, "Concatemers of alternating plus and minus strands are intermediates in adenovirus associated virus DNA synthesis," *Proc. Natl. Acad. Sci. U. S. A.*, vol. 73, no. 3, pp. 742–746, 1976.

[25] R. J. Samulski, L. S. Chang, and T. Shenk, "A recombinant plasmid from which an infectious adeno-associated virus genome can be excised in vitro and its use to study viral replication.," *J. Virol.*, vol. 61, no. 10, pp. 3096–3101, Oct. 1987.

[26] L. Galibert and O. W. Merten, "Latest developments in the large-scale production of adeno-associated virus vectors in insect cells toward the treatment of neuromuscular diseases," *Journal of Invertebrate Pathology*, vol. 107, no. SUPPL. Jul-2011.

[27] D. J. Pereira, D. M. McCarty, and N. Muzyczka, "The adeno-associated virus (AAV) Rep protein acts as both a repressor and an activator to regulate AAV transcription during a productive infection.," *J. Virol.*, vol. 71, no. 2, pp. 1079–88, Feb. 1997.

[28] S. R. Kyöstiö, R. A. Owens, M. D. Weitzman, B. A. Antoni, N. Chejanovsky, and B. J. Carter, "Analysis of adeno-associated virus (AAV) wild-type and mutant Rep proteins for their abilities to negatively regulate AAV p5 and p19 mRNA levels.," *J. Virol.*, vol. 68, no. 5, pp. 2947–57, May 1994.

[29] J. A. King, R. Dubielzig, D. Grimm, and J. A. Kleinschmidt, "DNA helicase-mediated packaging of adeno-associated virus type 2 genomes into preformed capsids," *EMBO J.*, vol. 20, no. 12, pp. 3282–3291, Jun. 2001.

[30] R. M. Kotin, R. M. Linden, and K. I. Berns, "Characterization of a preferred site on human chromosome 19q for integration of adeno-associated virus DNA by non-homologous recombination.," *EMBO J.*, vol. 11, no. 13, pp. 5071–5078, Dec. 1992.

[31] S. Smith-Moore *et al.*, "Adeno-associated virus Rep proteins antagonize phosphatase PP1 to counteract KAP1 repression of the latent viral genome," *Proc. Natl. Acad. Sci. U. S. A.*, vol. 115, no. 15, pp. E3529–E3538, 2018.

[32] A. Girod *et al.*, "The VP1 capsid protein of adeno-associated virus type 2 is carrying a phospholipase A2 domain required for virus infectivity.," *J. Gen. Virol.*, vol. 83, no. Pt 5, pp. 973–8, May 2002.

[33] Z. Zádori *et al.*, "A Viral Phospholipase A2 Is Required for Parvovirus Infectivity," *Dev. Cell*, vol. 1, no. 2, pp. 291–302, Aug. 2001.

[34] J. J. Kurian *et al.*, "Adeno-associated virus VP1u exhibits protease activity," *Viruses*, vol. 11, no. 5, May 2019.

[35] S. P. Becerra, F. Koczot, P. Fabisch, and J. A. Rose, "Synthesis of adeno-associated virus structural proteins requires both alternative mRNA splicing and alternative initiations from a single transcript.," *J. Virol.*, vol. 62, no. 8, pp. 2745–54, Aug. 1988.

[36] K. H. Warrington, O. S. Gorbatyuk, J. K. Harrison, S. R. Opie, S. Zolotukhin, and N. Muzyczka, "Adeno-Associated Virus Type 2 VP2 Capsid Protein Is Nonessential and Can Tolerate Large Peptide Insertions at Its N Terminus," *J. Virol.*, vol. 78, no. 12, pp. 6595–6609, Jun. 2004.

[37] F. Sonntag *et al.*, "The assembly-activating protein promotes capsid assembly of different adeno-associated virus serotypes.," *J. Virol.*, vol. 85, no. 23, pp. 12686–97, Dec. 2011.

[38] L. F. Earley *et al.*, "Adeno-associated Virus (AAV) Assembly-Activating Protein Is Not an Essential Requirement for Capsid Assembly of AAV Serotypes 4, 5, and 11," *J. Virol.*, vol. 91, no. 3, Feb. 2017.

[39] M. Naumer *et al.*, "Properties of the adeno-associated virus assembly-activating protein.," *J. Virol.*, vol. 86, no. 23, pp. 13038–48, Dec. 2012.

[40] M. S. Chapman and M. G. Rossmann, "Structure, sequence, and function

correlations among parvoviruses," *Virology*, vol. 194, no. 2, pp. 491–508, 1993.

[41] B. Akache *et al.*, "A two-hybrid screen identifies cathepsins B and L as uncoating factors for adeno-associated virus 2 and 8.," *Mol. Ther.*, vol. 15, no. 2, pp. 330–9, Feb. 2007.

[42] S. Kronenberg, B. Böttcher, C. W. von der Lieth, S. Bleker, and J. A. Kleinschmidt, "A conformational change in the adeno-associated virus type 2 capsid leads to the exposure of hidden VP1 N termini.," *J. Virol.*, vol. 79, no. 9, pp. 5296–303, May 2005.

[43] Q. Xie *et al.*, "The atomic structure of adeno-associated virus (AAV-2), a vector for human gene therapy.," *Proc. Natl. Acad. Sci. U. S. A.*, vol. 99, no. 16, pp. 10405–10, Aug. 2002.

[44] Y.-S. Tseng and M. Agbandje-McKenna, "Mapping the AAV Capsid Host Antibody Response toward the Development of Second Generation Gene Delivery Vectors.," *Front. Immunol.*, vol. 5, p. 9, Jan. 2014.

[45] Z. Wu, E. Miller, M. Agbandje-McKenna, and R. J. Samulski, "Alpha2,3 and alpha2,6 N-linked sialic acids facilitate efficient binding and transduction by adeno-associated virus types 1 and 6.," *J. Virol.*, vol. 80, no. 18, pp. 9093–103, Sep. 2006.

[46] N. Kaludov, K. E. Brown, R. W. Walters, J. Zabner, and J. A. Chiorini, "Adeno-Associated Virus Serotype 4 (AAV4) and AAV5 Both Require Sialic Acid Binding for Hemagglutination and Efficient Transduction but Differ in Sialic Acid Linkage Specificity," *J. Virol.*, vol. 75, no. 15, pp. 6884–6893, Aug. 2001.

[47] R. W. Walters *et al.*, "Binding of Adeno-associated Virus Type 5 to 2,3-Linked Sialic Acid is Required for Gene Transfer," *J. Biol. Chem.*, vol. 276, no. 23, pp. 20610–20616, Jun. 2001.

[48] S. Shen, K. D. Bryant, S. M. Brown, S. H. Randell, and A. Asokan, "Terminal n-linked galactose is the primary receptor for adeno-associated virus," *J. Biol. Chem.*, vol. 286, no. 15, pp. 13532–13540, Apr. 2011.

[49] C. Summerford, J. S. Bartlett, and R. J. Samulski, "αVβ5 integrin: A co-receptor for adeno-associated virus type 2 infection," *Nat. Med.*, vol. 5, no. 1, pp. 78–82, 1999.

[50] C. Kurzeder, B. Koppold, G. Sauer, S. Pabst, R. Kreienberg, and H. Deissler, "CD9 promotes adeno-associated virus type 2 infection of mammary carcinoma cells with low cell surface expression of heparan sulphate proteoglycans," *Int. J. Mol. Med.*, vol. 19, no. 2, pp. 325–333, Feb. 2007.

[51] M. Nonnenmacher and T. Weber, "Adeno-associated virus 2 infection requires endocytosis through the CLIC/GEEC pathway.," *Cell Host Microbe*, vol. 10, no. 6, pp. 563–76, Dec. 2011.

[52] S. Sanlioglu, P. K. Benson, J. Yang, E. M. Atkinson, T. Reynolds, and J. F. Engelhardt, "Endocytosis and Nuclear Trafficking of Adeno-Associated Virus Type 2 Are Controlled by Rac1 and Phosphatidylinositol-3 Kinase Activation," *J. Virol.*, vol. 74, no. 19, pp. 9184–9196, Oct. 2000.

[53] J. S. Bartlett, R. Wilcher, and R. J. Samulski, "Infectious entry pathway of adeno-associated virus and adeno-associated virus vectors.," *J. Virol.*, vol. 74, no. 6, pp. 2777–85, Mar. 2000.

[54] A. M. Douar, K. Poulard, D. Stockholm, and O. Danos, "Intracellular trafficking of adeno-associated virus vectors: routing to the late endosomal compartment and proteasome degradation.," *J. Virol.*, vol. 75, no. 4, pp. 1824–33, Feb. 2001.

[55] S. Stahnke *et al.*, "Intrinsic phospholipase A2 activity of adeno-associated virus is involved in endosomal escape of incoming particles," *Virology*, vol. 409, no. 1, pp. 77–83, Jan. 2011.

[56] A. Girod *et al.*, "The VP1 capsid protein of adeno-associated virus type 2 is carrying a phospholipase A2 domain required for virus infectivity," *J. Gen. Virol.*, vol. 83, no. 5, pp. 973–978, 2002.

[57] S. C. Nicolson and R. J. Samulski, "Recombinant Adeno-Associated Virus Utilizes Host Cell Nuclear Import Machinery To Enter the Nucleus," *J. Virol.*, vol. 88, no. 8, pp. 4132–4144, Apr. 2014.

[58] J. C. Grieger, S. Snowdy, and R. J. Samulski, "Separate basic region motifs within the adeno-associated virus capsid proteins are essential for infectivity and assembly.," *J. Virol.*, vol. 80, no. 11, pp. 5199–210, Jun. 2006.

[59] F. Sonntag, S. Bleker, B. Leuchs, R. Fischer, and J. A. Kleinschmidt, "Adeno-Associated Virus Type 2 Capsids with Externalized VP1/VP2 Trafficking Domains Are Generated prior to Passage through the Cytoplasm and Are Maintained until Uncoating Occurs in the Nucleus," *J. Virol.*, vol. 80, no. 22, pp. 11040–11054, Nov. 2006.

[60] M. E. Nonnenmacher, J.-C. Cintrat, D. Gillet, and T. Weber, "Syntaxin 5-dependent retrograde transport to the trans-Golgi network is required for adeno-associated virus transduction.," *J. Virol.*, vol. 89, no. 3, pp. 1673–87, Feb. 2015.

[61] U. Bantel-Schaal, B. Hub, and J. Kartenbeck, "Endocytosis of Adeno-Associated Virus Type 5 Leads to Accumulation of Virus Particles in the Golgi Compartment," *J. Virol.*, vol. 76, no. 5, pp. 2340–2349, Mar. 2002.

[62] J. S. Johnson and R. J. Samulski, "Enhancement of adeno-associated virus infection by mobilizing capsids into and out of the nucleolus.," *J. Virol.*, vol. 83, no. 6, pp. 2632–44, Mar. 2009.

[63] S. F. Cotmore, A. M. D'Abramo, C. M. Ticknor, and P. Tattersall, "Controlled conformational transitions in the MVM virion expose the VP1 N-terminus and viral genome without particle disassembly," *Virology*, vol. 254, no. 1, pp. 169–181, Feb. 1999.

[64] C. Ros, C. Baltzer, B. Mani, and C. Kempf, "Parvovirus uncoating in vitro reveals a mechanism of DNA release without capsid disassembly and striking differences in encapsidated DNA stability," *Virology*, vol. 345, no. 1, pp. 137–147, Feb. 2006.

[65] I. Sipo *et al.*, "Differential internalization and nuclear uncoating of self-complementary adeno-associated virus pseudotype vectors as determinants of cardiac cell transduction," *Gene Ther.*, vol. 14, no. 18, pp. 1319–1329, Sep. 2007.

[66] C. E. Thomas, T. A. Storm, Z. Huang, and M. A. Kay, "Rapid Uncoating of Vector Genomes Is the Key to Efficient Liver Transduction with Pseudotyped Adeno-Associated Virus Vectors," *J. Virol.*, vol. 78, no. 6, pp. 3110–3122, Mar. 2004.

[67] S. Daya and K. I. Berns, "Gene therapy using adeno-associated virus vectors.," *Clin. Microbiol. Rev.*, vol. 21, no. 4, pp. 583–93, Oct. 2008.

[68] S. Pillay and J. E. Carette, "Host determinants of adeno-associated viral vector entry," *Current Opinion in Virology*, vol. 24. Elsevier B.V., pp. 124–131, 01-Jun-2017.

[69] R. J. Samulski and T. Shenk, "Adenovirus E1B 55-Mr polypeptide facilitates timely cytoplasmic accumulation of adeno-associated virus mRNAs.," *J. Virol.*, vol. 62, no. 1, pp. 206–10, Jan. 1988.

[70] H. Nakai, T. A. Storm, and M. A. Kay, "Recruitment of Single-Stranded Recombinant Adeno-Associated Virus Vector Genomes and Intermolecular Recombination Are Responsible for Stable Transduction of Liver In Vivo," *J. Virol.*, vol. 74, no. 20, pp. 9451–9463, Oct. 2000.

[71] K. J. Fisher, G. P. Gao, M. D. Weitzman, R. DeMatteo, J. F. Burda, and J. M. Wilson, "Transduction with recombinant adeno-associated virus for gene therapy is limited by leading-strand synthesis.," *J. Virol.*, vol. 70, no. 1, pp. 520–32, Jan. 1996.

[72] F. K. Ferrari, T. Samulski, T. Shenk, and R. J. Samulski, "Second-strand synthesis is a rate-limiting step for efficient transduction by recombinant adeno-associated virus vectors.," *J. Virol.*, vol. 70, no. 5, pp. 3227–34, May 1996.

[73] T. H. Ni *et al.*, "Cellular proteins required for adeno-associated virus DNA replication in the absence of adenovirus coinfection.," *J. Virol.*, vol. 72, no. 4, pp. 2777–87, Apr. 1998.

[74] N. Chejanovsky and B. J. Carter, "Mutagenesis of an AUG codon in the adeno-associated virus rep gene: Effects on viral DNA replication," *Virology*, vol. 173, no. 1, pp. 120–128, 1989.

[75] B. J. Carter, C. J. Marcus-Sekura, C. A. Laughlin, and G. Ketner, "Properties of an adenovirus type 2 mutant, Ad2dl807, having a deletion near the right-hand genome terminus: failure to help AAV replication.," *Virology*, vol. 126, no. 2, pp. 505–16, Apr. 1983.

[76] L. S. Chang and T. Shenk, "The adenovirus DNA-binding protein stimulates the rate of transcription directed by adenovirus and adeno-associated virus promoters.," *J. Virol.*, vol. 64, no. 5, pp. 2103–9, May 1990.

[77] J. E. Janik, M. M. Huston, K. Cho, and J. A. Rose, "Efficient synthesis of adeno-associated virus structural proteins requires both adenovirus DNA binding protein and VA I RNA.," *Virology*, vol. 168, no. 2, pp. 320–9, Feb. 1989.

[78] J. A. King, R. Dubielzig, D. Grimm, and J. A. Kleinschmidt, "DNA helicase-mediated packaging of adeno-associated virus type 2 genomes into preformed capsids.,"

EMBO J., vol. 20, no. 12, pp. 3282–91, Jun. 2001.

[79] S. Bleker, F. Sonntag, and J. A. Kleinschmidt, "Mutational analysis of narrow pores at the fivefold symmetry axes of adeno-associated virus type 2 capsids reveals a dual role in genome packaging and activation of phospholipase A2 activity.," *J. Virol.*, vol. 79, no. 4, pp. 2528–40, Feb. 2005.

[80] M.-C. Geoffroy and A. Salvetti, "Helper functions required for wild type and recombinant adeno-associated virus growth.," *Curr. Gene Ther.*, vol. 5, no. 3, pp. 265–71, Jun. 2005.

[81] C. Balagúe, M. Kalla, and W. W. Zhang, "Adeno-associated virus Rep78 protein and terminal repeats enhance integration of DNA sequences into the cellular genome.," *J. Virol.*, vol. 71, no. 4, pp. 3299–306, Apr. 1997.

[82] J. A. Chiorini, S. M. Wiener, R. A. Owens, S. R. Kyöstió, R. M. Kotin, and B. Safer, "Sequence requirements for stable binding and function of Rep68 on the adeno-associated virus type 2 inverted terminal repeats.," *J. Virol.*, vol. 68, no. 11, pp. 7448–7457, Nov. 1994.

[83] A. Ö. Yalklnoglu, R. Heilbronn, A. Bürkle, J. R. Schlehofer, and H. Zur Hausen, "Dna amplification of adeno-associated virus as a response to cellular genotoxic stress," *Cancer Res.*, vol. 48, no. 11, pp. 3123–3129, 1988.

[84] X. Xiao, J. Li, and R. J. Samulski, "Production of high-titer recombinant adeno-associated virus vectors in the absence of helper adenovirus.," *J. Virol.*, vol. 72, no. 3, pp. 2224–32, Mar. 1998.

[85] T. Matsushita *et al.*, "Adeno-associated virus vectors can be efficiently produced without helper virus," *Gene Ther.*, vol. 5, no. 7, pp. 938–945, 1998.

[86] D. Grimm, A. Kern, K. Rittner, and J. A. Kleinschmidt, "Novel tools for production and purification of recombinant adenoassociated virus vectors," *Hum. Gene Ther.*, vol. 9, no. 18, pp. 2745–2760, Dec. 1998.

[87] C. Qiao, B. Wang, X. Zhu, J. Li, and X. Xiao, "A Novel Gene Expression Control System and Its Use in Stable, High-Titer 293 Cell-Based Adeno-Associated Virus Packaging Cell Lines," *J. Virol.*, vol. 76, no. 24, pp. 13015–13027, Dec. 2002.

[88] G. Chadeuf *et al.*, "Efficient recombinant adeno-associated virus production by a stable rep-cap HeLa cell line correlates with adenovirus-induced amplification of the integrated rep-cap genome.," *J. Gene Med.*, vol. 2, no. 4, pp. 260–8.

[89] G. P. Gao *et al.*, "High-titer adeno-associated viral vectors from a Rep/Cap cell line and hybrid shuttle virus," *Hum. Gene Ther.*, vol. 9, no. 16, pp. 2353–2362, Nov. 1998.

[90] M. Urabe, C. Ding, and R. M. Kotin, "Insect cells as a factory to produce adeno-associated virus type 2 vectors," *Hum. Gene Ther.*, vol. 13, no. 16, pp. 1935–1943, 2002.

[91] A. Auricchio, M. Hildinger, E. O'Connor, G. P. Gao, and J. M. Wilson, "Isolation of highly infectious and pure adeno-associated virus type 2 vectors with a single-

step gravity-flow column," *Hum. Gene Ther.*, vol. 12, no. 1, pp. 71–76, Jan. 2001.

[92] A. Auricchio, E. O'Connor, M. Hildinger, and J. M. Wilson, "A single-step affinity column for purification of serotype-5 based adeno-associated viral vectors," *Mol. Ther.*, vol. 4, no. 4, pp. 372–374, 2001.

[93] N. Kaludov, B. Handelman, and J. A. Chiorini, "Scalable purification of adeno-associated virus type 2, 4, or 5 using ion-exchange chromatography," *Hum. Gene Ther.*, vol. 13, no. 10, pp. 1235–1243, 2002.

[94] J. E. Rabinowitz and R. J. Samulski, "Building a better vector: The manipulation of AAV virions," *Virology*, vol. 278, no. 2, pp. 301–308, 2000.

[95] D. Grimm and M. Kay, "From Virus Evolution to Vector Revolution: Use of Naturally Occurring Serotypes of Adeno-associated Virus (AAV) as Novel Vectors for Human Gene Therapy," *Curr. Gene Ther.*, vol. 3, no. 4, pp. 281–304, Jul. 2005.

[96] B. E. Deverman *et al.*, "Cre-dependent selection yields AAV variants for widespread gene transfer to the adult brain," *Nat. Biotechnol.*, vol. 34, no. 2, pp. 204–209, Feb. 2016.

[97] M. A. Kotterman and D. V. Schaffer, "Engineering adeno-associated viruses for clinical gene therapy," *Nat. Rev. Genet.*, vol. 15, no. 7, pp. 445–451, 2014.

[98] J. Weinmann and D. Grimm, "Next-generation AAV vectors for clinical use: an ever-accelerating race," *Virus Genes*, vol. 53, no. 5. Springer New York LLC, pp. 707–713, 01-Oct-2017.

[99] Z. Yan, T. C. Ritchie, D. Duan, and J. F. Engelhardt, "Recombinant AAV-mediated gene delivery using dual vector heterodimerization.," *Methods Enzymol.*, vol. 346, pp. 334–57, 2002.

[100] J. C. Grieger and R. J. Samulski, "Packaging Capacity of Adeno-Associated Virus Serotypes: Impact of Larger Genomes on Infectivity and Postentry Steps," *J. Virol.*, vol. 79, no. 15, pp. 9933–9944, Aug. 2005.

[101] A. Ghosh and D. Duan, "Expanding adeno-associated viral vector capacity: A tale of two vectors," *Biotechnol. Genet. Eng. Rev.*, vol. 24, no. 1, pp. 165–178, 2007.

[102] P. E. Monahan *et al.*, "Proteasome inhibitors enhance gene delivery by AAV virus vectors expressing large genomes in hemophilia mouse and dog models: A strategy for broad clinical application," *Mol. Ther.*, vol. 18, no. 11, pp. 1907–1916, 2010.

[103] C. D. Scallan *et al.*, "Phenotypic correction of a mouse model of hemophilia A using AAV2 vectors encoding the heavy and light chains of FVIII," *Blood*, vol. 102, no. 12, pp. 3919–3926, Dec. 2003.

[104] J. Li, W. Sun, B. Wang, X. Xiao, and X. Q. Liu, "Protein trans-splicing as a means for viral vector-mediated in vivo gene therapy," *Hum. Gene Ther.*, vol. 19, no. 9, pp. 958–964, Sep. 2008.

[105] D. M. McCarty, P. E. Monahan, and R. J. Samulski, "Self-complementary

recombinant adeno-associated virus (scAAV) vectors promote efficient transduction independently of DNA synthesis," *Gene Ther.*, vol. 8, no. 16, pp. 1248–1254, 2001.

[106] A. C. Nathwani *et al.*, "Long-term safety and efficacy following systemic administration of a self-complementary AAV vector encoding human FIX pseudotyped with serotype 5 and 8 capsid proteins," *Mol. Ther.*, vol. 19, no. 5, pp. 876–885, 2011.

[107] J. R. Mendell *et al.*, "Single-dose gene-replacement therapy for spinal muscular atrophy," *N. Engl. J. Med.*, vol. 377, no. 18, pp. 1713–1722, Nov. 2017.

[108] S. Russell *et al.*, "Efficacy and safety of voretigene neparvovec (AAV2-hRPE65v2) in patients with RPE65-mediated inherited retinal dystrophy: a randomised, controlled, open-label, phase 3 trial," *Lancet*, vol. 390, no. 10097, pp. 849–860, Aug. 2017.

[109] D. Gaudet *et al.*, "Long-Term Retrospective Analysis of Gene Therapy with Alipogene Tiparvovec and Its Effect on Lipoprotein Lipase Deficiency-Induced Pancreatitis," *Hum. Gene Ther.*, vol. 27, no. 11, pp. 916–925, Nov. 2016.

[110] V. Ferreira *et al.*, "Immune responses to intramuscular administration of alipogene tiparvovec (AAV1-LPLS447X) in a phase II Clinical trial of lipoprotein lipase deficiency gene therapy," *Hum. Gene Ther.*, vol. 25, no. 3, pp. 180–188, Mar. 2014.

[111] S. Al-Zaidy *et al.*, "Health outcomes in spinal muscular atrophy type 1 following AVXS-101 gene replacement therapy," *Pediatr. Pulmonol.*, vol. 54, no. 2, pp. 179–185, Feb. 2019.

[112] J.-M. Peters, W. W. Frankes, and J. A. Kleinschmidt, "Distinct 19 S and 20 S Subcomplexes of the 26 S Proteasome and Their Distribution in the Nucleus and the Cytoplasm.," 1994.

[113] A. Hershko and A. Ciechanover, "The Ubiquitin System for Protein Degradation," *Annu. Rev. Biochem.*, vol. 61, no. 1, pp. 761–807, Jun. 1992.

[114] J. H. Seol *et al.*, "Cdc53/cullin and the essential Hrt1 RING-H2 subunit of SCF define a ubiquitin ligase module that activates the E2 enzyme Cdc34," *Genes Dev.*, vol. 13, no. 12, pp. 1614–1626, Jun. 1999.

[115] T. Kamura *et al.*, "Rbx1, a component of the VHL tumor suppressor complex and SCF ubiquitin ligase," *Science (80-.).*, vol. 284, no. 5414, pp. 657–661, Apr. 1999.

[116] T. Ohta, J. J. Michel, A. J. Schottelius, and Y. Xiong, "ROC1, a homolog of APC11, represents a family of cullin partners with an associated ubiquitin ligase activity," *Mol. Cell*, vol. 3, no. 4, pp. 535–541, 1999.

[117] J. M. Huibregtse, M. Scheffner, and P. M. Howley, "A cellular protein mediates association of p53 with the E6 oncoprotein of human papillomavirus types 16 or 18.," *EMBO J.*, vol. 10, no. 13, pp. 4129–4135, Dec. 1991.

[118] M. Scheffner, J. M. Huibregtse, R. D. Vierstra, and P. M. Howley, "The HPV-16 E6 and E6-AP complex functions as a ubiquitin-protein ligase in the ubiquitination of

p53," *Cell*, vol. 75, no. 3, pp. 495–505, Nov. 1993.

[119] J. M. Huibregtse, M. Scheffner, S. Beaudenon, and P. M. Howley, "A family of proteins structurally and functionally related to the E6-AP ubiquitin-protein ligase," *Proc. Natl. Acad. Sci. U. S. A.*, vol. 92, no. 7, pp. 2563–2567, Mar. 1995.

[120] T. Kirisako *et al.*, "A ubiquitin ligase complex assembles linear polyubiquitin chains," *EMBO J.*, vol. 25, no. 20, pp. 4877–4887, Oct. 2006.

[121] F. Tokunaga *et al.*, "Involvement of linear polyubiquitylation of NEMO in NF-κB activation," *Nat. Cell Biol.*, vol. 11, no. 2, pp. 123–132, 2009.

[122] A. Plechanovov, E. G. Jaffray, M. H. Tatham, J. H. Naismith, and R. T. Hay, "Structure of a RING E3 ligase and ubiquitin-loaded E2 primed for catalysis," *Nature*, vol. 489, no. 7414, pp. 115–120, Sep. 2012.

[123] E. Maspero *et al.*, "Structure of the HECT:ubiquitin complex and its role in ubiquitin chain elongation," *EMBO Rep.*, vol. 12, no. 4, pp. 342–349, Apr. 2011.

[124] J. F. Trempe *et al.*, "Structure of parkin reveals mechanisms for ubiquitin ligase activation," *Science (80-.).*, vol. 340, no. 6139, pp. 1451–1455, 2013.

[125] D. M. Duda *et al.*, "Structure of HHARI, a RING-IBR-RING ubiquitin ligase: Autoinhibition of an Ariadne-family E3 and insights into ligation mechanism," *Structure*, vol. 21, no. 6, pp. 1030–1041, Jun. 2013.

[126] D. Komander, M. J. Clague, and S. Urbé, "Breaking the chains: Structure and function of the deubiquitinases," *Nature Reviews Molecular Cell Biology*, vol. 10, no. 8. pp. 550–563, Aug-2009.

[127] Q. Zheng *et al.*, "Dysregulation of ubiquitin-proteasome system in neurodegenerative diseases," *Frontiers in Aging Neuroscience*, vol. 8, no. DEC. Frontiers Media S.A., 2016.

[128] D. Skowyra, K. L. Craig, M. Tyers, S. J. Elledge, and J. W. Harper, "F-box proteins are receptors that recruit phosphorylated substrates to the SCF ubiquitin-ligase complex.," *Cell*, vol. 91, no. 2, pp. 209–19, Oct. 1997.

[129] R. M. R. Feldman, C. C. Correll, K. B. Kaplan, and R. J. Deshaies, "A complex of Cdc4p, Skp1p, and Cdc53p/cullin catalyzes ubiquitination of the phosphorylated CDK inhibitor Sic1p," *Cell*, vol. 91, no. 2, pp. 221–230, Oct. 1997.

[130] A. Saha and R. J. Deshaies, "Multimodal Activation of the Ubiquitin Ligase SCF by Nedd8 Conjugation," *Mol. Cell*, vol. 32, no. 1, pp. 21–31, Oct. 2008.

[131] B. K. Boh, P. G. Smith, and T. Hagen, "Neddylation-induced conformational control regulates cullin RING ligase activity in vivo," *J. Mol. Biol.*, vol. 409, no. 2, pp. 136–145, Jun. 2011.

[132] A. C. Andérica-Romero, I. G. González-Herrera, A. Santamaría, and J. Pedraza-Chaverri, "Cullin 3 as a novel target in diverse pathologies," *Redox Biology*, vol. 1, no. 1. Elsevier B.V., pp. 366–372, 2013.

[133] L. Xu *et al.*, "BTB proteins are substrate-specific adaptors in an SCF-like modular

ubiquitin ligase containing CUL-3," *Nature*, vol. 425, no. 6955, pp. 316–321, Sep. 2003.

[134] R. Geyer, S. Wee, S. Anderson, J. Yates, and D. A. Wolf, "BTB/POZ domain proteins are putative substrate adaptors for cullin 3 ubiquitin ligases.," *Mol. Cell*, vol. 12, no. 3, pp. 783–90, Sep. 2003.

[135] M. Furukawa, Y. J. He, C. Borchers, and Y. Xiong, "Targeting of protein ubiquitination by BTB-Cullin 3-Roc1 ubiquitin ligases," *Nat. Cell Biol.*, vol. 5, no. 11, pp. 1001–1007, Nov. 2003.

[136] S. Zollman, D. Godt, G. G. Privé, J. L. Couderc, and F. A. Laski, "The BTB domain, found primarily in zinc finger proteins, defines an evolutionarily conserved family that includes several developmentally regulated genes in Drosophila," *Proc. Natl. Acad. Sci. U. S. A.*, vol. 91, no. 22, pp. 10717–10721, Oct. 1994.

[137] P. J. Stogios, G. S. Downs, J. J. S. Jauhal, S. K. Nandra, and G. G. Privé, "Sequence and structural analysis of BTB domain proteins.," *Genome Biol.*, vol. 6, no. 10, 2005.

[138] P. Canning *et al.*, "Structural basis for Cul3 protein assembly with the BTB-Kelch family of E3 ubiquitin ligases," *J. Biol. Chem.*, vol. 288, no. 11, pp. 7803–7814, Mar. 2013.

[139] M. Zhuang *et al.*, "Structures of SPOP-substrate complexes: insights into molecular architectures of BTB-Cul3 ubiquitin ligases.," *Mol. Cell*, vol. 36, no. 1, pp. 39–50, Oct. 2009.

[140] D. Moreau *et al.*, "Genome-Wide RNAi Screens Identify Genes Required for Ricin and PE Intoxications," *Dev. Cell*, vol. 21, no. 2, pp. 231–244, Aug. 2011.

[141] S. Luke-Glaser, L. Pintard, M. Tyers, and M. Peter, "The AAA-ATPase FIGL-1 controls mitotic progression, and its levels are regulated by the CUL-3MEL-26 E3 ligase in the C. elegans germ line," *J. Cell Sci.*, vol. 120, no. 18, pp. 3179–3187, Sep. 2007.

[142] D. D. Zhang, S.-C. Lo, J. V. Cross, D. J. Templeton, and M. Hannink, "Keap1 Is a Redox-Regulated Substrate Adaptor Protein for a Cul3-Dependent Ubiquitin Ligase Complex," *Mol. Cell. Biol.*, vol. 24, no. 24, pp. 10941–10953, Dec. 2004.

[143] A. Kobayashi *et al.*, "Oxidative Stress Sensor Keap1 Functions as an Adaptor for Cul3-Based E3 Ligase To Regulate Proteasomal Degradation of Nrf2," *Mol. Cell. Biol.*, vol. 24, no. 16, pp. 7130–7139, Aug. 2004.

[144] Y. Chen *et al.*, "Cullin Mediates Degradation of RhoA through Evolutionarily Conserved BTB Adaptors to Control Actin Cytoskeleton Structure and Cell Movement," *Mol. Cell*, vol. 35, no. 6, pp. 841–855, Sep. 2009.

[145] J. D. Singer, M. Gurian-West, B. Clurman, and J. M. Roberts, "Cullin-3 targets cyclin E for ubiquitination and controls S phase in mammalian cells," *Genes Dev.*, vol. 13, no. 18, pp. 2375–2387, Sep. 1999.

[146] Y. Nagai *et al.*, "Identification of a novel nuclear speckle-type protein, SPOP.," *FEBS Lett.*, vol. 418, no. 1–2, pp. 23–6, Nov. 1997.

[147] I. Hernández-Muñoz *et al.*, "Stable X chromosome inactivation involves the PRC1 Polycomb complex and requires histone MACROH2A1 and the CULLIN3/SPOP ubiquitin E3 ligase.," *Proc. Natl. Acad. Sci. U. S. A.*, vol. 102, no. 21, pp. 7635–40, May 2005.

[148] J. E. Kwon *et al.*, "BTB domain-containing speckle-type POZ protein (SPOP) serves as an adaptor of Daxx for ubiquitination by Cul3-based ubiquitin ligase.," *J. Biol. Chem.*, vol. 281, no. 18, pp. 12664–72, May 2006.

[149] T. Sakaue *et al.*, "The CUL3-SPOP-DAXX axis is a novel regulator of VEGFR2 expression in vascular endothelial cells," *Sci. Rep.*, vol. 7, Feb. 2017.

[150] L. K. Van Geersdaele *et al.*, "Structural basis of high-order oligomerization of the cullin-3 adaptor SPOP," *Acta Crystallogr. Sect. D Biol. Crystallogr.*, vol. 69, no. 9, pp. 1677–1684, Sep. 2013.

[151] M. R. Marzahn *et al.*, " Higher-order oligomerization promotes localization of SPOP to liquid nuclear speckles ," *EMBO J.*, vol. 35, no. 12, pp. 1254–1275, Jun. 2016.

[152] J. J. Bouchard *et al.*, "Cancer Mutations of the Tumor Suppressor SPOP Disrupt the Formation of Active, Phase-Separated Compartments," *Mol. Cell*, vol. 72, no. 1, pp. 19-36.e8, Oct. 2018.

[153] M. S. Ostertag, A. C. Messias, M. Sattler, and G. M. Popowicz, "The Structure of the SPOP-Pdx1 Interface Reveals Insights into the Phosphorylation-Dependent Binding Regulation," *Structure*, vol. 27, no. 2, pp. 327-334.e3, Feb. 2019.

[154] G. Polekhina *et al.*, "Siah ubiquitin ligase is structurally related to traf and modulates tnf-α signaling," *Nat. Struct. Biol.*, vol. 9, no. 1, pp. 68–75, 2002.

[155] Q. Yin *et al.*, "E2 interaction and dimerization in the crystal structure of TRAF6," *Nat. Struct. Mol. Biol.*, vol. 16, no. 6, pp. 658–666, Jun. 2009.

[156] G. Li *et al.*, "SPOP promotes tumorigenesis by acting as a key regulatory hub in kidney cancer," *Cancer Cell*, vol. 25, no. 4, pp. 455–468, Apr. 2014.

[157] L. Zhang *et al.*, "Tumor suppressor SPOP ubiquitinates and degrades EglN2 to compromise growth of prostate cancer cells," *Cancer Lett.*, vol. 390, pp. 11–20, Apr. 2017.

[158] C. Li *et al.*, "Tumor-suppressor role for the SPOP ubiquitin ligase in signal-dependent proteolysis of the oncogenic co-activator SRC-3/AIB1," *Oncogene*, vol. 30, no. 42, pp. 4350–4364, Oct. 2011.

[159] K. Gao *et al.*, "Tumor suppressor SPOP mediates the proteasomal degradation of progesterone receptors (PRs) in breast cancer cells.," *Am. J. Cancer Res.*, vol. 5, no. 10, pp. 3210–20, 2015.

[160] J. Luo, Y. chen Bao, X. xiu Ji, B. Chen, Q. fang Deng, and S. wen Zhou, "SPOP promotes SIRT2 degradation and suppresses non-small cell lung cancer cell growth," *Biochem. Biophys. Res. Commun.*, vol. 483, no. 2, pp. 880–884, Feb. 2017.

[161] X. Dai, Z. Wang, and W. Wei, "SPOP-mediated degradation of BRD4 dictates cellular

sensitivity to BET inhibitors," *Cell Cycle*, vol. 16, no. 24, pp. 2326–2329, Dec. 2017.

[162] X. Zhi, J. Tao, L. Zhang, R. Tao, L. Ma, and J. Qin, "Silencing speckle-type POZ protein by promoter hypermethylation decreases cell apoptosis through upregulating hedgehog signaling pathway in colorectal cancer," *Cell Death Dis.*, vol. 7, no. 12, 2016.

[163] C. Zeng *et al.*, "SPOP suppresses tumorigenesis by regulating Hedgehog/Gli2 signaling pathway in gastric cancer," *J. Exp. Clin. Cancer Res.*, vol. 33, no. 1, 2014.

[164] L. G. Ju *et al.*, "SPOP suppresses prostate cancer through regulation of CYCLIN E1 stability," *Cell Death Differ.*, vol. 26, no. 6, pp. 1156–1168, Jun. 2019.

[165] H. Zhu *et al.*, "SPOP E3 Ubiquitin Ligase Adaptor Promotes Cellular Senescence by Degrading the SENP7 deSUMOylase," *Cell Rep.*, vol. 13, no. 6, pp. 1183–1193, Nov. 2015.

[166] W. J. Errington, M. Q. Khan, S. A. Bueler, J. L. Rubinstein, A. Chakrabartty, and G. G. Privé, "Adaptor protein self-assembly drives the control of a cullin-RING ubiquitin ligase," *Structure*, vol. 20, no. 7, pp. 1141–1153, Jul. 2012.

[167] M. Gschweitl *et al.*, "A SPOPL/Cullin-3 ubiquitin ligase complex regulates endocytic trafficking by targeting EPS15 at endosomes.," *Elife*, vol. 5, p. e13841, Mar. 2016.

[168] N. Fang, I. H. Frazer, and G. J. P. Fernando, "Differences in the post-translational modifications of human papillomavirus type 6b major capsid protein expressed from a baculovirus system compared with a vaccinia virus system," *Biotechnol. Appl. Biochem.*, vol. 32, no. 1, p. 27, Aug. 2000.

[169] A. R. Fattaey and R. A. Consigli, "Synthesis, posttranslational modifications, and nuclear transport of polyomavirus major capsid protein VP1.," *J. Virol.*, vol. 63, no. 7, pp. 3168–75, Jul. 1989.

[170] S. Bergström Lind, K. A. Artemenko, L. Elfineh, Y. Zhao, J. Bergquist, and U. Pettersson, "Post translational modifications in adenovirus type 2," *Virology*, vol. 447, no. 1–2, pp. 104–111, Dec. 2013.

[171] B. Mary, S. Maurya, S. Arumugam, V. Kumar, and G. R. Jayandharan, "Post-translational modifications in capsid proteins of recombinant adeno-associated virus (<scp>AAV</scp>) 1-rh10 serotypes," *FEBS J.*, p. febs.15013, Aug. 2019.

[172] D. Duan, Y. Yue, Z. Yan, J. Yang, and J. F. Engelhardt, "Endosomal processing limits gene transfer to polarized airway epithelia by adeno-associated virus.," *J. Clin. Invest.*, vol. 105, no. 11, pp. 1573–87, Jun. 2000.

[173] A. M. Mitchell and R. J. Samulski, "Mechanistic insights into the enhancement of adeno-associated virus transduction by proteasome inhibitors.," *J. Virol.*, vol. 87, no. 23, pp. 13035–41, Dec. 2013.

[174] N. Gabriel *et al.*, "Bioengineering of AAV2 Capsid at Specific Serine, Threonine, or Lysine Residues Improves Its Transduction Efficiency *in Vitro* and *in Vivo*," *Hum. Gene Ther. Methods*, vol. 24, no. 2, pp. 80–93, Apr. 2013.

[175] B. Li *et al.*, "Site-Directed Mutagenesis of Surface-Exposed Lysine Residues Leads to Improved Transduction by AAV2, But Not AAV8, Vectors in Murine Hepatocytes *In Vivo*," *Hum. Gene Ther. Methods*, vol. 26, no. 6, pp. 211–220, Dec. 2015.

[176] D. Sen *et al.*, "Targeted Modifications in Adeno-Associated Virus Serotype 8 Capsid Improves Its Hepatic Gene Transfer Efficiency *In Vivo*," *Hum. Gene Ther. Methods*, vol. 24, no. 2, pp. 104–116, Apr. 2013.

[177] L. Zhong *et al.*, "Next generation of adeno-associated virus 2 vectors: Point mutations in tyrosines lead to high-efficiency transduction at lower doses," *Proc. Natl. Acad. Sci. U. S. A.*, vol. 105, no. 22, pp. 7827–7832, Jun. 2008.

[178] F. Burkart, "Identification of cellular interaction partners of Adeno-associated viruses, PhD thesis." 2012.

[179] A. M. Mitchell and R. J. Samulski, "Mechanistic Insights into the Enhancement of Adeno-Associated Virus Transduction by Proteasome Inhibitors," *J. Virol.*, vol. 87, no. 23, pp. 13035–13041, Dec. 2013.

[180] M. Gschweitl *et al.*, "A SPOPL/cullin-3 ubiquitin ligase complex regulates endocytic trafficking by targeting EPS15 at endosomes," *Elife*, vol. 5, no. MARCH2016, Mar. 2016.

[181] Q. Zhang, L. Zhang, B. Wang, C.-Y. Ou, C.-T. Chien, and J. Jiang, "A hedgehog-induced BTB protein modulates hedgehog signaling by degrading Ci/Gli transcription factor.," *Dev. Cell*, vol. 10, no. 6, pp. 719–29, Jun. 2006.

[182] J. Liu *et al.*, "Analysis of Drosophila segmentation network identifies a JNK pathway factor overexpressed in kidney cancer," *Science (80-.).*, vol. 323, no. 5918, pp. 1218–1222, Feb. 2009.

[183] E. Hinoshita *et al.*, "Decreased expression of an ATP-binding cassette transporter, MRP2, in human livers with hepatitis C virus infection," *J. Hepatol.*, vol. 35, no. 6, pp. 765–773, 2001.

[184] L. Chen, H. Rao, W. Zhang, F. Liu, D. Jiang, and L. Wei, "Association of ATP-binding cassette transporter (ABC) gene polymorphisms with viral load in patients with genotype 1 hepatitis C virus infection," *Clin. Lab.*, vol. 62, no. 9, pp. 1643–1649, 2016.

[185] V. J. Madigan *et al.*, "Ring finger protein 121 is a potent regulator of adeno-associated viral genome transcription," *PLoS Pathog.*, vol. 15, no. 8, 2019.

[186] W. Ji and F. Rivero, "Atypical Rho GTPases of the RhoBTB Subfamily: Roles in Vesicle Trafficking and Tumorigenesis," *Cells*, vol. 5, no. 2, p. 28, Jun. 2016.

[187] K. Taguchi, H. Motohashi, and M. Yamamoto, "Molecular mechanisms of the Keap1-Nrf2 pathway in stress response and cancer evolution," *Genes to Cells*, vol. 16, no. 2. pp. 123–140, Feb-2011.

[188] W. J. Errington, M. Q. Khan, S. A. Bueler, J. L. Rubinstein, A. Chakrabartty, and G. G. Privé, "Adaptor Protein Self-Assembly Drives the Control of a Cullin-RING Ubiquitin Ligase," *Structure*, vol. 20, no. 7, pp. 1141–1153, 2012.

[189] D. Duan, Q. Li, A. W. Kao, Y. Yue, J. E. Pessin, and J. F. Engelhardt, "Dynamin is required for recombinant adeno-associated virus type 2 infection.," *J. Virol.*, vol. 73, no. 12, pp. 10371–6, Dec. 1999.

[190] B. L. Ellis, M. L. Hirsch, J. C. Barker, J. P. Connelly, R. J. Steininger, and M. H. Porteus, "A survey of ex vivo/in vitro transduction efficiency of mammalian primary cells and cell lines with Nine natural adeno-associated virus (AAV1-9) and one engineered adeno-associated virus serotype," *Virology Journal*, vol. 10. 2013.

[191] S. Polyak *et al.*, "Identification of adeno-associated viral vectors suitable for intestinal gene delivery and modulation of experimental colitis," *Am. J. Physiol. - Gastrointest. Liver Physiol.*, vol. 302, no. 3, Feb. 2012.

[192] A. Frattini *et al.*, "High variability of genomic instability and gene expression profiling in different HeLa clones," *Sci. Rep.*, vol. 5, Oct. 2015.

[193] D. M. Duda, L. A. Borg, D. C. Scott, H. W. Hunt, M. Hammel, and B. A. Schulman, "Structural Insights into NEDD8 Activation of Cullin-RING Ligases: Conformational Control of Conjugation," *Cell*, vol. 134, no. 6, pp. 995–1006, Sep. 2008.

[194] S. Tong, Y. Si, H. Yu, L. Zhang, P. Xie, and W. Jiang, "MLN4924 (Pevonedistat), a protein neddylation inhibitor, suppresses proliferation and migration of human clear cell renal cell carcinoma," *Sci. Rep.*, vol. 7, no. 1, Dec. 2017.

[195] C. Geng *et al.*, "SPOP regulates prostate epithelial cell proliferation and promotes ubiquitination and turnover of c-MYC oncoprotein," *Oncogene*, Apr. 2017.

[196] P. Zhang *et al.*, "Intrinsic BET inhibitor resistance in SPOP-mutated prostate cancer is mediated by BET protein stabilization and AKT-mTORC1 activation," *Nat. Med.*, vol. 23, no. 9, pp. 1055–1062, Sep. 2017.

[197] X. Dai *et al.*, "Prostate cancer-Associated SPOP mutations confer resistance to BET inhibitors through stabilization of BRD4," *Nat. Med.*, vol. 23, no. 9, pp. 1063–1071, Sep. 2017.

[198] R. Nayak and D. J. Pintel, "Positive and Negative Effects of Adenovirus Type 5 Helper Functions on Adeno-Associated Virus Type 5 (AAV5) Protein Accumulation Govern AAV5 Virus Production," *J. Virol.*, vol. 81, no. 5, pp. 2205–2212, Mar. 2007.

[199] J. K. Gustin, A. V. Moses, K. Früh, and J. L. Douglas, "Viral takeover of the host ubiquitin system," *Frontiers in Microbiology*, vol. 2, no. JULY. Frontiers Research Foundation, 2011.

[200] A. Wistuba, A. Kern, S. Weger, D. Grimm, J. Ju¨, and J. A. Kleinschmidt, "Subcellular Compartmentalization of Adeno-Associated Virus Type 2 Assembly," 1997.

[201] C. Fraefel, A. G. Bittermann, H. Bueler, I. Heid, T. Bachi, and M. Ackermann, "Spatial and Temporal Organization of Adeno-Associated Virus DNA Replication in Live Cells," *J. Virol.*, vol. 78, no. 1, pp. 389–398, Jan. 2004.

[202] A. M. Mitchell, M. L. Hirsch, C. Li, and R. J. Samulski, "Promyelocytic Leukemia Protein Is a Cell-Intrinsic Factor Inhibiting Parvovirus DNA Replication," *J. Virol.*, vol. 88, no. 2, pp. 925–936, Jan. 2014.

[203] C. Geng *et al.*, "Prostate cancer-associated mutations in speckle-type POZ protein (SPOP) regulate steroid receptor coactivator 3 protein turnover," *Proc. Natl. Acad. Sci. U. S. A.*, vol. 110, no. 17, pp. 6997–7002, Apr. 2013.

[204] S. Grosse *et al.*, "Relevance of Assembly-Activating Protein for Adeno-associated Virus Vector Production and Capsid Protein Stability in Mammalian and Insect Cells," *J. Virol.*, vol. 91, no. 20, Oct. 2017.

7 Appendix

7.1 List of figures

7.2 List of Tables

7.3 List of abbreviations

	Description
#	Number
%	Percent
φ	Non-Polar Amino Acid
π	Polar Amino Acid
°C	Degree Celsius
µ	micro
aa	Amino Acid
A	Alanine
A20	Mouse Monoclonal Antibody Raised Against VP1 Capsid of various AAV Serotypes
A69	Mouse Monoclonal Antibody Raised Against VP1 and VP2 Capsid Proteins of various AAV Serotypes
ABC	ATP-Binding Cassette
Ad	Adenovirus
AAP	Assembly-Activating Protein
AAV	Adeno-Associated Virus
AAVR	AAV Receptor
Amp	Ampicillin
APS	Ammonium Peroxydisulfate
ATP	Adenosine Triphosphate
BACK	BTB and C-Terminal Kelch Domain
B1	Mouse Monoclonal Antibody Raised Against VP1, VP2 and VP3 Capsid Proteins of various AAV Serotypes

BC	Basic Cluster
BET	Bromodomain and Extra-Terminal Motif
BLAST	Basic Local Alignment Search Tool
bp	Base Pairs
BRD	Bromodomain Family
BSA	Bovine Serum Albumin
BTB	Bric-A-Brac, Tram-Track and Broad Complex
C-	Carboxy Terminus
CLIC/GEEC	Clathrin-Independent Carriers/ Gpi-Enriched Early Endosomal Compartment
c-MET	Hepatocyte Growth Factor Receptor
c-myc	Master Regulator of Cell Cycle Entry and Proliferative Metabolism
Cas9	CRISPR-Associated Protein 9
cm	Centimetre
CNS	Central Nervous System
CO_2	Carbon Dioxide
CRISPR	Clustered Regularly Interspaced Short Palindromic Repeats
CRL	Cullin-RING Ubiquitin Ligases
crRNA	CRISPR Locus Encoded RNA
CSA	Cockayne Syndrome Group A Protein
Cul	Cullin
DAPI	4′,6-Diamidino-2-Phenylindole
DAXX	Death Domain Associated Protein
DNA	Deoxyribonucleic Acid
DDB	Damage-Specific DNA Binding Protein
DMEM	Dulbecco's Modified Eagle Medium
DMSO	Dimethyl Sulfoxide
dsDNA	Double Stranded DNA
DUB	Deubiquitinating Enzyme
EDTA	Ethylenediaminetetraacetic Acid
eGFP	Enhanced GFP
EGFR	Epidermal Growth Factor Receptor
EGFR-PTK	Epidermal Growth Factor Receptor Tyrosine Kinase
EglN	Egln Prolyl Hydroxylases
EPS15	Epidermal Growth Factor Receptor Substrate 15
ER	Endoplasmic Reticulum
ERG	ETS-Related Gene
ERK	Extracellular Signal-Regulated Kinase
FGFR	Fibroblast Growth Factor Receptor
g	Gravitational
GAMPO	Goat-Anti-Rabbit, Coupled with Peroxidase
GARPO	Goat-Anti-Mouse, Coupled with Peroxidase
GFP	Green Fluorescent Protein
Gli2	GLI Family Zinc Finger 2
HAT	Hypoxanthine-Aminopterin-Thymidine
H_2O	Water

HCV	Hepatitis C Virus
HECT	Homologous to E6AP C-Terminus
HET 293T	Human Embryonic Kidney Cells 293 with a T Antigen
HEK 293TT	Human Embryonic Kidney Cells 293 with two T Antigens
HIB	Roadkill (Rdx)
HPV	Human Papillomavirus
HRP	Horse Radish Peroxidase
HSPG	Heparin Sulfate Proteoglycan
hSPOP	Human Speckle-Type POZ Protein
IAV	Influenza A Virus
IBR	In-Between-RING Domain
ITR	Inverted Terminal Repeats
K	Lysine
K/O	Knockout
KCl	Potassium Chloride
KD	Knockdown
kDa	Kilo Dalton
KH_2PO4	Monopotassium Phosphate
l	Litre
LamR	Laminin Receptor
LB	Luria-Bertani Broth
Lys	Lysine
M	Molar
MATH	Meprin and TRAF Homology
min	Minute
mL	Millilitre
Mm	Millimetre
MOI	Multiplicity of Infection
N-	Amino-Terminus
nm	Nanometre
Na_2HPO_4	Disodium Hydrogen Phosphate
NaCl	Sodium Chloride
NaOH	Sodium Hydroxide
ND-10	Promyelocytic Leukemia (PML) Nuclear Bodies
NLS	Nuclear Localizing Signal
ORF	Open Reading Frame
PCR	Polymerase Chain Reaction
PBS	Phosphate Buffered Saline
PBS-MK	PBS-Magnesium-Potassium
PBS-T	PBS-Tween
PDGF-R	Platelet-Derived Growth Factor Receptors
Pdx1	Pancreatic and Duodenal homeobox 1 (Also known as insulin promoter factor 1)
PFA	Paraformaldehyde
PEI	Polyethylenimine
PI	Proteasome Inhibitor

PLA2	Phospholipase A2 Domain
PML	Promyelocytic Leukemia Protein
POZ	Poxvirus and Zinc Finger Domain
PPi	Inorganic Pyrophosphate
pTAV 2.0	Vector encoding the AAV2 WT Genome
pTAVORF1cm	Vector encoding the AAV2 WT Without The 2nd ORF
pTAVORF2stopB	Vector encoding the AAV2 With a STOP In AAP
PTEN	Phosphatase and Tensin Homolog
PTM	Post Translational Modification
qPCR	Quantitative PCR
RBR	RING-Between-RING
Rbx1	RING-Box Protein (Also known as ROC1)
RNF	Ring Finger Protein
RPE	Retinal Pigment Epithelium
RING	Really Interesting New Gene
RLU	Relative Light Units
RNA	Ribonucleic Acid
RNAi	RNA Interference
rpm	Revolutions Per Minute
RT	Room Temperature
Sae2	SUMO-Activating Enzyme E1 Subunit 2
SBC	SPOP Binding Consensus
SBS	SPOP Binding Site
scAAV	Self-Complementary AAV Vectors
SDS	Sodium Dodecyl Sulfate
SENP	Sentrin-Specific Proteases
Ser	Serine
Skp1	S-Phase Kinase-Associated Protein 1
Siah	Seven in Absentia Homolog
siRNA	Small Interfering RNA
Sirt2	NAD-Dependent Deacetylase Sirtuin 2
SOC	Super Optimal broth with Catabolite repression
SOCS	Suppressors of Cytokine Signalling Protein
SPOP	Speckle-Type Poxvirus and Zinc Finger Domain (POZ) Protein
SPOPL	Speckle-Type POZ Protein-Like
SRC	Steroid Receptor Co-activator
SRS	Substrate Recognition Subunit
ssDNA	Single-Stranded DNA
SUMO	Small Ubiquitin-like Modifier
TAE	Tris-Acetate-EDTA
TAP	Tandem-Affinity Purification
TE	Tris EDTA
TEMED	N,N,N',N'-Tetramethylethylendiamin
TGS	Tris-Glycine-SDS
Thr	Threonine
TRAF6	Tumour Necrosis Factor Receptor Associated Factor 6

tracrRNA	*Trans*-Acting CRISPR RNA
Tris	Tris (Hydroxymethyl)-Aminomethan
trs	Terminal Resolution Site
U	Unit
UPS	Ubiquitin-Proteasome System
V	Volt
VEGFR	Vascular Endothelial Cell Growth Factor Receptor
VP	Virus Protein
VP1	Viral Capsid Protein 1
VP1u	VP1 Unique N-Terminus
VP2	Viral Capsid Protein 2
VP3	Viral Capsid Protein 3
Y2H	Yeast-2-Hybrid
WT	Wild Type

8 Acknowledgements

First and foremost, my gratitude goes to God almighty. Looking at my life, I can clearly see how His hand has guided my path.

Secondly, I would like to thank the big boss, Prof. Dr. Martin Müller. Thank you for the opportunity to work in your lab, for the guidance and belief in me and the project (even at times when mine wavered). Your jokes and approachable nature eased the pressure of the PhD and created a supportive atmosphere on the project.

I would like to thank my TAC committee Prof. Dr. Oliver Müller and Dr. Steeve Boulant, for having my best interests at heart all through the PhD, both with scientific and non-scientific issues. I appreciate your confidence in me and my capabilities. Thank you for fruitful discussions and numerous ideas. A special thanks also goes to Prof. Jürgen Kleinschmidt, a Godfather in the AAV field. I am grateful for availing your time, ideas and endless support to me and the SPOP project. Our meetings were very insightful and taught me a lot about how to plan and execute science successfully.

My gratitude goes out to Dr. Barbara Leuchs, for the AAV titer quantifications, Dr. Damir Krunic for all the help with microscopy, macros and general scientific advice, and the core facilities at the DKFZ. I would also like to thank the DKFZ PhD program especially to Dr. Lindsay Murrells and Dr. Franziska Schmidt for running a great program with the right amount of co- and extra-curricular activities.

Next, I would like to thank current and past members of F035! Over the last 4 years you have become like family to me. I am so grateful to have had such great work colleagues. Thank you for the scientific support, the friendship, the conversations, the food and the bonding. I shall miss the lab atmosphere primarily because of you guys! I would like to thank Greta Jaschkowitz and Anja Brauchle, for being great students and testing my teaching capabilities. It was such an honor to have you under my wing and to see you grow in your scientific thinking, AAV and lab knowledge, experimental planning and execution. A special shout out goes to Qingxin Chen, my favorite member of the AAV group. Thank you for the guidance and partnership as we explored our little virus and aspired to contribute to AAV biology.

I would also like to extend my thanks to my educators over the years- Teacher Njeri, Mr. Tulesi, Mr. Kihumba, Mr . Githiomi, Mrs. Ombeta, Mr. Gee and Mrs. Lee. Thank you for believing in me from a very young age and challenging me to strive for more. To my university professors- Prof. Sebastian Springer, Dr. Susan Illenberger, Prof. Klaudia Brix, Dr. Sophia Tedelind, Prof. Christian Hammann, Prof. Matthias Ulrich, Prof. Alexander Dalpke and Prof.

Volker Lohmann. Thank you for sparking an interest in molecular biology within me, by letting your passion for science shine through you.

The good friends I have made in Heidelberg- Monica, Diana, Vlad, Ruki, Raissa, Julius, Veronica, Dorcas, Mendi, Basti, Kevin, Albina, Charlotte, James, Bryan and Ayo; as well as my awesome past and present housemates-Flo, Maira, Lea, Jaro. Sisi, Tomasso, Bertille, Sara and Jay. Thank you so much for your friendship and for all the fun times. You really made HD feel that much warmer and gave me that work-life balance! I am also grateful for my good friends outside HD- Njeri, Irene, Nadja, Anne, Sibulele, Patience, Martina, Octavian, Manuela, Robin, Johnny, Eric, Tenzin, Elnathan, Kisila, Arnold, Louis, Theuri, Ashwin, Makena, Ngina, Sylvia, Viona, Kushi, BG, Hope, Viyerrah, Krystal and Stacie. Thank you for checking up on me over the years, for inspiring me, making me laugh, providing great distractions and for your life-long friendship.

My gratitude also goes out to my host mum: Marlene Georgi and the entire Georgi and Schwann clans. Thank you so much for letting me be a part of your family, for the laughter, advice and love over the past 10 years. My insight and appreciation of German culture and food is mostly thanks to you Nene and I thank God that He put you in my life.

I would like to especially thank my parents- Njenga Mwangi and Jane Njenga. Not only for educating me, feeding me and loving me unconditionally, but for guiding me and trusting me as I made choices throughout my life. For giving me independence from a very young age and for going beyond parenting to actually being friends. My younger sister Zafrina Muthoni Njenga, thank you for being a great listener, a sharer of memes and lame jokes, and a kick-ass musical taste. As I always say you are wise beyond your years and an amazing kid sis, with a great future ahead! My sister Njambi, brothers- Alex and Mwangi, all my cousins especially Shiro Fiona and my aunts and uncles from both the Njora and Mwangi sides. Thank you for being the warmest, tight-knit family ever and for surrounding me with love and affirmation my whole life.

Finally, I would like to thank Bett David Kipruiyot Korir, for being my rock these last two years. For your fresh perspective, calmness, endless love and care; and for your mental, psychological and emotional support. Thank you for keeping me sane through it all and being my biggest cheerleader.